UNIVERSITY OF CALIFORNIA
RIVERSIDE

Age-Related Changes to Auditory Temporal Processing in Mice with and without Age-Related Hearing Loss

A Dissertation submitted in partial satisfaction
of the requirements for the degree of

Doctor of Philosophy

in

Neuroscience

by

Jeffrey Alexander Rumschlag

December 2020

Dissertation Committee:
Dr. Khaleel Razak, Chairperson
Dr. Megan Peters
Dr. Edward Zagha

The Dissertation of Jeffrey Alexander Rumschlag is approved:

_____

_____

_____

Committee Chairperson

University of California, Riverside

Acknowledgments

The text of this dissertation, in part, is a reprint of the material as it appears in Rumschlag et al., 2020. The co-author, Khaleel Razak, directed and supervised the research. Co-author Jonathan Lovelace provided advice on statistical analysis and suggested edits to the manuscript. Chapter 2 is reproduced in its entirety from the publication, Rumschlag, J. A., Lovelace, J. W., & Razak, K. A. (2020). Age- and movement-related modulation of cortical oscillations in a mouse model of presbycusis. Hearing Research, Advance online publication. https://doi.org/10.1016/j.heares.2020.108095, under the Creative Commons license.

I would like to acknowledge and thank the Hearing Health Foundation, UC MRPI, and UCR for each funding portions of this research.

I would like to personally acknowledge several people who provided essential support to me during my graduate studies.

To my parents, who have supported me every step of the way. Your guidance and positivity have made the last 6 years possible.

To everyone in the Razak lab, past and present: Jonny, Stephen, Jamiela, Mawaheb, Xin, Kati, Teresa, Sarah, Anna, Brad, Katherine, Anjana, Victoria, and Max. You all made the basement a warm and welcome place to be. I can only hope that I will be so lucky to find such wonderful coworkers and friends in the future.

To Jim, my climbing buddy during the good times and my virtual friend during the pandemic.

To Jonny, a friend, colleague, and fellow night owl.

To the mice who participated in my experiments. Your sacrifices were not in vain.

And finally, and most importantly, to Khaleel Razak, a dedicated mentor and brilliant scientist. Thank you for your unending support and guidance.

Dedication

This dissertation is dedicated to my parents, Tony and Hella, who have encouraged my scientific pursuits, starting with my first science fair in kindergarten. You inspired me to think critically and question everything, which turned out to be very helpful, eventually. Thank you for your patience, love, and support. This dissertation would not have been possible without you.

ABSTRACT OF THE DISSERTATION

Age-Related Changes to Auditory Temporal Processing in Mice with and without Age-Related Hearing Loss

by

Jeffrey Alexander Rumschlag

Doctor of Philosophy, Graduate Program in Neuroscience
University of California, Riverside, December 2020
Dr. Khaleel Razak, Chairperson

Most older adults experience age-related changes to their hearing, either in the form of hearing loss, or in a more subtle form of hearing impairment, causing difficulties understanding speech in acoustically challenging environments. As the population grows older, better solutions will be needed to alleviate age-related hearing deficits. To test new potential therapies for age-related changes to hearing, preclinical models must be identified and characterized. The studies included in this dissertation measure translationally relevant electrophysiological signals from mice at multiple ages, with and without severe hearing loss, to identify age-related changes to cortical activity, both at baseline and in response to acoustic stimuli. Acoustic stimuli were used to test various aspects of auditory processing, including amplitude modulated signal processing, which supports speech comprehension. We found that age-related changes in the responses to the acoustic stimuli selected for this study mirror many of the changes observed in older humans. We observed age-related deficits in responses to more challenging amplitude modulated signals, even in the absence of hearing loss. In mice with hearing loss, we

observed evidence of central gain and disrupted temporal processing. Both results, which mirror age-related changes to human hearing, suggest that aging mice are a useful model for auditory processing in older humans. We then evaluated the therapeutic potential of nicotine for treating age-related changes to auditory temporal processing, with promising results. Nicotine appeared to improve temporal processing in old mice, partially reversing age-related, frequency-specific changes in event-related spectral perturbations and amplitude modulation following responses. This dissertation characterizes translationally relevant preclinical measures of age-related changes to auditory processing, with the aim of testing interventions and therapeutics, such as nicotine, for the treatment of age-related auditory temporal processing deficits.

Table of Contents

List of Tables

List of Figures

Abbreviations

ANOVA: Analysis of variance

ARHL: Age-related hearing loss

ASSR: Auditory steady-state response

dB SPL: decibel sound pressure level

ECoG: Electrocorticogram

EEG: Electroencephalogram

EFR: Envelope-following response

ERP: Event-related potential

ERSP: Event-related spectral perturbations

ITPC: Inter-trial phase clustering

PV: Parvalbumin

SPIN: Speech perception in noise

Chapter 1

Introduction

Shifting age demographics highlight the need to study age-related auditory system changes

Understanding speech in challenging environments is difficult for most older adults. Studies have demonstrated that hearing loss, communication difficulties, and the ensuing isolation, often go hand in hand with cognitive decline. As reviewed by Davis et al. (2016), data from the World Health Organization shows that around 33% of people older than 65 have significant age-related hearing loss (ARHL; presbycusis) (WHO: Prevention of blindness and deafness: Estimates, 2012; WHO: Deafness and hearing loss, 2015). The age distribution of the US population is trending older, as baby boomers enter the 65 and older population. This means that there will be a significantly larger portion of the population affected by age-related hearing difficulties in the coming years. The need for hearing preservation and restoration therapies is growing along with the growth of the older population. The studies included in this dissertation are intended to provide improved and translation relevant preclinical measures of age-related changes to auditory processing, and identify if nicotine administration provides therapeutic benefit.

Older individuals without hearing loss also have difficulty understanding speech in adverse environments

Even without hearing loss, many older adults report difficulties in understanding speech in challenging environments, such as crowded rooms, reverberant spaces, and

internet-based audiovisual communication (Humes & Dubno, 2010; Zamir et al., 2018). Although hearing aids have improved significantly in the past decades, they are still unable to improve understanding in all situations, and unfortunately continue to be associated with stigma. Increasing gain does not necessarily improve auditory temporal processing, which is necessary for speech comprehension (Gürses et al., 2020).

Speech processing relies on high fidelity auditory temporal processing

Auditory temporal processing refers to the ability of the auditory system to register changes in acoustic signals over time. This includes distinguishing between voice onset times (VOTs), to distinguish between words like 'dye' and 'tie', the difference between which lies in the gap between the consonant and the voiced vowel. Some studies show age-related deficiencies in gap detection (He et al., 1999; Schneider et al., 1994), while others, especially those that present gaps in acoustically clean environments, do not (Moore et al., 1992). Auditory temporal processing includes the ability to follow changes in pitch (frequency modulation; FM), and in sound level (amplitude modulation; AM). Studies have demonstrated that AM and FM information are both important for speech comprehension. In my dissertation, I focused on AM, but the techniques used to study age-related changes in AM could also be adapted to examine changes in FM. Auditory steady-state responses (ASSR), which are responses to AM signals, have been linked with word recognition scores in humans (Dimitrijevic et al., 2004).

Animal models of age-related changes to the auditory system

To identify therapeutic potential of treatments, it is vital to first describe and validate objective biomarkers at the preclinical level. Therefore, one of the major goals

of this dissertation is to focus on the aging murine auditory system, and identify electrophysiological biomarkers of age-related changes in auditory processing. Other animal models have been used to study age-related changes in hearing, including rats, gerbils, guinea pigs, and cats. We use mice because many aspects of age-related hearing loss have been characterized in specific mouse strains, and studying mice provides the opportunity to perform complex genetic manipulations, which is one of the next steps in this line of research. This study uses two inbred strains of mice, the well-studied model of age-related hearing loss, the C57bl/6J (C57) strain, and the FVB.129P2−Pde6b+Tyrc-ch/AntJ (FVB) strain, which appears to age similarly to the more commonly studied CBA/CaJ strain. The C57 mouse serves as a model for presbycusis, because its audiometric trajectory mimics the changes observed in humans: a severe decline in high-frequency hearing, along with an overall increase in hearing thresholds. However, the C57 mouse loses its hearing due to genetic mutations, the most commonly cited of which is a splice variant of the gene expressing the stereocilia tip-link protein, cadherin 23 (CDH23, coded by *Cdh23*) (Johnson et al., 2010). This leads to a rapid decline in the number of inner and outer hair cells (Johnson et al., 2010). This hair cell loss mimics the age-related hair cell loss in most aging humans (Wu et al., 2020), making it a useful model for severe age-related hearing loss.

Behavioral testing of auditory temporal processing in aging models

Previous studies have measure age-related changes to some aspects of temporal processing in aging animals. Behavioral gap detection has been used to measure auditory temporal processing. In these studies, the animal is trained to respond to a silent gap in an

acoustic stimulus, and the width of the gap is varied to find the limit (Gleich & Strutz, 2011; Šuta et al., 2011). Some studies, especially those that have tested in challenging environments, have found age-related deficits in detecting short gaps (Šuta et al., 2011; Walton et al., 1998).

Electrophysiological testing of auditory temporal processing in aging models

Electrophysiological changes in the aging rat auditory system have been well characterized by Bartlett and Parthasarathay (Herrmann et al., 2017; Parthasarathy & Bartlett, 2011, 2012; Parthasarathy et al., 2014, 2019). In summary, they found age-related decreases in temporal processing fidelity, as measured by envelope following responses (EFRs) in the inferior colliculus of anesthetized rats. The Bartlett lab found that responses to sinusoidally amplitude modulated (SAM) tones were increased in old rats when the modulation depth was 100%, but not when it was 25%, which suggests an age-related increase in central gain (Lai et al., 2017). In the experiments contained in this dissertation, I measured EEG signals from the cortex of awake, freely moving mice. The results in this dissertation complement the previous studies done in anesthetized rats and describe additional ways to measure changes in central gain and auditory processing with age.

Auditory steady-state responses (ASSR) are oscillatory population activity in response to periodic stimuli and have been well-characterized in animal models (Hwang et al., 2020). Some studies have found age-related changes to the ASSR in animals (Sanz-Fernández et al., 2015). EFRs can be elicited by an amplitude modulated noise stimulus (chirp), for which the amplitude modulation frequency steadily increases (Ethridge et al.,

2017). In the following studies, we measure both ASSR and chirp responses to assess auditory temporal processing. While the ASSR is limited to 40 Hz, the chirp response evokes oscillations at multiple frequencies. This may allow for the disentanglement of the contributions of different interneuron populations, based on studies suggesting frequency-specific contributions to neural oscillations (Cardin et al., 2009; Chen et al., 2017; Sohal et al., 2009).

Neural responses to gaps have been measured at the single-neuron and population level in animal models (Keller et al., 2018; Walton et al., 2008; Weible et al., 2014; Zhao et al., 2015). Electrophysiological and behavioral gap detection thresholds are strongly related (Eggermont, 2000). In the 4th chapter, a novel stimulus is demonstrated, which combines aspects of ASSR and gap responses, and may serve as a useful preclinical biomarker of subtle age-related changes to temporal processing.

Defining mouse models for age-related hearing changes with and without severe hearing loss

The purpose of this research is to identify age-related electrophysiological outcome measures in mice, to find measures that differentiate cortical responses in mice with cochlear hearing loss and those with relatively healthy cochlear aging, and to test acute nicotine as a potential intervention for age-related changes in auditory processing. Because we are interested in using these measures to develop a preclinical model, we recorded EEG responses, a method commonly used to study humans. Mice were implanted with epidural screw electrodes, which yield recordings comparable to human EEG or electrocorticography (ECoG). We recorded baseline brain activity from freely

moving mice, in addition to responses to a variety of stimuli designed to assess auditory system function. We chose to measure responses to 12 kHz low-pass noise to minimize the effect of normal age-related high-frequency hearing loss. We used specific temporal patterns of noise to measure different aspects of auditory processing, from a simple noise burst, to periodic stimuli, and a novel stimulus eliciting an auditory steady-state response with gaps. The chapters are organized as three papers that are in various stages of the publication process.

Chapter 2: Age- and movement-related modulation of cortical oscillations in a mouse model of presbycusis

Young and old C57 mice are recorded during rest and while passively listening to sound stimuli. Baseline gamma activity is significantly decreased in older mice. The mice show significant event-related potentials in response to noise bursts, but do not show phase-locking in response to a dynamic amplitude-modulated noise stimulus.

Chapter 3: Nicotine partially reverses age-related changes in cortical neural oscillations

In this chapter, mice without severe hearing loss (FVB) are tested for age-related changes to auditory processing, baseline cortical activity, and movement-related modulation of cortical activity. Following an acute administration of nicotine, the old mice show reversals in multiple measurements of age-related changes in cortical gamma activity.

Chapter 4: Age-Related Changes to Gap-Evoked Auditory Steady State Responses in Mice with and without Pathological Hearing Loss

This chapter directly compares C57 and FVB mice to demonstrate a measure that differentiates between changes in auditory temporal processing due to age-related hearing loss and changes simply due to aging.

References

Cardin, J. A., Carlén, M., Meletis, K., Knoblich, U., Zhang, F., Deisseroth, K., Tsai, L. H., & Moore, C. I. (2009). Driving fast-spiking cells induces gamma rhythm and controls sensory responses. *Nature*, *459*(7247), 663–667. https://doi.org/10.1038/nature08002

Chen, G., Zhang, Y., Li, X., Zhao, X., Ye, Q., Lin, Y., Tao, H. W., Rasch, M. J., & Zhang, X. (2017). Distinct inhibitory circuits orchestrate cortical beta and gamma band oscillations. *Neuron*, *96*(6), 1403-1418. https://doi.org/10.1016/j.neuron.2017.11.033

Davis, A., McMahon, C. M., Pichora-Fuller, K. M., Russ, S., Lin, F., Olusanya, B. O., Chadha, S., & Tremblay, K. L. (2016). Aging and hearing health: the life-course approach. *Gerontologist*, *56*, S256–S267. https://doi.org/10.1093/geront/gnw033

Dimitrijevic, A., John, M. S., & Picton, T. W. (2004). Auditory steady-state responses and word recognition scores in normal-hearing and hearing-impaired adults. *Ear and Hearing*, *25*(1), 68–84. https://doi.org/10.1097/01.AUD.0000111545.71693.48

Eggermont, J. J. (2000). Neural responses in primary auditory cortex mimic psychophysical, across-frequency-channel, gap-detection thresholds. *Journal of Neurophysiology*, *84*(3), 1453–1463. https://doi.org/10.1152/jn.2000.84.3.1453

Ethridge, L. E., White, S. P., Mosconi, M. W., Wang, J., Pedapati, E. V., Erickson, C. A., Byerly, M. J., & Sweeney, J. A. (2017). Neural synchronization deficits linked to cortical hyper-excitability and auditory hypersensitivity in fragile X syndrome. *Molecular Autism*, *8*(1), 1–11. https://doi.org/10.1186/s13229-017-0140-1

Gleich, O., & Strutz, J. (2011). The effect of gabapentin on gap detection and forward masking in young and old gerbils. *Ear and Hearing*, *32*(6), 741–749. https://doi.org/10.1097/AUD.0b013e318222289f

Gürses, E., Türkyılmaz, M. D., & Sennaroğlu, G. (2020). Evaluation of auditory temporal processing in patients fitted with bone-anchored hearing aids. *European Archives of Oto-Rhino-Laryngology*, *277*(2), 351–359. https://doi.org/10.1007/s00405-019-05701-4

He, N., Horwitz, A. R., Dubno, J. R., & Mills, J. H. (1999). Psychometric functions for gap detection in noise measured from young and aged subjects. *The Journal of the Acoustical Society of America*, *106*(2), 966. https://doi.org/10.1121/1.427109

Herrmann, B., Parthasarathy, A., & Bartlett, E. L. (2017). Ageing affects dual encoding of periodicity and envelope shape in rat inferior colliculus neurons. *European Journal of Neuroscience*, *45*(2), 299-311. https://doi.org/10.1111/ejn.13463

Humes, L. E., Busey, T. A., Craig, J., & Kewley-Port, D. (2013). Are age-related changes in cognitive function driven by age-related changes in sensory processing?. *Attention, Perception, & Psychophysics*, *75*(3), 508-524. https://doi.org/10.3758/s13414-012-0406-9

Hwang, E., Han, H. B., Kim, J. Y., & Choi, J. H. (2020). High-density EEG of auditory steady-state responses during stimulation of basal forebrain parvalbumin neurons. *Scientific Data*, *7*(1), 1–9. https://doi.org/10.1038/s41597-020-00621-z

Johnson, K. R., Yu, H., Ding, D., Jiang, H., Gagnon, L. H., & Salvi, R. J. (2010). Separate and combined effects of Sod1 and Cdh23 mutations on age-related hearing loss and cochlear pathology in C57BL/6J mice. *Hearing Research*, *268*(1–2), 85–92. https://doi.org/10.1016/j.heares.2010.05.002

Keller, C. H., Kaylegian, K., & Wehr, M. (2018). Gap encoding by parvalbumin-expressing interneurons in auditory cortex. *Journal of Neurophysiology*, *120*(1), 105–114. https://doi.org/10.1152/jn.00911.2017

Lai, J., Sommer, A. L., & Bartlett, E. L. (2017). Age-related changes in envelope-following responses at equalized peripheral or central activation. *Neurobiology of Aging*, *58*, 191–200. https://doi.org/10.1016/j.neurobiolaging.2017.06.013

Moore, B. C. J., Peters, R. W., & Glasberg, B. R. (1992). Detection of temporal gaps in sinusoids by elderly subjects with and without hearing loss. *The Journal of the Acoustical Society of America*, *92*(4), 1923–1932. https://doi.org/10.1121/1.405240

Parthasarathy, A, & Bartlett, E. L. (2011). Age-related auditory deficits in temporal processing in F-344 rats. *Neuroscience, 192*, 619–630. https://doi.org/https://doi.org/10.1016/j.neuroscience.2011.06.042

Parthasarathy, A., & Bartlett, E. L. (2012). Two-channel recording of auditory-evoked potentials to detect age-related deficits in temporal processing. *Hearing Research, 289*(1–2), 52–62. https://doi.org/10.1016/j.heares.2012.04.014

Parthasarathy, A., Datta, J., Torres, J. A. L., Hopkins, C., & Bartlett, E. L. (2014). Age-related changes in the relationship between auditory brainstem responses and envelope-following responses. *Journal of the Association for Research in Otolaryngology*, *15*(4), 649–661. https://doi.org/10.1007/s10162-014-0460-1

Parthasarathy, A., Herrmann, B., & Bartlett, E. L. (2019). Aging alters envelope representations of speech-like sounds in the inferior colliculus. *Neurobiology of Aging, 73*, 30–40. https://doi.org/10.1016/j.neurobiolaging.2018.08.023

Sanz-Fernández, R., Sánchez-Rodriguez, C., Granizo, J. J., Durio-Calero, E., & Martín-Sanz, E. (2015). Utility of auditory steady-state and brainstem responses in age-related hearing loss in rats. *Acta Oto-Laryngologica*, *135*(1), 35–41. https://doi.org/10.3109/00016489.2014.953203

Schneider, B. A., Pichora-Fuller, M. K., Kowalchuk, D., & Lamb, M. (1994). Gap detection and the precedence effect in young and old adults. *The Journal of the Acoustical Society of America*, *95*(2), 980–991. https://doi.org/10.1121/1.408403

Sohal, V. S., Zhang, F., Yizhar, O., & Deisseroth, K. (2009). Parvalbumin neurons and gamma rhythms enhance cortical circuit performance. *Nature, 459*(7247), 698–702. https://doi.org/10.1038/nature07991

Šuta, D., Rybalko, N., Pelánová, J., Popelář, J., & Syka, J. (2011). Age-related changes in auditory temporal processing in the rat. *Experimental Gerontology*, *46*(9), 739–746. https://doi.org/10.1016/j.exger.2011.05.004

Walton, J. P., Barsz, K., & Wilson, W. W. (2008). Sensorineural hearing loss and neural correlates of temporal acuity in the inferior colliculus of the C57bl/6 mouse. *Journal of the Association for Research in Otolaryngology*, *9*(1), 90–101. https://doi.org/10.1007/s10162-007-0101-z

Walton, J. P., Frisina, R. D., & O'Neill, W. E. (1998). Age-related alteration in processing of temporal sound features in the auditory midbrain of the CBA mouse. *Journal of Neuroscience, 18*(7), 2764–2776. https://doi.org/10.1523/JNEUROSCI.18-07-02764.1998

Weible, A. P., Moore, A. K., Liu, C., Deblander, L., Wu, H., Kentros, C., & Wehr, M. (2014). Perceptual gap detection is mediated by gap termination responses in auditory cortex. *Current Biology*, *24*(13), 1447–1455. https://doi.org/10.1016/j.cub.2014.05.031

Wu, P. Z., O'Malley, J. T., de Gruttola, V., & Charles Liberman, M. (2020). Age-related hearing loss is dominated by damage to inner ear sensory cells, not the cellular battery that powers them. *Journal of Neuroscience*, *40*(33), 6357–6366. https://doi.org/10.1523/JNEUROSCI.093720.2020

Zamir, S., Hennessy, C. H., Taylor, A. H., & Jones, R. B. (2018). Video-calls to reduce loneliness and social isolation within care environments for older people: An implementation study using collaborative action research. *BMC Geriatrics*, *18*(1), 1–13. https://doi.org/10.1186/s12877-018-0746-y

Zhao, Y., Xu, X., He, J., Xu, J., & Zhang, J. (2015). Age-related changes in neural gap detection thresholds in the rat auditory cortex. *European Journal of Neuroscience, 41*(3), 285–292. https://doi.org/10.1111/ejn.12791

Chapter 2

Age- and movement-related modulation of cortical oscillations in a mouse model of presbycusis

Abstract

Brain oscillations are associated with specific cognitive and sensory processes. How age-related hearing loss (presbycusis) alters cortical oscillations is unclear. Altered inhibitory neurotransmission and temporal processing deficits contribute to speech recognition impairments in presbycusis. Specifically, age-related reduction in parvalbumin positive interneurons and perineuronal nets in the auditory cortex predicts a reduction in gamma oscillations that may lead to a decline in temporal precision and attention. To test the hypothesis that resting and evoked gamma oscillations decline with presbycusis, EEGs were recorded from the auditory and frontal cortex of awake, freely moving C57BL/6J mice at three ages (3, 14 and 24 months). Resting EEG data were analyzed according to movement state (move *versus* still). Evoked responses were recorded following presentation of noise bursts or amplitude modulated noise with time varying modulation frequencies. We report an age-related decrease in resting gamma power, a decline in gamma-range synchrony to time varying stimuli, and an increase in noise evoked and induced gamma power. A decline in temporal processing is seen in aged mice that exhibit robust auditory-evoked potentials, dissociating hearing loss from temporal processing deficits. We also report an increase in gamma power when mice moved compared to the still state. However, the movement-related modulation of gamma oscillations did not

change with age. Together, these data identify a number of novel markers of presbycusis-related changes in auditory and frontal cortex. Because EEGs are commonly recorded in humans, the mouse data may serve as translation relevant preclinical biomarkers to facilitate the development of therapeutics to delay or reverse central auditory processing deficits in presbycusis.

Introduction

Age-related changes in auditory processing in humans include degraded temporal fine structure processing, spectrotemporal sweep detection, phoneme discrimination and word recognition (Fitzgibbons et al., 2006; Gordon-Salant & Fitzgibbons, 2001; He et al., 1998, 2007; Hopkins & Moore, 2011). Physiological studies in humans indicate altered representation of time-varying speech cues, including reduced temporal precision and increased response variability of evoked responses (Anderson et al., 2012; Tremblay et al., 2003). These age-related deficits are further compounded by hearing loss (presbycusis or age-related hearing loss). Presbycusis is the most prevalent form of hearing impairment affecting ~35-45% of humans older than 65 years (Gates & Mills, 2005). Declining speech recognition contributes to social isolation and may lead to cognitive impairment (Frisina, 2009; Humes et al., 2013; Gates & Mills, 2005; López-Torres Hidalgo et al., 2009; Weinstein & Ventry, 1982). Indeed, a Lancet Commission report indicated that hearing loss is a leading risk factor in age-related cognitive decline (Livingston et al., 2017). Hearing aids amplify sounds but do not necessarily improve speech recognition (Hogan & Turner, 1998), suggesting altered central auditory

processing. Currently there are no treatments to delay or reverse central auditory system changes. To identify and test potential therapeutics, translationally relevant pre-clinical biomarkers are necessary.

Studies of aging rodents show altered spectral representation (tonotopy and tuning curves, Turner et al., 2005; Willott et al., 1993), declining temporal processing (gap detection, amplitude-modulated signals, Barsz et al., 2002; De Villers-Sidani et al., 2010; Parthasarathy & Bartlett, 2011; Simon et al., 2004; Walton et al., 1998; Walton et al., 2002, 2008) and declining spectrotemporal selectivity (Mendelson & Ricketts, 2001; Trujillo & Razak, 2013). Trujillo et al., (2013) showed increasing variability in responses and shifts in selectivity to slower modulations that may be correlates of observed deficits in humans (Anderson et al., 2012; Tremblay et al., 2003). Histological studies of aging rodent brains abnormal or reduced inhibitory neurotransmission (Burianova et al., 2009; Caspary et al., 2008). Martin del Campo et al., (2012) and Brewton et al. (2016) showed a loss of parvalbumin (PV) positive inhibitory neuron density and the perineuronal nets (PNN) that cover PV cells in the auditory cortex of mice with presbycusis (C57BL/6J).

Parvalbumin neurons are involved in shaping gamma band (30-80 Hz) oscillations in the forebrain that are implicated in sensory processing, timing precision and attention (Sohal et al., 2009; Cardin et al., 2009). Schneider et al., (2014) showed that activation of auditory cortex PV cells by projections from the secondary motor cortex modulates responses in the auditory cortex. These studies suggest that the age-related loss of PV cells, and their altered excitability due to loss of PNNs, will lead to reduced gamma band oscillations and a reduction in the movement-related modulation of auditory cortex

activity. However, these predictions have not been tested in any species. Changes in oscillations may underlie age-related deficits in sensory processing, attention and movement related gain modulation of cortex. Because EEG recordings of brain oscillations in humans are relatively more feasible (Harris et al., 2008; Polich, 1997), and widely used, compared to single unit recordings and brain histology, rodent EEG studies will facilitate the preclinical to clinical biomarker pipeline for developing therapies for presbycusis related deficits in speech processing. The main goal of this study was therefore to quantify the changes in resting and sound-evoked neural oscillations using EEG recordings in auditory and frontal cortex of awake and freely moving mice across three different ages (young, middle-age and old). By analyzing EEGs when mice were still *versus* moving, age- and movement-related modulations of EEG power distributions were quantified.

Methods

All procedures were approved by the Institutional Animal Care and Use Committee at the University of California, Riverside. Mice were obtained from an in-house breeding colony that originated from Jackson Laboratory (Bar Harbor, ME). One to four mice were housed in each cage under a 12:12-h light-dark cycle and fed *ad libitum*. The following age ranges and sample sizes were used in this study: young (n=10, 5 females, mean = 3.0 mo), middle age (n=8, 4 females, mean =13.8 mo) and old (n=17, 9 females, mean = 24.2 mo). The groups are referred to as 3, 14 and 24 mo old mice.

Surgery to implant EEG electrodes

The aseptic surgical procedures used are described in detail in Lovelace et al., (2018). Briefly, mice were anesthetized with ketamine/xylazine/acepromazine (80/10/1 mg/kg, i.p.) and 1 mm diameter holes were drilled (Foredom dental drill) in the skull overlying the right auditory cortex, right frontal cortex, and the left occipital cortex. The auditory screw position was determined using skull landmarks which have been validated previously using tonotopic mapping, single unit recordings (Trujillo et al., 2011; Willott et al., 1993) and epidural EEG recordings (Lovelace et al., 2018) in the C57 mice (~AP 2.2-2.3 mm relative to Bregma and ~ML 4.3-4.4 mm). The frontal screw was placed just caudal to the frontal sinus and just lateral to the sagittal suture. The occipital screw was placed in the parietal bone, just lateral to the intersection of the sagittal suture and lambdoid suture. The wires extending from three-channel posts (P1 Technologies, Roanoke, VA) were stripped and wrapped around 1mm screws (P1 Technologies, Roanoke, VA), which were screwed into the pre-drilled holes. Dental cement (Kuraray Dental, New York, NY) was used to cover the exposed skull and screws. Recovering mice were injected (subcutaneous) with 0.1 mg/kg buprenorphine every 6-8 hours for 48 hours after surgery. The mice had at least 4 days to recover following surgery, and at least 3 days after the last buprenorphine injection, before the first recording.

EEG recordings from awake, freely-moving mice

The mouse was briefly anesthetized with isoflurane inhalation, and a three-channel cable was plugged into the implanted post. This cable was connected *via* freely-

rotating commutator to a TDT (Tucker Davis Technologies, FL) RA4LI/RA4PA headstage/pre-amp, which was connected to a TDT RZ6 multi-I/O processor. The frontal and auditory cortical screw electrodes were referenced and grounded to the occipital screw electrode. Motion detection was achieved using a 27 mm piezoelectric pressure sensor (AW-PZT27L, Audiowell, Guangdong, China) placed beneath the arena, in addition to an infrared video camera mounted above the arena. OpenEx (TDT) was used to record EEG signals, record pressure signals and operate the LED light used to synchronize the video and waveform data. The EEG signals were captured at a sampling rate of 24.414 kHz and down-sampled to 1024 Hz. EEG Recordings were visually examined for artifacts, which are characterized by a temporary loss of signal, or by vertical lines indicative of clipping. Any recordings that included artifacts would have been eliminated from the study, but none did, so no EEG data were rejected.

Auditory stimulus presentation

Sounds were presented to freely moving mice through a TDT MF1 speaker placed 20 cm above the arena. The sound levels were calibrated using a ¼" Bruel and Kjaer (Nærum, Denmark) microphone. The broadband noise pulses and chirps were presented at 70 dB SPL to young mice (3 mo) and 90 dB SPL to old mice (24 mo), to account for age-related hearing loss (Hunter & Willott, 1987; Johnson et al., 1997). The stimuli were generated with a TDT RZ6 with a sampling rate of 24.414 kHz.

Spectral analysis of resting EEG data

To quantify age-related changes in EEG spectral power distribution, and how movement influences EEG power at different ages, we measured resting EEG power spectral densities in both auditory and frontal cortex (AC and FC) across the different age groups. The phrase 'resting EEG' is used to describe data collected when there was no specific auditory stimulation. Five minutes of resting EEG was recorded from each mouse. This data was then split into periods of movement (referred as 'move') and non-movement (referred as 'still'), based on analysis of the pressure and video signal of motion (custom MATLAB scripts). The two conditions ('still' vs. 'move') were analyzed separately to identify movement-dependent differences in power spectral density of resting EEG. The traces from each condition were split into Hanning-windowed 1-second segments with 50% overlap, which were then transformed to the frequency domain *via* Fourier transform. The average power spectra for each condition were calculated by averaging the spectra from each of the 1-second segments. Each average power spectrum was then split into canonical EEG frequency bands (theta: 3-7 Hz, alpha: 8-13 Hz, beta: 14-29 Hz, low gamma: 30-59 Hz, high gamma: 61-100 Hz, and high-frequency oscillations: 101-250 Hz). Delta band power was not analyzed because the pre-amplifier has a built-in high-pass filter at 2.2 Hz. The average power from each frequency band was calculated. Kruskall-Wallis tests were run on each frequency band (SPSS, IBM, NY), and the resulting p-values were adjusted for multiple comparisons within each region. To calculate relative power, the power at each frequency was divided by the total

power across the frequency spectrum. The relative power spectra were then analyzed as described above.

Analysis of movement-related modulation of EEG spectral power

To correlate EEG power with movement, videos recorded during EEG recordings were analyzed for motion. A custom MATLAB script was used to determine the location of the mouse in each frame, and to calculate instantaneous velocity. During recordings, a red LED light controlled by the RZ6 system flashed briefly every 5 minutes, and simultaneously a TTL pulse was recorded alongside the EEG signal. The video and EEG signals were synchronized via the on/off times of the LED. The EEG signal was transformed using a complex Morlet wavelet transform, with a constant wavelet parameter of 7, to provide instantaneous spectral power at frequencies ranging from 1-250 Hz. For each frequency, this spectral power was correlated with the velocity calculated from the video, using Spearman's Rho. These measurements will allow us to determine if there were changes to movement velocity and/or EEG power with age, and if there were correlations between these measures.

Analysis of Auditory Responses

For auditory ERP analysis, we averaged responses to 120 repetitions of a 100 ms-duration noise burst and performed time-frequency analysis using a dynamic complex Morlet wavelet transform with Gabor normalization, in which the wavelet parameter was set for each frequency to optimize time-frequency resolution. The baseline-normalized power was measured by averaging time-frequency power matrices across stimulus

presentations, measuring mean baseline power for each frequency, and calculating the dB change from baseline due to the stimulus. We measured inter-trial phase clustering (Cohen, 2014; phase-locking factor: Tallon-Baudry et al., 1996), which quantifies the consistency of the responses across trials, by extracting the phase time-series for each frequency during each stimulus presentation, and calculating the average vector, plotted on the unit circle, at each time-frequency point.

Correlations of resting gamma power with N1 amplitude

To examine associations between resting gamma power and N1 amplitude in individual mice, Spearman correlations were calculated for low and high gamma with N1 amplitude values for mice from each age group. The N1 amplitudes and gamma power values recorded from the AC and FC are shown as ratios of the 3mo group mean values. Least-squares trendlines were calculated with the "polyfit" function in MATLAB.

Amplitude-Modulated Chirp Stimulus (swept-frequency AM noise)

To analyze how temporal fidelity of responses to dynamic stimuli changed with age, we used a 'chirp' stimulus (Lovelace et al., 2018; Purcell et al., 2004). The chirp stimulus allows a quantification of the fidelity with which neural generators synchronize responses to a time varying auditory stimulus. The stimulus consisted of sinusoidally amplitude modulated broadband noise, for which the frequency of modulation was increased from 1 to 100 Hz over the course of 2 seconds. A 500 ms broadband noise ramp was presented immediately before the chirp stimulus onset to avoid confounding

the chirp response with an onset response. The stimulus was repeated 300 times, with an inter-stimulus interval of 1 second.

Statistical Analysis of Auditory Responses

To compare the responses across age-groups, a non-parametric permutation test was used, to find clusters of significant values (Maris & Oostenveld, 2007). First, a t-test was run on each time-frequency point for the two groups being compared, yielding the T-values for each TF point. T-values corresponding to $p<0.025$ were considered significant. Clusters of significant T-values were found and their area was measured. Next, the group assignments were shuffled randomly, and the t-tests and cluster-measurements were run again on the surrogate groups. This was performed 2000 times to generate a distribution of cluster sizes that we would expect to find by chance. In the original comparison, clusters that were larger than 95% of the surrogate clusters were considered to be significant. This method allows for the discovery of significant differences between groups without performing hundreds of thousands of comparisons, and without making assumptions about normality or homogeneity of variance between groups.

Results

We recorded EEG signals from auditory and frontal cortex (AC and FC) at three different ages in freely moving C57BL/6J mice. The hypotheses tested were, 1) old mice have reduced power in the gamma band of neural oscillations in both AC and FC, 2) old mice show reduced movement-related modulation of EEG oscillations. Both hypotheses

were based on the findings of declining PV neuron density and PNNs in aging C57BL/6J mice.

Resting EEG power shows frequency- and region-specific decreases with age

Figure 2.1 shows the resting EEG power in each frequency band (from theta to high frequency oscillations) in each age group as a ratio of power in the 3 mo group. These analyses are for the entire 5 minutes of resting EEG, regardless of movement state. Kruskal-Wallis one-way analysis of variance tests were used to measure differences among group means, and Dunn-Bonferroni tests were used to examine pairwise comparisons. The p-values obtained from the Kruskal-Wallis tests were multiplied by 6 to correct for the number of frequency-band comparisons (corrected p-values exceeding 1 were set to 1). Pairwise comparisons for bands that showed significant K-W p-values prior to correction for multiple comparisons are shown. The full results of the statistical analyses are shown in Table 2.1. In the AC (left column), there is an age-related decline in alpha ($H=10.081$, $p=0.036$), beta ($H=12.439$, $p=0.012$), and low-gamma power ($H=13.761$, $p=0.006$), with the young and old groups showing significant differences (alpha: $p=0.004$, beta: $p=0.001$, low-gamma: $p=0.001$, high-gamma: $p=0.018$). In the FC (right column), resting EEG power was decreased in the alpha ($H=9.454$, $p=0.054$) and high-frequency oscillation bands ($H=11.427$, $p=0.018$). Taken together, these data indicate frequency-, age- and region-specific changes in the absolute power of resting EEG.

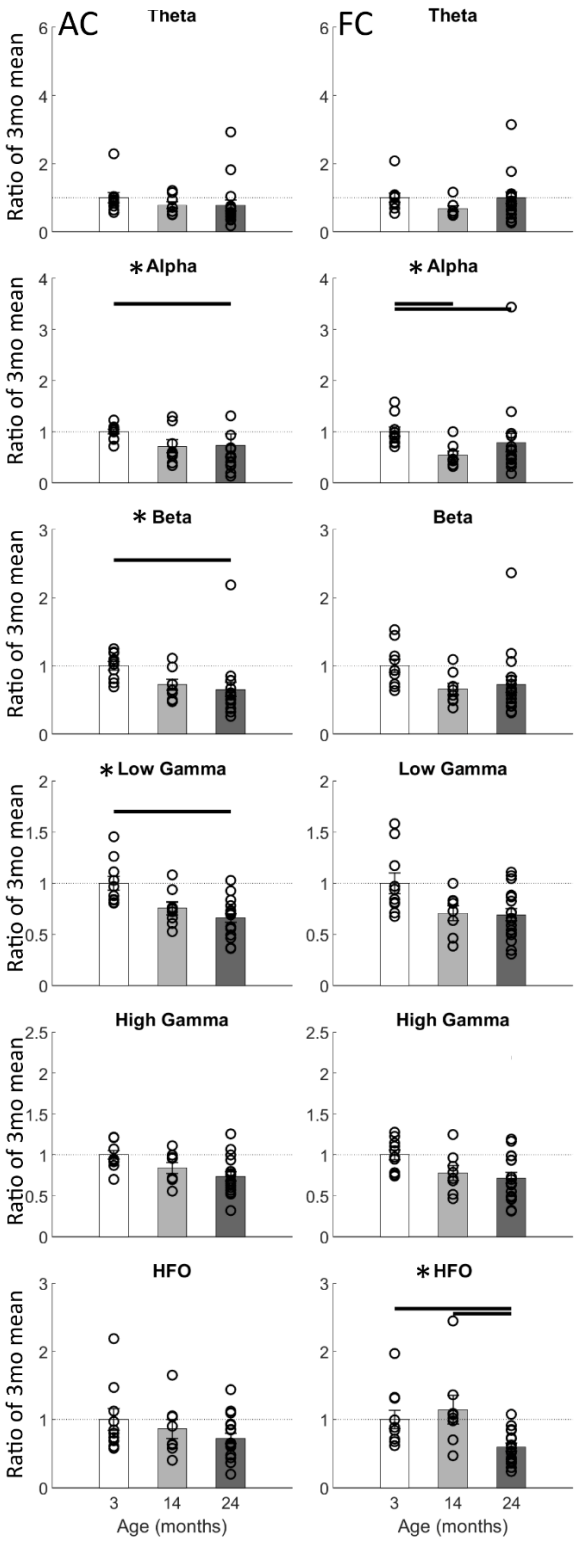

Figure 2.1: Resting EEG power in several frequency bands decreases with age in a cortical region-specific manner. Five minutes of resting EEG data was recorded from electrodes implanted in the auditory (left column) and frontal (right column) cortices (AC and FC). Average power was calculated within canonical frequency bands and expressed as a ratio of corresponding spectral band power in the 3mo old group. Ratios higher than 1 indicate increase compared to 3mo mice and values below 1 indicate an age-related decrease. There is a general reduction of absolute EEG power from 3mo to 24mo, which is most pronounced in the alpha, beta and low-gamma range in the AC, and alpha, beta and high frequency oscillations in the FC. There was no band of power that showed any increase with age. * denotes a significant Bonferroni-corrected p-value obtained from K-W tests; black lines represent significant Dunn-Bonferroni post-hoc pairwise comparisons.

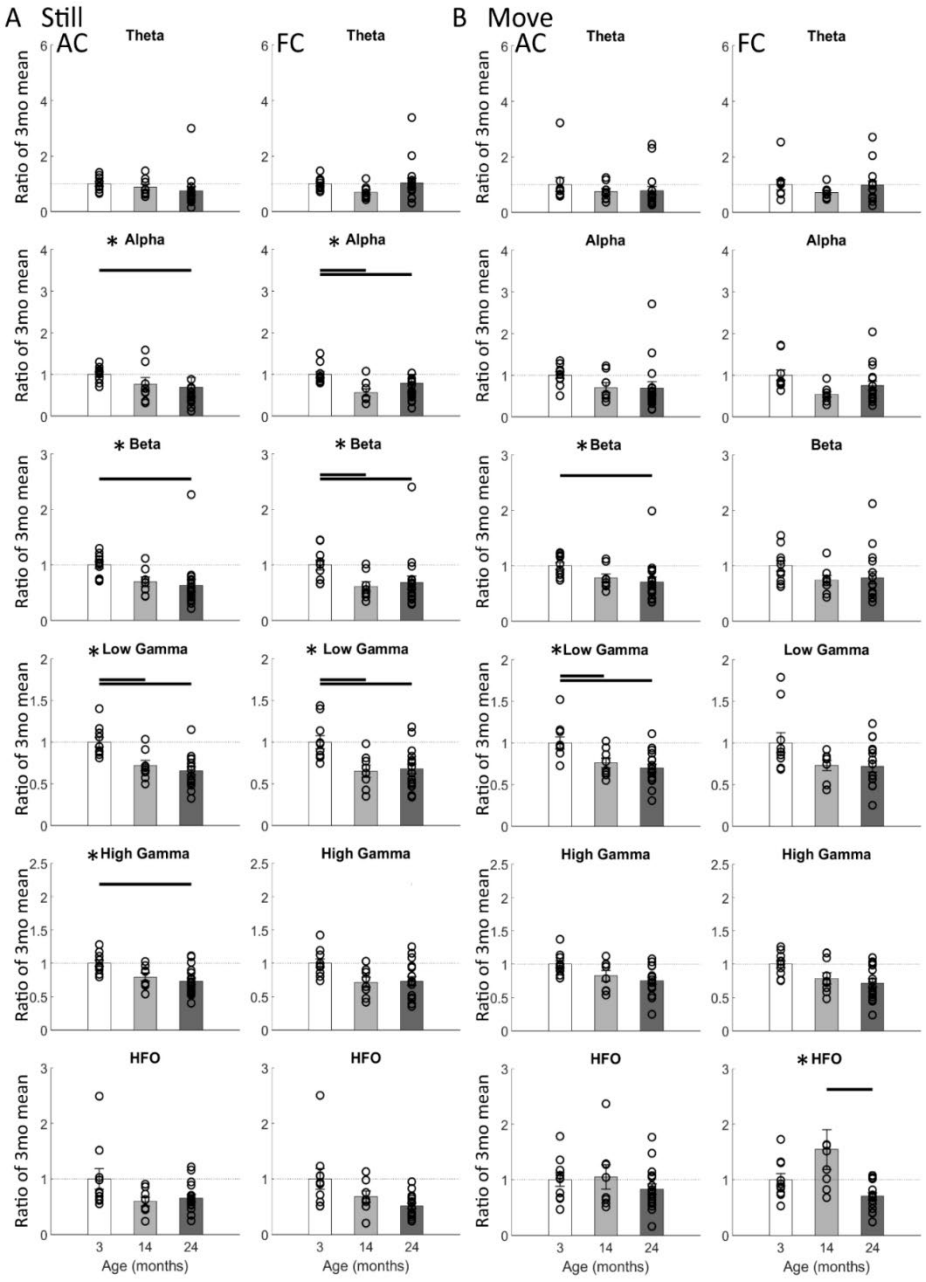

Figure 2.2. Frequency- and movement-specific decrease in resting EEG power with age. Spectral power in each band and age is represented as ratio of corresponding spectral power in the 3mo group (as in Figure 2.1). While the mice were still (**A**), theta, alpha, beta, low gamma, and high gamma power in the AC are all lower in 24mo mice compared to 3mo mice. In the FC, alpha and high frequency oscillation power are lower in the old mice compared to the young mice. (**B**) During movement, old mice show decreased low gamma and high gamma power in the AC compared to young mice. In the FC, 14mo mice have lower alpha power compared to 3mo mice, and 24mo mice have lower HFO power compared to 14mo mice.

Given the significant age-related decrease in absolute AC gamma power, we determined whether the relative gamma power (gamma power as a percentage of overall power) showed age-related changes. Relative power was calculated by dividing the summed power within low- and high-gamma bands by the sum of power across the frequency spectrum and then compared across age groups. Relative low- or high- gamma power was not different across age groups ($p>0.05$ for Kruskal-Wallis tests). This indicates that gamma band does not represent a relatively lower percentage of the overall power spectra in the aged mice compared to young mice, but instead shows a decline in absolute power.

Figure 2.2 and Table 2.1 show the results for resting EEG power with age after the data were classified according to movement states (still *versus* move). Figure 2.2 (as in Figure 2.1) shows the power in canonical EEG bands as a ratio of power in the 3 mo group. When mice were still (Figure 2.2, first 2 columns), EEG power declined significantly between the 3 mo and 24 mo groups in every frequency band in the AC except for theta and high frequency oscillations (Figure 2.2, 1st column; alpha: $H=13.128$, $p=0.006$, beta: $H=12.992$, $p=0.012$, low-gamma: $H=15.024$, $p=0.006$, high-gamma: $H=9.849$, $p=0.042$). In the FC (Figure 2.2, 2nd column), significant decline in power was seen for the alpha ($H=11.379$, $p=0.018$), beta ($H=9.872$, $p=0.042$), and low-gamma ($H=10.109$, $p=0.036$) bands. These data are mostly similar to those observed when the entire 5 minutes of resting EEG was analyzed (Figure 2.1). When the mice were moving (Figure 2.2, 2 right columns), only the beta ($H=10.749$, $p=0.030$) and low-gamma ($H=10.879$, $p=0.024$) bands showed a significant decline with age in the AC

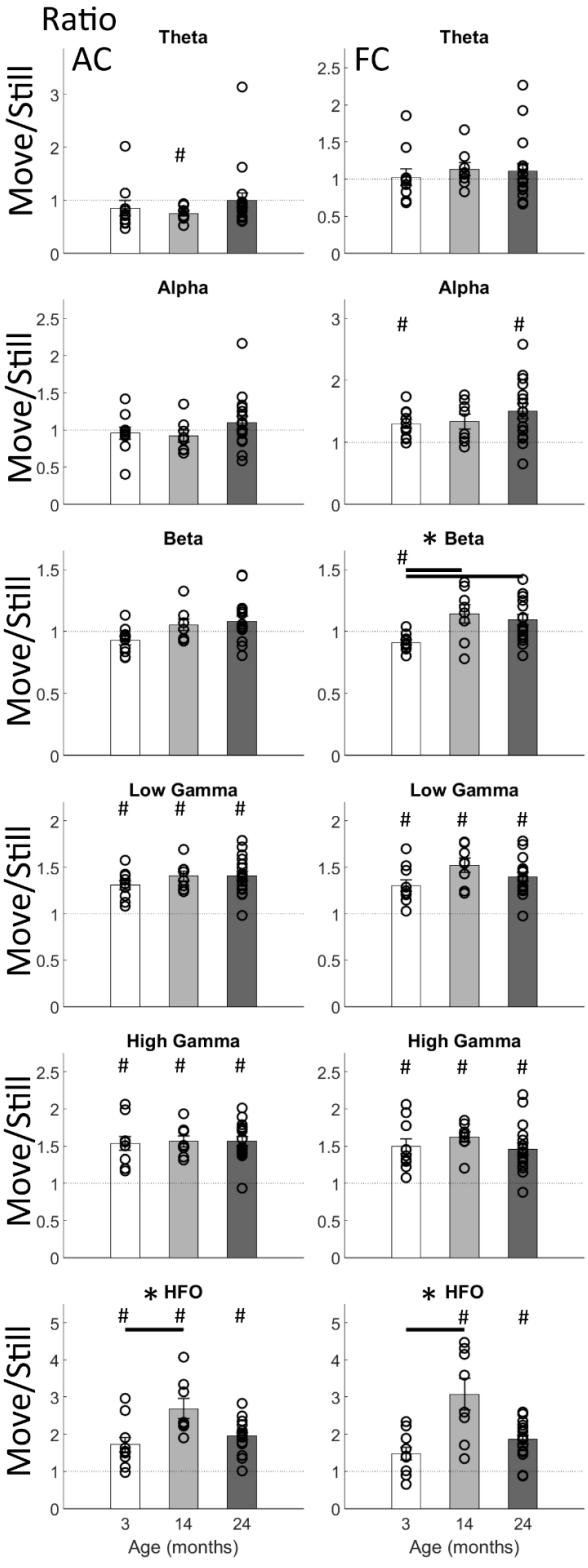

Figure 2.3. The ratio of power between the movement and still conditions shows age-related changes. The power during movement was divided by the power during still periods to calculate the effect of movement on power. The move:still ratio is shown for both AC (left column) and FC (right column). The movement-related modulation of beta power changes from a decrease (ratio < 1) to an increase (ratio > 1) between 3mo and 14mo and is significantly higher in 24mo compared to 3mo mice. Low gamma, high gamma, and HFO power are increased during movement for all age groups. Low gamma power modulation is increased from 3mo to 12mo in the FC. In the AC and FC, HFO power is modulated to a greater degree in 14mo mice compared to 3mo and 24mo mice.

(Figure 2.2, 3rd column). In the FC, the high frequency oscillations declined between 14 and 24 mo (Figure 2.2, 4th column, H=10.847, p=0.024), but no other age-related differences were seen. These data show that most of the EEG declines observed with age primarily affected the AC, compared to the FC, and were more robust when the mice were still.

Movement-related modulation of EEG power across age groups

Given that age-related changes in cortical EEG power are different for movement states (Figure 2.2), we examined the ratio of power between movement and still conditions within each age groups (Figure 2.3 and Table 2.1). The power during movement was divided by the power during still periods to calculate the effect of movement on power. The theta and alpha frequency bands do not show movement related modulations in power. This is shown quantitatively in Table 2.1, which contains p-values from 1-sample t-tests, comparing the ratio distributions against a normal distribution with a mean of 1. The p-values are Bonferroni-corrected for six comparisons. A significant p-value means that the move:still ratios are significantly different from 1 and that there is a significant modulation of that frequency band by movement. These significant modulations are represented in Figure 2.3 as '#' signs. Examination of the 3 mo data in the AC (Figure 2.3, left column) and FC (Figure 2.3, right column) shows that the ratio of

low- and high-gamma power and high frequency oscillations is greater than 1, indicating the power in these bands increased with movement. This is shown quantitatively in Table 2.2. With age, and contrary to our hypothesis, there was no decrease in the modulation of gamma band power by movement. The ratio of power between movement and still

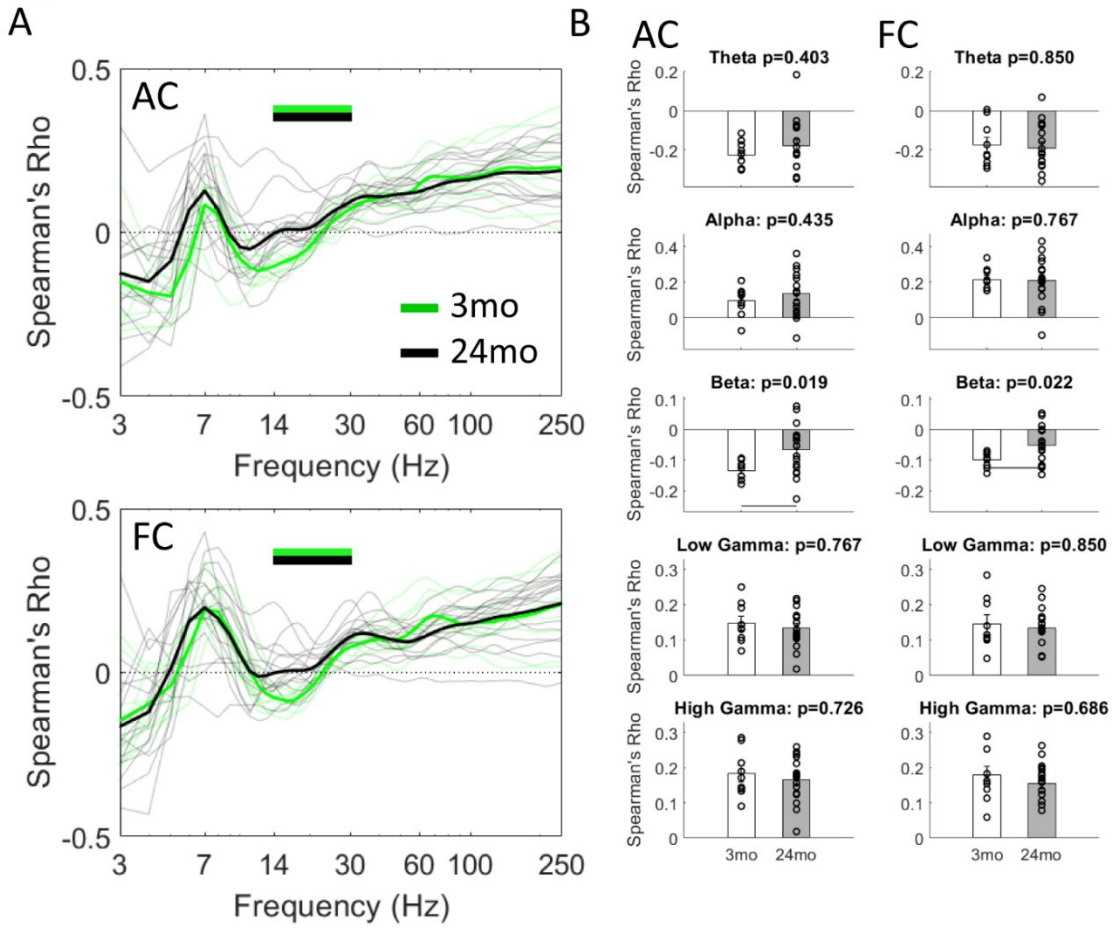

Figure 2.4. The correlation of velocity with EEG spectral power shows decreased modulation of cortical activity by movement. (**A**) The correlation of velocity with spectral power from a Morlet wavelet transform shows a distinct frequency-specific pattern. (**B**) Canonical EEG frequency bands show differences in modulation by movement. The theta and beta bands are negatively correlated with velocity, whereas the alpha, low gamma, and high gamma bands are positively correlated with velocity. In young mice (3mo), beta power is negatively correlated with velocity. In old mice (24mo), the correlation is significantly weaker.

conditions in the low and high gamma bands did not change with age in the AC. In both AC and FC, there was an increase in the move:still ratio of high frequency oscillation power from young to middle age. Overall, we interpret these results to indicate that movement related modulation of cortical resting EEG activity does not decrease with age in either AC or FC.

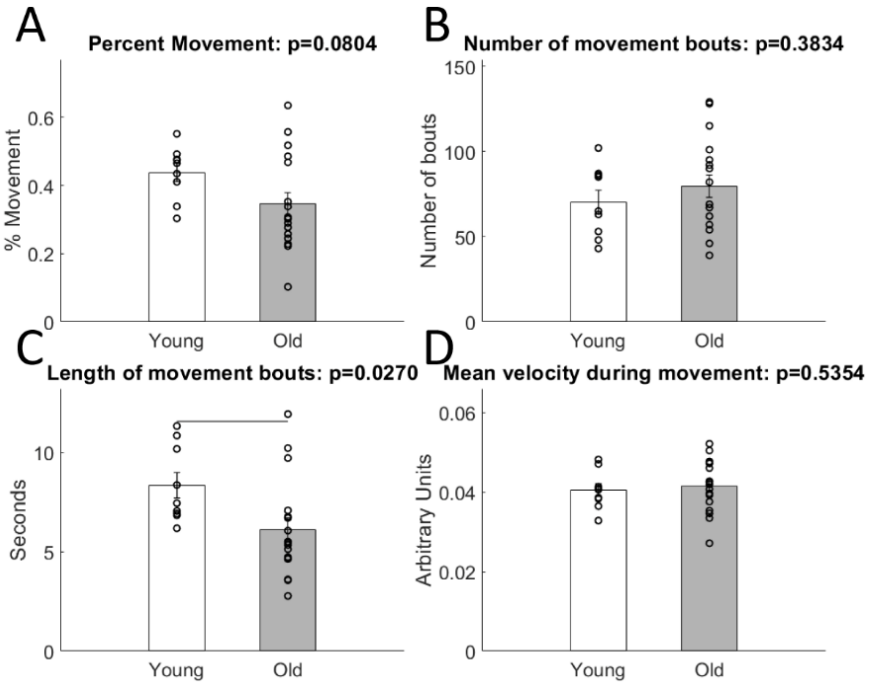

Figure 2.5. Analysis of movement characteristics shows few changes in ambulation properties between age groups. Young and old mice do not show differences in percentage of time moving (**A**), number of movement bouts (**B**), or average movement velocities (**D**). When moving, however, the movement bouts of young mice last longer than those of old mice (**C**).

Movement speed alters EEG power in different frequency bands and areas of the brain (Niell & Stryker, 2010; Polack et al., 2013; Schneider et al., 2014; Schneider & Mooney, 2018; Zhou et al., 2014). Therefore, we quantified the correlation of speed with EEG spectral power across age groups (Figure 2.4). The correlations between movement speed and EEG power across bands show a similar pattern in the AC and FC. The theta and beta bands are negatively correlated with speed, whereas the alpha, low gamma, and high gamma bands are positively correlated with speed. However, with age, there was only one frequency band that showed a difference in the correlation between movement speed and EEG power, with AC and FC beta band correlations showing a decrease in the old mice. Because movement properties may explain age-related change in the correlation between EEG power and speed, we next compared the ambulatory properties between the 3 and 24 mo old groups (Figure 2.5). The average velocity, percentage of time spent moving, average movement bout length, and number of movement bouts were calculated for each mouse. Young and old mice do not have different average movement speeds ($p=0.53$) or different number of movement bouts ($p=0.38$) nor do they move for a different percentage of time during the recording ($p=0.080$). However, when young mice move, their movement bouts last longer than those of old mice ($p=0.027$). Our overall interpretation is that movement speed influences EEG band power in a frequency-specific manner, but these correlations are affected by aging only in the beta band. In particular, movement-related influences on gamma band power are not reduced with age.

ERP spectral (gamma) power is enhanced with age, but temporal processing declines.

Young (3mo) and old (24mo) mice were presented with broadband noise bursts and AM chirps. The sounds were presented at 70 dB SPL to the young mice and 90 dB SPL to the old mice, to account for age-related hearing loss. The grand average ERPs for the young and old groups are shown within the time-frequency plots in Figure 2.6B. ERP component analyses statistics are provided in Figure 2.6A and Table 2.3. In the AC, there was a significant increase in N1 amplitude and P1 latency in the old mice. In the FC, N1 latency was significantly longer in the old mice, and a trending increase in N1 amplitude.

When a time-frequency analysis was carried out on the ERPs, an increase in total evoked and ongoing power was observed in the old group. The ERPs were transformed to the time-frequency domain using a wavelet transform (Figure 2.6B). The heatmaps in Figure 2.6B show baseline-normalized power, where red hues represent an increase from baseline, and blue hues represent a decrease from baseline. Significant differences between the age groups were found using a non-parametric permutation testing approach. In both the AC and FC, there is an increase in onset response in the old mice shown as contours in the bottom row. There is also a longer-latency increase in gamma power following the noise stimulus. Taken together, these data show enhanced total gamma band power in the ERPs in the old group compared to the young group. There were no significant differences in lower frequency bands, indicating a specific gamma band change with age.

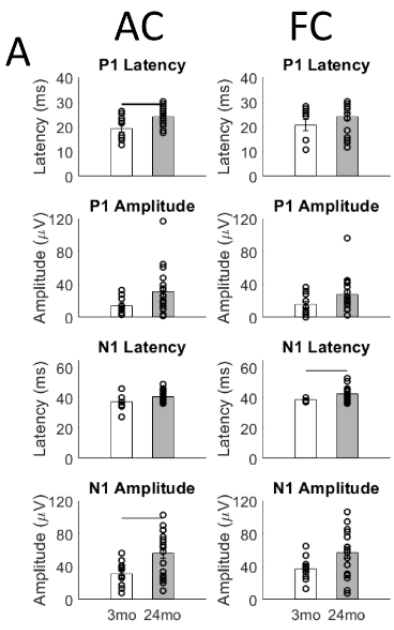

Figure 2.6. ERP N1 amplitude and gamma power is increased with age. Young (3mo) and old (24mo) mice were presented with broadband noise bursts at 70 dB SPL and 90 dB SPL, respectively. (**A**) Analysis of latency of amplitude of individual ERP components show that old mice had higher N1 amplitude and longer P1 latencies in AC (top row). Old mice showed longer N1 latencies in FC (bottom row). Full statistical analyses are shown in Table 2.3. The grand averaged ERPs are shown in (**B**). (**B**) The heatmaps show baseline-normalized power, where red hues represent an increase from baseline, and blue hues represent a decrease from baseline. Significant differences between the age groups were found using a non-parametric permutation testing approach. In both the AC and FC, there is an increase in onset response in the old mice. In the AC, there is also a longer-latency increase in gamma power following the noise stimulus.

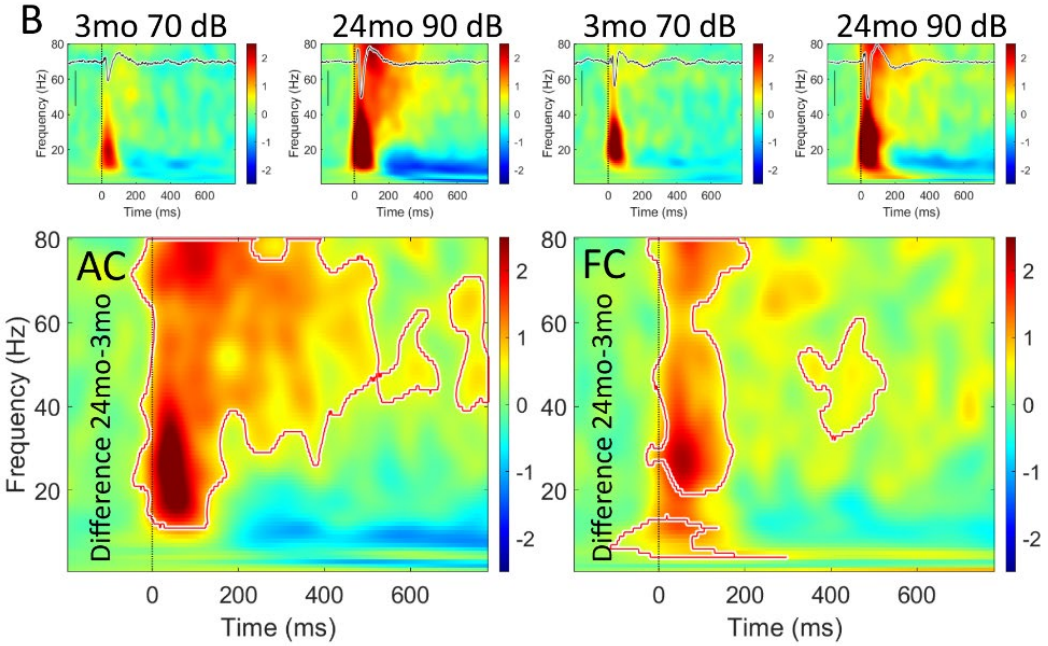

To examine the relationships between evoked responses and resting power in the low gamma band, Spearman correlations of ERP N1 amplitude and low gamma power were calculated. Figure 2.7 shows the relationships between these values for young and

old mice, with resting power values shown as ratios of younger group's mean values, as in Figures 2.1-2.2. In the young group, there was a trend for a negative correlation between N1 amplitude and low gamma power in the AC (rho=-0.60, p=0.067, thick black trendline). No other correlations between gamma power and N1 amplitude approached significance. These data suggest that potentially different mechanisms underlie the synchrony related to ERP N1 amplitude compared to gamma oscillations.

To develop an EEG-based method to examine age-related changes in temporal processing, the consistency of responses to AM chirp stimuli was calculated as inter-trial phase clustering (ITPC, Figure 2.8). Despite the strong ERPs to auditory stimuli in old mice, both AC and FC showed a significant reduction in ITPC to the chirp stimuli, even though the sounds were presented at 90 dB for the old mice. These data indicate that trial-to-trial phase locking to the AM chirp stimulus is more variable in the old group compared to the young.

Discussion

This study examined resting and sound evoked EEG responses in the C57BL/6J mice, a commonly used strain for studying age-related hearing loss. We identified a number of novel response measures to examine age-related changes in neural oscillations and temporal processing in awake and freely moving mice. Comparison of young and old

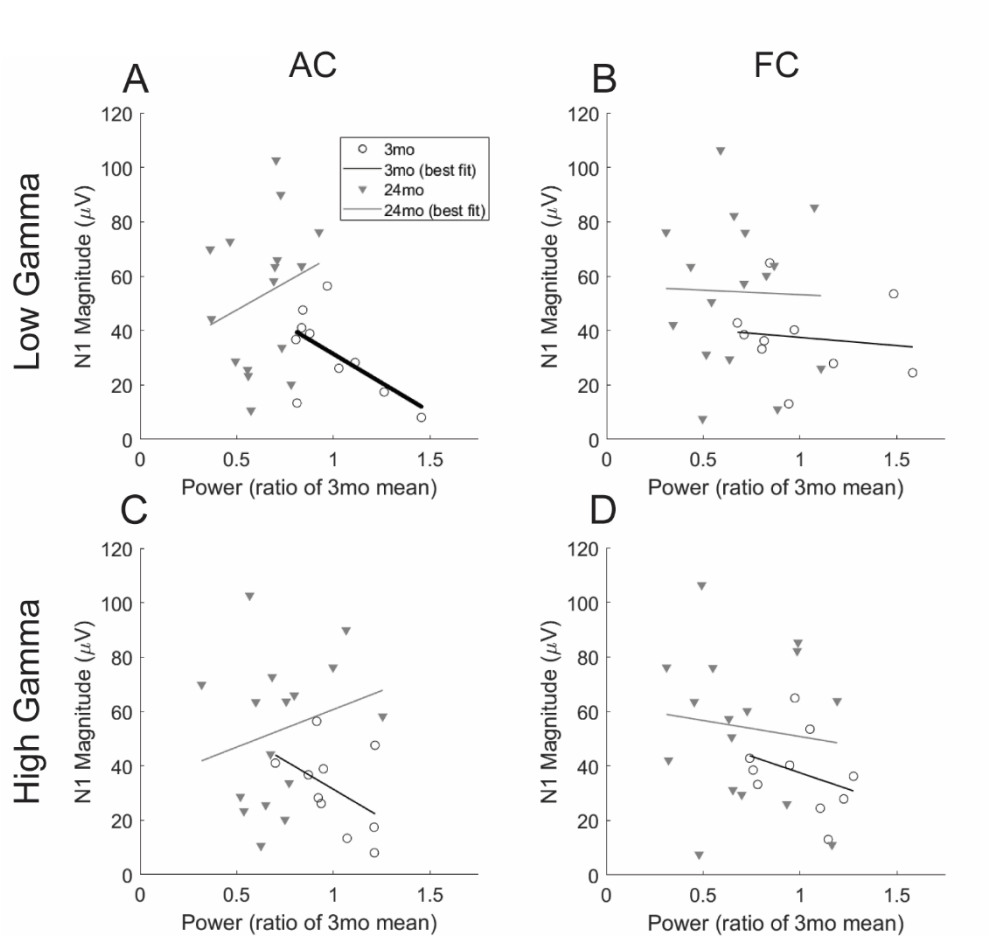

Figure 2.7. ERP N1 amplitudes are not correlated with gamma power. The relationship between N1 amplitudes and gamma power values were examined using Spearman's correlation coefficient. Gamma power values are each shown as ratios of the mean values for the 3mo group. The top row (**A** & **B**), show the relationships between low gamma power (still and move combined) and N1 amplitude for the young (triangles open black circles) and old mice (filled gray), in the AC and FC, respectively. The bottom row (**C** & **D**), show the relationships between high gamma power and N1 amplitude, in AC and FC, respectively. There is a marginally significant negative relationship (rho=-0.60, p=0.067) between low gamma power and N1 amplitude in the 3mo age group (thick black trendline), showing that higher resting low gamma power may be associated with lower N1 amplitudes. None of the other correlations approach significance (thin trendlines).

mice reveal the following key findings: 1) resting EEG alpha, beta and low gamma band power declines with age in the AC, and less robustly in FC, 2) movement increases low and high gamma band power (compared to still) in both young and old mice, but there is no difference in movement-related modulation of gamma band power with age, 3) movement speed is correlated with power in different frequency bands, but these correlations show age-related change only in the beta band, 4) ERP N1 amplitude and onset and long-latency gamma band power in ERP increases with age in both AC and FC, and 5) ITPC for AM chirps declines with age. Taken together, our data provide novel insights into frequency, cortical region and movement-specific changes in resting and evoked neural oscillations. These changes in neural oscillations may be correlates of sensory-perceptual declines in speech processing with age and may provide a number of objective physiological biomarkers of cortical processing in presbycusis.

Neural oscillations are related to specific sensory and cognitive processes and behavioral states. One major finding of this study is that the power of gamma band oscillations in resting EEG (Figures 2.1-2.2), and ITPC in the gamma range for the chirp stimuli (Figure 2.8) are reduced with presbycusis in the auditory cortex. Gamma oscillations are linked with sensory processing and cognitive functions such as attention and memory. Timing of spikes with respect to the phase of the gamma oscillations may provide temporal precision in sensory encoding. The phase of an ongoing oscillation becomes less reliable if the amplitude of the oscillation is reduced. The decrease in resting and entrained gamma power in the cortex of the C57BL/6J mice may underlie age-related decline in sensory encoding and fidelity of responses to repeated stimulation.

The decline in gamma power is consistent with the role of PV cells in generating this rhythm (Cardin et al., 2009; Sohal et al., 2009; Volman et al., 2011), and the loss of cortical PV expression with age (Brewton et al., 2016; Martin del Campo et al., 2012; Ouda et al., 2008; Ouellet & de Villers-Sidani, 2014). Optogenetic activation of fast spiking (putative PV neurons) inhibitory interneurons with periodic light stimulus was more effective in eliciting gamma oscillations than activation of pyramidal neurons (Cardin et al., 2009). Each cortical PV neuron provides synchronized inhibition to multiple pyramidal cells (Packer & Yuste, 2011). The PV neurons themselves are connected to each other via gap junctions (Hestrin & Galarreta, 2005). This neural architecture combined with the ~25 msec spike interval for fast spiking neurons have been suggested to give rise to synchronized output of population of pyramidal cells at ~40 Hz (Hasenstaub et al., 2005). The EEG reflects synchronized signals in the apical dendrites of such pyramidal cells (Kirschstein & Köhling, 2009). GABAergic signaling generally, and PV neuron density more specifically, declines in aging rodent and human brain (Caspary et al., 1999, 2008, 2013; Ling et al., 2005; Raza et al., 1994; Richardson et al., 2013). Loss of PV cell function is also exacerbated by the loss of perineuronal nets (PNNs), a specialized assembly of extracellular matrix components that mostly target PV cells and increase their excitability (Wen et al., 2018).

Cortical EEG spectral power shows frequency and region specific modulation by movement, consistent with data in humans (Ball et al., 2008; Cheyne et al., 2008). Across all age groups, movement increased low and high gamma power and high frequency oscillations, but not for the lower frequencies. At both cortical and midbrain levels,

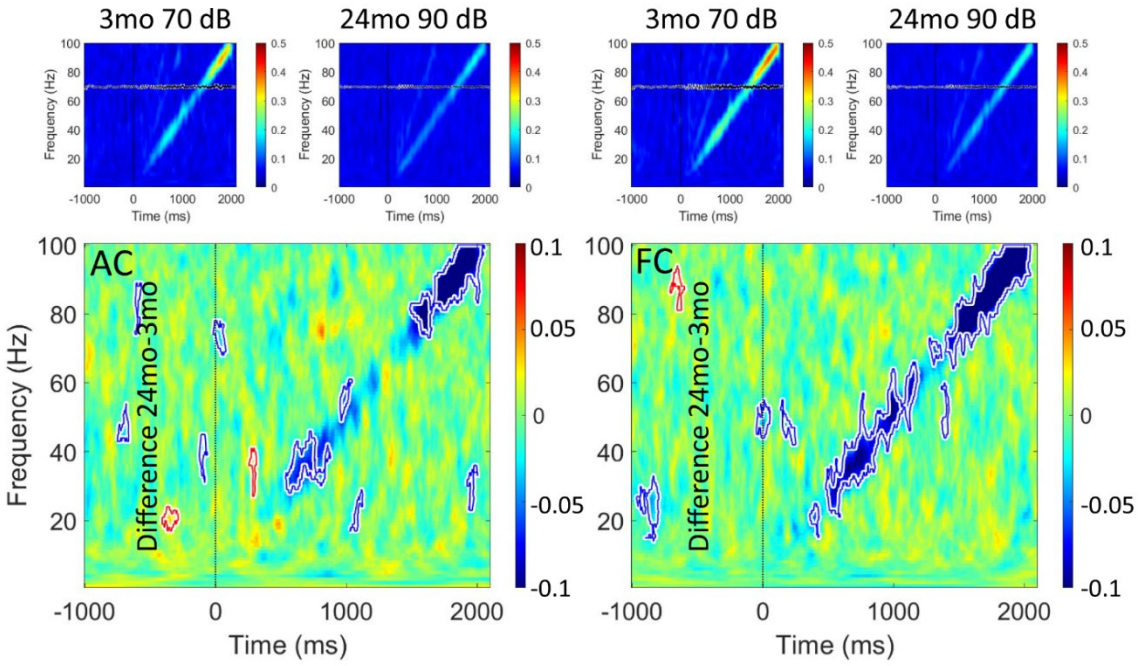

Figure 2.8. Temporal processing declines with age. Young (3mo) and old (24mo) mice were presented with amplitude modulated chirps. The responses were transformed to the time-frequency domain using a dynamic complex Morlet wavelet transform. The consistency of responses to AM chirp stimuli is calculated as inter-trial phase clustering (ITPC). In the AC and FC, responses recorded from old mice are less consistent in the low gamma and high gamma frequency ranges.

movement alters auditory neurons' spontaneous and evoked responses (Schneider et al., 2014). Tone driven activity in the auditory cortex mostly decreases with movement. In the auditory cortex, this effect is driven by connections between the secondary motor cortex and auditory cortex PV neurons. Because of this link, and the loss of PV neurons with age, we hypothesized that movement related modulation of resting EEG gamma power would be altered with age. Across all age groups we found that gamma power was indeed increased during movement compared to still. However, movement-related modulation of gamma power was not different across the age groups. This may be

because of overall decrease in gamma power in both still and move conditions in the older animals. There was also correlation between movement speed and EEG spectral band power with theta and beta bands showing negative correlation with speed, and with alpha and gamma power showing positive correlations. The only significant age-related change occurred in the beta power – speed correlations in the auditory and frontal cortices. Movement speed itself was not different between the young and the old mice. Taken together, these data indicate that movement modulates EEG power in the gamma band, but this modulation is not significantly altered in presbycusis.

In addition to changes in gamma power, we observed a decline in alpha and beta band power with age (Figures 2.1-2.2). Alpha power and peak alpha frequency decline with age in humans (Chiang et al., 2011; Harris & Dubno, 2017). Decline in alpha power and subsequent reduction in reliable phase estimation with age is predicted to affect stimulus detection thresholds and reaction times (Samuel et al., 2018; VanRullen et al., 2011), which can lead to difficulties with speech recognition in noise. The reduced alpha power may also mark elevated cortical load or arousal levels (Barry et al., 2007) and changes in cerebral perfusion (Cook et al., 1998) in the old mice (reviewed in Bazanova & Vernon, 2014). Power fluctuations in the EEG beta band are related to motor performance and sensorimotor integration in humans (Feurra et al., 2011). The decrease in correlation between speed and beta power in both AC and FC may be a readout of the age-related changes in motor and sensorimotor functions.

Consistent with visual and auditory ERP data in aging humans (Finnigan et al., 2011; Karayanidis et al., 1995), N1 amplitude of ERP is increased in older mice perhaps

reflecting reduced inhibition in cortex with age. While the sound level used in the older mice was 20 dB louder than that used for young mice, the level relative to hearing level is likely to have been lower for the old mice. Click-evoked ABR thresholds in 24 mo C57 mice are at least 30 dB higher than 3 mo old mice (Trujillo & Razak, 2013). Therefore, when relative sound levels are considered the observed increase in N1 amplitude may be an under-estimate.

Time frequency analyses reveal two type of gamma oscillations following a stimulus (Galambos, 1992; Pantev, 1995; Pfurtscheller & Lopes da Silva, 1999). Evoked gamma, occurring within 100 msec of sound onset is phase locked to the stimulus. Induced gamma, occurs with longer latency in the 150-400 msec window following sound onset, is not phase locked to the stimulus (Brosch et al., 2002; Crone et al., 2001; Franowicz & Barth, 1995; Jeschke et al., 2008). We observed both evoked and induced gamma oscillations following broadband noise stimulus in young and old mice (Figure 2.6), with the same time course and frequency ranges observed in the macaque and rat cortex (Brosch et al., 2002; Franowicz and Barth, 1995). The power of both components was increased in aged mice revealing a novel marker of age-related change in auditory processing. Using a cortical slice preparation, Metherate & Cruikshank (1999) showed that thalamic stimulation caused an early glutamatergic potential in the input layer. This was followed by gamma-band fluctuations driven by polysynaptic activity. This long latency gamma band activity was dominant in the middle and superficial layers and propagated intracortically. This may facilitate formation of transient neural assemblies by synchronizing activity across rapidly changing pools of neurons. The hearing loss in C57

mice starts by affecting high-frequencies and subsequently incorporates lower frequencies. The cortical tonotopic representation in C57 mice is plastic, with the majority of neurons responding to low frequencies following loss of high-frequency hearing (Trujillo & Razak, 2013; Willott et al., 1993). This renders the cortex more homogeneous in terms of frequency representation as the mouse ages. Broadband noise stimulus may incorporate more neurons with similar tuning into the synchronized ensemble of cells potentially leading to the higher power in induced gamma oscillations in the old mice.

Based on the chirp ITPC data, there was a robust decrease in the fidelity of temporal synchronization with age. Accuracy in temporal processing is important in fundamental functions of the auditory system including sound localization using binaural cues and discrimination of amplitude and frequency modulations in behaviorally relevant sounds. These functions aid speech perception, and the age-related decline in speech processing may arise from changes in temporal processing (Gordon-Salant et al., 2011; Mazelová et al., 2003; Tremblay et al., 2002). The deficits become more apparent when task is made more difficult by either decreasing the modulation depth or increasing the modulation rate (Clinard & Cotter, 2015; Parthasarathy & Bartlett, 2012, 2011; Trujillo & Razak, 2013). These effects are seen at multiple levels of the auditory system.

Conclusions

The major contribution of our study is the identification of a broad range of EEG phenotypes of declining temporal processing and altered sensory fidelity. These EEG

phenotypes facilitate the development of hypotheses regarding circuit level changes (e.g., PV neuron and gamma power decrease) as well as specific sensory and cognitive functions (e.g., gamma and sensory encoding, attention). These studies also report for the first time how frequency, region and movement specific modulation of EEG power changes with age. These EEG based responses can be recorded from the scalp of humans (e.g., Harris & Dubno, 2017), providing the opportunity to using these age-related phenotypes as pre-clinical biomarkers in developing therapeutics that reverse or delay central auditory system changes.

All	Bonferroni-corrected p	K-W H	p	Dunn's Test z	p	Dunn's Test z	p	Dunn's Test z
AC	Main Effect of Age		**3mo-14mo**		**3mo-24mo**		**14mo-24mo**	
Theta (3-7 Hz)	1.000	5.541						
Alpha (8-13 Hz)	**0.036**	**10.081**	0.260	-8.325	**0.004**	**-12.965**	0.873	4.640
Beta (14-29 Hz)	**0.012**	**12.439**	0.109	-10.175	**0.001**	**-14.359**	1.000	4.184
Low Gamma (30-59 Hz)	**0.006**	**13.761**	0.079	-10.800	**0.001**	**-15.094**	0.985	4.294
High Gamma (60-100 Hz)	0.132	7.613	0.669	-5.925	**0.018**	**-11.212**	0.687	5.287
HFO (101-250 Hz)	1.000	2.322						
FC	Main Effect of Age		**3mo-14mo**		**3mo-24mo**		**14mo-24mo**	
Theta	0.894	3.809						
Alpha	**0.054**	**9.454**	**0.013**	-13.850	**0.039**	**-10.159**	1.000	-3.691
Beta	0.114	7.910	0.089	-10.575	**0.023**	**-10.876**	1.000	0.301
Low Gamma	1.000	5.854						
High Gamma	0.132	7.629	0.225	-8.650	**0.019**	**-11.165**	1.000	2.515
HFO	**0.018**	**11.427**	1.000	2.725	**0.034**	**-10.341**	**0.009**	**13.066**
Still								
AC	Main Effect of Age		**3mo-14mo**		**3mo-24mo**		**14mo-24mo**	
Theta	0.102	8.161	0.827	-5.300	**0.015**	**-11.506**	0.473	6.206
Alpha	**0.006**	**13.128**	0.208	-8.825	**0.001**	**-14.788**	0.524	5.963
Beta	**0.012**	**12.992**	0.098	-10.375	**0.001**	**-14.676**	0.983	4.301
Low Gamma	**0.006**	**15.024**	**0.022**	**-13.000**	**0.000**	**-15.500**	1.000	2.500
High Gamma	**0.042**	**9.849**	0.133	-9.775	**0.006**	**-12.694**	1.000	2.919
HFO	0.39	5.462						
FC	Main Effect of Age		**3mo-14mo**		**3mo-24mo**		**14mo-24mo**	
Theta	0.744	4.181						
Alpha	**0.018**	**11.379**	**0.009**	**-14.475**	**0.011**	**-11.924**	1.000	-2.551
Beta	**0.042**	**9.872**	**0.033**	**-12.350**	**0.011**	**-11.894**	1.000	-0.456
Low Gamma	**0.036**	**10.109**	**0.029**	**-12.575**	**0.010**	**-11.994**	1.000	-0.581

High Gamma	0.114	7.925	0.064	-11.200	**0.029**	**-10.582**	1.000	-0.618
HFO	0.066	9.062	0.723	-5.700	**0.009**	**-12.141**	0.428	6.441
Move								
AC	Main Effect of Age		**3mo-14mo**		**3mo-24mo**		**14mo-24mo**	
Theta	1.000	3.220						
Alpha	0.138	7.547	0.339	-7.700	**0.018**	**-11.200**	1.000	3.500
Beta	**0.030**	**10.749**	0.173	-9.225	**0.003**	**-13.365**	1.000	4.140
Low Gamma	**0.024**	**10.879**	**0.080**	**-10.775**	**0.004**	**-13.253**	1.000	2.478
High Gamma	0.156	7.335	0.354	-7.600	**0.021**	**-11.041**	1.000	3.441
HFO	1.000	1.096						
FC	Main Effect of Age		**3mo-14mo**		**3mo-24mo**		**14mo-24mo**	
Theta	1.000	1.981						
Alpha	0.156	7.281	**0.027**	**-12.675**	0.147	-8.035	0.873	-4.640
Beta	0.516	4.918						
Low Gamma	0.792	4.045						
High Gamma	0.090	8.453	0.177	-9.175	**0.012**	**-11.741**	1.000	2.566
HFO	**0.024**	**10.847**	0.940	4.900	0.100	-8.688	**0.006**	**13.588**
Ratio								
AC	Main Effect of Age		**3mo-14mo**		**3mo-24mo**		**14mo-24mo**	
Theta	1.000	2.309						
Alpha	1.000	2.671						
Beta	0.162	7.200	0.167	9.300	**0.027**	**10.653**	1.000	-1.353
Low Gamma	1.000	2.244						
High Gamma	1.000	0.090						
HFO	**0.048**	**9.600**	**0.006**	**14.975**	0.531	5.512	0.094	9.463
FC	Main Effect of Age		**3mo-14mo**		**3mo-24mo**		**14mo-24mo**	
Theta	1.000	1.975						
Alpha	1.000	1.675						
Beta	**0.048**	**9.769**	**0.022**	**13.000**	**0.016**	**11.382**	1.000	1.618
Low Gamma	0.390	5.465						
High Gamma	1.000	2.652						
HFO	**0.048**	**9.701**	**0.006**	**15.125**	0.375	6.265	0.131	8.860

Table 2.1. Full statistical results table for resting data analysis. Results of Kruskal-Wallis tests, corrected for multiple comparisons within each condition and each recording site, are shown. Pairwise Dunn-Bonferroni comparisons are shown for frequency bands for which a significant effect of age on power ($p<0.05$) was found.

AC	3mo	14mo	24mo
Theta Ratio	1.942	**0.008**	5.971
Alpha Ratio	3.674	1.924	1.576
Beta Ratio	0.339	1.866	0.423
Low-Gamma Ratio	**0.001**	**0.001**	**0.000**
High-Gamma Ratio	**0.002**	**0.001**	**0.000**
HFO Ratio	**0.035**	**0.002**	**0.000**

FC			
Theta Ratio	4.971	1.081	1.973
Alpha Ratio	**0.019**	0.147	**0.003**
Beta Ratio	**0.012**	0.632	0.223
Low-Gamma Ratio	**0.006**	**0.001**	**0.000**
High-Gamma Ratio	**0.006**	**0.000**	**0.000**
HFO Ratio	0.136	**0.012**	**0.000**

Table 2.2. Results of 1-sample t-tests on move:still ratio data. Distributions of move:still ratios were compared to normal distributions with a mean of 1, to determine whether power in each band was significantly modulated by movement. The p-values shown have been Bonferroni-corrected for comparisons across six frequency bands.

AC		M-W U	p
P1	Amplitude	54	0.61
	Latency	43.5	0.025
N1	Amplitude	138	0.021
	Latency	55.5	0.094
P2	Amplitude	56	0.103
	Latency	74.5	0.448
N2	Amplitude	92	0.924
	Latency	93.5	0.867

FC		M-W U	p
P1	Amplitude	53	0.076
	Latency	57.5	0.117
N1	Amplitude	128	0.068
	Latency	38	0.011
P2	Amplitude	79	0.598
	Latency	552	0.066
N2	Amplitude	104	0.502
	Latency	89	0.962

Table 2.3: Statistical results table for ERP component analysis. Results of Mann-Whitney U tests on ERP components are shown.

References

Anderson, S., Parbery-Clark, A., White-Schwoch, T., & Kraus, N. (2012). Aging affects neural precision of speech encoding. *The Journal of Neuroscience*, *32*(41), 14156–14164. https://doi.org/10.1523/JNEUROSCI.2176-12.2012

Ball, T., Demandt, E., Mutschler, I., Neitzel, E., Mehring, C., Vogt, K., Aertsen, A., & Schulze-Bonhage, A. (2008). Movement related activity in the high gamma range of the human EEG. *NeuroImage*, *41*(2), 302–310. https://doi.org/10.1016/j.neuroimage.2008.02.032

Barry, R. J., Clarke, A. R., Johnstone, S. J., Magee, C. A., & Rushby, J. A. (2007). EEG differences between eyes-closed and eyes-open resting conditions. *Clinical Neurophysiology*, *118*(12), 2765–2773. https://doi.org/10.1016/j.clinph.2007.07.028

Barsz, K., Ison, J. R., Snell, K. B., & Walton, J. P. (2002). Behavioral and neural measures of auditory temporal acuity in aging humans and mice. *Neurobiology of Aging*, *23*(4), 565–578. https://doi.org/10.1016/S0197-4580(02)00008-8

Bazanova, O. M., & Vernon, D. (2014). Interpreting EEG alpha activity. *Neuroscience and Biobehavioral Reviews*, *44*, 94–110. https://doi.org/10.1016/j.neubiorev.2013.05.007

Brewton, D. H., Kokash, J., Jimenez, O., Pena, E. R., & Razak, K. A. (2016). Age-related deterioration of perineuronal nets in the primary auditory cortex of mice. *Frontiers in Aging Neuroscience*, *8*, 270. https://doi.org/10.3389/fnagi.2016.00270

Brosch, M., Budinger, E., & Scheich, H. (2002). Stimulus-related gamma oscillations in primate auditory cortex. *Journal of Neurophysiology*, *87*(6), 2715–2725. https://doi.org/10.1152/jn.00583.2001

Burianova, J., Ouda, L., Profant, O., & Syka, J. (2009). Age-related changes in GAD levels in the central auditory system of the rat. *Experimental Gerontology*, *44*(3), 161–169. https://doi.org/10.1016/j.exger.2008.09.012

Cardin, J. A., Carlén, M., Meletis, K., Knoblich, U., Zhang, F., Deisseroth, K., Tsai, L. H., & Moore, C. I. (2009). Driving fast-spiking cells induces gamma rhythm and controls sensory responses. *Nature*, *459*(7247), 663–667. https://doi.org/10.1038/nature08002

Caspary, D. M., Holder, T. M., Hughes, L. F., Milbrandt, J. C., McKernan, R. M., & Naritoku, D. K. (1999). Age-related changes in GABA(A) receptor subunit composition and function in rat auditory system. *Neuroscience*, *93*(1), 307–312. https://doi.org/10.1016/S0306-4522(99)00121-9

Caspary, D. M., Hughes, L. F., & Ling, L. L. (2013). Age-related GABAA receptor changes in rat auditory cortex. *Neurobiology of Aging*, *34*(5), 1486–1496. https://doi.org/10.1016/j.neurobiolaging.2012.11.009

Caspary, D. M., Ling, L., Turner, J. G., & Hughes, L. F. (2008). Inhibitory neurotransmission, plasticity and aging in the mammalian central auditory system. *Journal of Experimental Biology*, *211*(11), 1781–1791. https://doi.org/10.1242/jeb.013581

Cheyne, D., Bells, S., Ferrari, P., Gaetz, W., & Bostan, A. C. (2008). Self-paced movements induce high-frequency gamma oscillations in primary motor cortex. *NeuroImage*, *42*(1), 332–342. https://doi.org/10.1016/j.neuroimage.2008.04.178

Chiang, A. K. I., Rennie, C. J., Robinson, P. A., van Albada, S. J., & Kerr, C. C. (2011). Age trends and sex differences of alpha rhythms including split alpha peaks. *Clinical Neurophysiology*, *122*(8), 1505–1517. https://doi.org/10.1016/j.clinph.2011.01.040

Clinard, C. G., & Cotter, C. M. (2015). Neural representation of dynamic frequency is degraded in older adults. *Hearing Research*, *323*, 91–98. https://doi.org/10.1016/j.heares.2015.02.002

Cohen, M. X. (2014). Analyzing neural time series data: theory and practice. *MIT press*.

Cook, I. A., O'Hara, R., Uijtdehaage, S. H. J., Mandelkern, M., & Leuchter, A. F. (1998). Assessing the accuracy of topographic EEG mapping for determining local brain function. *Electroencephalography and Clinical Neurophysiology*, *107*(6), 408–414. https://doi.org/10.1016/S0013-4694(98)00092-3

Crone, N., Boatman, D., Gordon, B., & Hao, L. (2001). Induced electrocorticographic gamma activity during auditory perception. *Clinical Neurophysiology*, *112*, 565–582. https://doi.org/10.1016/S1388-2457(00)00545-9

De Villers-Sidani, E., Alzghoul, L., Zhou, X., Simpson, K. L., Lin, R. C. S., & Merzenich, M. M. (2010). Recovery of functional and structural age-related changes in the rat primary auditory cortex with operant training. *Proceedings of the National Academy of Sciences of the United States of America*, *107*(31), 13900–13905. https://doi.org/10.1073/pnas.1007885107

Feurra, M., Bianco, G., Santarnecchi, E., del Testa, M., Rossi, A., & Rossi, S. (2011). Frequency-dependent tuning of the human motor system induced by transcranial oscillatory potentials. *Journal of Neuroscience*, *31*(34), 12165–12170. https://doi.org/10.1523/JNEUROSCI.0978-11.2011

Finnigan, S., O'Connell, R. G., Cummins, T. D. R., Broughton, M., & Robertson, I. H. (2011). ERP measures indicate both attention and working memory encoding decrements in aging. *Psychophysiology*, *48*(5), 601–611. https://doi.org/10.1111/j.1469-8986.2010.01128.x

Fitzgibbons, P. J., Gordon-Salant, S., & Friedman, S. A. (2006). Effects of age and sequence presentation rate on temporal order recognition. *The Journal of the Acoustical Society of America*, *120*(2), 991–999. https://doi.org/10.1121/1.2214463

Franowicz, M. N., & Barth, D. S. (1995). Comparison of evoked potentials and high-frequency (gamma-band) oscillating potentials in rat auditory cortex. *Journal of Neurophysiology*, *74*(1), 96–112. https://doi.org/10.1152/jn.1995.74.1.96

Frisina, R. D. (2009). Age-related hearing loss: ear and brain mechanisms. *Annals of the New York Academy of Sciences*, *1170*, 708–717. https://doi.org/10.1111/j.1749-6632.2009.03931.x

Galambos, R. (1992). A comparison of certain gamma band (40-Hz) brain rhythms in cat and man. In E. Baar & T. H. Bullock (Eds.), Induced Rhythms in the Brain, 201–216. *Birkhäuser Boston*. https://doi.org/10.1007/978-1-4757-1281-0_11

Gates, G., & Mills, J. (2005). Presbycusis. *Lancet*, *366*, 1111–1120. https://doi.org/10.1016/S0140-6736(05)67423-5

Gordon-Salant, S., Fitzgibbons, P. J., & Yeni-Komshian, G. H. (2011). Auditory temporal processing and aging: implications for speech understanding of older people. *Audiology Research*, *1*(1), 9–15. https://doi.org/10.4081/audiores.2011.e4

Gordon-Salant, S., & Fitzgibbons, P. J. (2001). Sources of age-related recognition difficulty for time-compressed speech. *Journal of Speech Language and Hearing Research*, *44*(4), 709-719. https://doi.org/10.1044/1092-4388(2001/056)

Harris, K. C., & Dubno, J. R. (2017). Age-related deficits in auditory temporal processing: unique contributions of neural dyssynchrony and slowed neuronal processing. *Neurobiology of Aging*, *53*, 150–158. https://doi.org/10.1016/j.neurobiolaging.2017.01.008

Harris, K. C., Mills, J. H., He, N. J., & Dubno, J. R. (2008). Age-related differences in sensitivity to small changes in frequency assessed with cortical evoked potentials. *Hearing Research*, *243*(1–2), 47–56. https://doi.org/10.1016/j.heares.2008.05.005

Hasenstaub, A., Shu, Y., Haider, B., Kraushaar, U., Duque, A., & McCormick, D. A. (2005). Inhibitory postsynaptic potentials carry synchronized frequency information in active cortical networks. *Neuron*, *47*(3), 423–435. https://doi.org/10.1016/j.neuron.2005.06.016

He, N., Dubno, J. R., & Mills, J. H. (1998). Frequency and intensity discrimination measured in a maximum-likelihood procedure from young and aged normal-hearing subjects. *The Journal of the Acoustical Society of America*, *103*(1), 553–565. https://doi.org/10.1121/1.421127

He, N., Mills, J. H., & Dubno, J. R. (2007). Frequency modulation detection: effects of age, psychophysical method, and modulation waveform. *The Journal of the Acoustical Society of America*, *122*(1), 467–477. https://doi.org/10.1121/1.2741208

Hestrin, S., & Galarreta, M. (2005). Electrical synapses define networks of neocortical GABAergic neurons. *Trends in neurosciences, 28*(6), 304-309. https://doi.org/10.1016/j.tins.2005.04.001

Hidalgo, J. L. T., Gras, C. B., Lapeira, J. T., Verdejo, M. Á. L., del Campo, J. M. D. C., & Rabadán, F. E. (2009). Functional status of elderly people with hearing loss. *Archives of Gerontology and Geriatrics, 49*(1), 88–92. https://doi.org/10.1016/j.archger.2008.05.006

Hogan, C. A., & Turner, C. W. (1998). High-frequency audibility: benefits for hearing-impaired listeners. *The Journal of the Acoustical Society of America*, *104*(1), 432–441. https://doi.org/10.1121/1.423247

Hopkins, K., & Moore, B. C. J. (2011). The effects of age and cochlear hearing loss on temporal fine structure sensitivity, frequency selectivity, and speech reception in noise. *The Journal of the Acoustical Society of America*, *130*(1), 334–349. https://doi.org/10.1121/1.3585848

Humes, L. E., Busey, T. A., Craig, J., & Kewley-Port, D. (2013). Are age-related changes in cognitive function driven by age-related changes in sensory processing?. *Attention, Perception, & Psychophysics*, *75*(3), 508-524. https://doi.org/10.3758/s13414-012-0406-9

Hunter, K. P., & Willott, J. F. (1987). Aging and the auditory brainstem response in mice with severe or minimal presbycusis. *Hearing Research*, *30*(2–3), 207–218. https://doi.org/10.1016/0378-5955(87)90137-7

Jeschke, M., Lenz, D., Budinger, E., Herrmann, C. S., & Ohl, F. W. (2008). Gamma oscillations in gerbil auditory cortex during a target-discrimination task reflect matches with short-term memory. *Brain Research*, *1220*, 70-80. https://doi.org/10.1016/j.brainres.2007.10.047

Johnson, K. R., Erway, L. C., Cook, S. A., & Willott, J. F. (1997). A major gene affecting age-related hearing loss in C57BL / 6J mice. *Hearing Research*, *114*, 83–92. https://doi.org/10.1016/S0378-5955(97)00155-X

Karayanidis, F., Andrews, S., Ward, P. B., & Michie, P. T. (1995). ERP indices of auditory selective attention in aging and Parkinson's disease. *Psychophysiology*, *32*(4), 335–350. https://doi.org/10.1111/j.1469-8986.1995.tb01216.x

Kirschstein, T., & Köhling, R. (2009). What is the source of the EEG? *Clinical EEG and Neuroscience, 40*(3), 146–149. https://doi.org/10.1177/155005940904000305

Ling, L. L., Hughes, L. F., & Caspary, D. M. (2005). Age-related loss of the GABA synthetic enzyme glutamic acid decarboxylase in rat primary auditory cortex. *Neuroscience, 132*(4), 1103–1113. https://doi.org/10.1016/j.neuroscience.2004.12.043

Lisman, J. E., & Idiart, M. A. P. (1995). Storage of 7 +/- 2 short-term memories in oscillatory subcycles. *Science, 267*(5203), 1512–1515.

Liu, P., Chen, Z., Jones, J. A., Huang, D., & Liu, H. (2011). Auditory feedback control of vocal pitch during sustained vocalization: a cross-sectional study of adult aging. *PLoS ONE, 6*(7). https://doi.org/10.1371/journal.pone.0022791

Livingston, G., Sommerlad, A., Orgeta, V., Costafreda, S. G., Huntley, J., Ames, D., Ballard, C., Banerjee, S., Cohen-Mansfield, J., Cooper, C., Gitlin, L. N., & Howard, R. (2017). Dementia prevention, intervention, and care. *Lancet, 390*(2673–734). https://doi.org/10.1016/ S0140-6736(17)31363-6

Lovelace, J. W., Ethell, I. M., Binder, D. K., & Razak, K. A. (2018). Translation-relevant EEG phenotypes in a mouse model of Fragile X Syndrome. *Neurobiology of Disease, 115*, 39–48. https://doi.org/10.1016/j.nbd.2018.03.012

Maris, E., & Oostenveld, R. (2007). Nonparametric statistical testing of EEG- and MEG-data. *Journal of Neuroscience Methods, 164*(1), 177–190. https://doi.org/10.1016/j.jneumeth.2007.03.024

Martin del Campo, H. N., Measor, K. R., & Razak, K. A. (2012). Parvalbumin immunoreactivity in the auditory cortex of a mouse model of presbycusis. *Hearing Research, 294*(1–2), 31–39. https://doi.org/10.1016/j.heares.2012.08.017

Mazelová, J., Popelar, J., & Syka, J. (2003). Auditory function in presbycusis: peripheral vs. central changes. *Experimental Gerontology, 38*(1), 87–94. https://doi.org/https://doi.org/10.1016/S0531-5565(02)00155-9

Mendelson, J. R., & Ricketts, C. (2001). Age-related temporal processing speed deterioration in auditory cortex. *Hearing Research, 158*(1–2), 84–94. https://doi.org/10.1016/S0378-5955(01)00294-5

Metherate, R., & Cruikshank, S. J. (1999). Thalamocortical inputs trigger a propagating envelope of gamma-band activity in auditory cortex in vitro. *Experimental Brain Research, 126*(2), 160–174. https://doi.org/10.1007/s002210050726

Niell, C. M., & Stryker, M. P. (2010). Modulation of visual responses by behavioral state in mouse visual cortex. *Neuron, 65*(4), 472–479. https://doi.org/10.1016/j.neuron.2010.01.033

Ouda, L., Druga, R., & Syka, J. (2008). Changes in parvalbumin immunoreactivity with aging in the central auditory system of the rat. *Experimental Gerontology, 43*(8), 782–789. https://doi.org/10.1016/j.exger.2008.04.001

Ouellet, L., & de Villers-Sidani, E. (2014). Trajectory of the main GABAergic interneuron populations from early development to old age in the rat primary auditory cortex. *Frontiers in Neuroanatomy, 8*, 40. https://doi.org/10.3389/fnana.2014.00040

Packer, A. M., & Yuste, R. (2011). Dense, unspecific connectivity of neocortical parvalbumin-positive interneurons: a canonical microcircuit for inhibition? *Journal of Neuroscience, 31*(37), 13260–13271. https://doi.org/10.1523/JNEUROSCI.3131-11.2011

Pantev, C. (1995). Evoked and induced gamma-band activity of the human cortex. *Brain Topography, 7*(4), 321–330. https://doi.org/10.1007/BF01195258

Parthasarathy, A, & Bartlett, E. L. (2011). Age-related auditory deficits in temporal processing in F-344 rats. *Neuroscience, 192*, 619–630. https://doi.org/https://doi.org/10.1016/j.neuroscience.2011.06.042

Parthasarathy, A., & Bartlett, E. L. (2012). Two-channel recording of auditory-evoked potentials to detect age-related deficits in temporal processing. *Hearing Research, 289*(1–2), 52–62. https://doi.org/10.1016/j.heares.2012.04.014

Pfurtscheller, G., & Lopes da Silva, F. H. (1999). Event-related EEG/MEG synchronization and desynchronization: basic principles. *Clinical Neurophysiology, 110*, 1842–1857. https://doi.org/10.1016/S1388-2457(99)00141-8

Polack, P. O., Friedman, J., & Golshani, P. (2013). Cellular mechanisms of brain state-dependent gain modulation in visual cortex. *Nature Neuroscience, 16*(9), 1331–1339. https://doi.org/10.1038/nn.3464

Polich, J. (1997). EEG and ERP assessment of normal aging. *Electroencephalography and Clinical Neurophysiology/Evoked Potentials Section, 104*(3), 244–256. https://doi.org/https://doi.org/10.1016/S0168-5597(97)96139-6

Purcell, D. W., John, S. M., Schneider, B. A., & Picton, T. W. (2004). Human temporal auditory acuity as assessed by envelope following responses. *The Journal of the Acoustical Society of America, 116*(6), 3581–3593. https://doi.org/10.1121/1.1798354

Raza, A., Milbrandt, J. C., Arneric, S. P., & Caspary, D. M. (1994). Age-related changes in brainstem auditory neurotransmitters: measures of GABA and acetylcholine function. *Hearing Research, 77*(1–2), 221–230. https://doi.org/10.1016/0378-5955(94)90270-4

Richardson, B. D., Ling, L. L., Uteshev, V. V., & Caspary, D. M. (2013). Reduced GABAA receptor-mediated tonic inhibition in aged rat auditory thalamus. *Journal of Neuroscience, 33*(3), 1218–1227. https://doi.org/10.1523/JNEUROSCI.3277-12.2013

Samuel, I. B. H., Wang, C., Hu, Z., & Ding, M. (2018). The frequency of alpha oscillations: task-dependent modulation and its functional significance. *NeuroImage, 183*, 897–906. https://doi.org/10.1016/j.neuroimage.2018.08.063

Schneider, D. M., & Mooney, R. (2018). How movement modulates hearing. *Annual Review of Neuroscience, 41*, 553–572. https://doi.org/10.1146/annurev-neuro-072116-031215

Schneider, D. M., Nelson, A., & Mooney, R. (2014). A synaptic and circuit basis for corollary discharge in the auditory cortex. *Nature, 513*(7517), 189–194. https://doi.org/10.1038/nature13724

Simon, H., Frisina, R. D., & Walton, J. P. (2004). Age reduces response latency of mouse inferior colliculus neurons to AM sounds. *The Journal of the Acoustical Society of America, 116*(1), 469–477. https://doi.org/10.1121/1.1760796

Sohal, V. S., Zhang, F., Yizhar, O., & Deisseroth, K. (2009). Parvalbumin neurons and gamma rhythms enhance cortical circuit performance. *Nature, 459*(7247), 698–702. https://doi.org/10.1038/nature07991

Tallon-Baudry, C., Bertrand, O., Delpuech, C., & Pernier, J. (1996). Stimulus specificity of phase-locked and non-phase-locked 40 Hz visual responses in human. *Journal of Neuroscience, 16*(13), 4240–4249. https://doi.org/10.1523/jneurosci.16-13-04240.1996

Tremblay, K. L., Piskosz, M., & Souza, P. (2002). Aging alters the neural representation of speech cues. *NeuroReport, 13*(15), 1865–1870. https://doi.org/10.1097/00001756-200210280-00007

Tremblay, K. L., Piskosz, M., & Souza, P. (2003). Effects of age and age-related hearing loss on the neural representation of speech cues. *Clinical Neurophysiology, 114*(7), 1332–1343. https://doi.org/10.1016/S1388-2457(03)00114-7

Trujillo, M., & Razak, K. A. (2013). Altered cortical spectrotemporal processing with age-related hearing loss. *Journal of Neurophysiology, 110*(12), 2873–2886. https://doi.org/10.1152/jn.00423.2013

Trujillo, M., Measor, K., Carrasco, M. M., & Razak, K. A. (2011). Selectivity for the rate of frequency-modulated sweeps in the mouse auditory cortex. *Journal of Neurophysiology, 106*(6), 2825–2837. https://doi.org/10.1152/jn.00480.2011

Turner, J. G., Hughes, L. F., & Caspary, D. M. (2005). Affects of aging on receptive fields in rat primary auditory cortex layer V neurons. *Journal of Neurophysiology, 94*(4), 2738–2747. https://doi.org/10.1152/jn.00362.2005

VanRullen, R., Busch, N. A., Drewes, J., & Dubois, J. (2011). Ongoing EEG phase as a trial-by-trial predictor of perceptual and attentional variability. *Frontiers in Psychology, 2*, 60. https://doi.org/10.3389/fpsyg.2011.00060

Volman, V., Behrens, M. M., & Sejnowski, T. J. (2011). Downregulation of parvalbumin at cortical GABA synapses reduces network gamma oscillatory activity. *Journal*

of Neuroscience, 31(49), 18137–18148. https://doi.org/10.1523/JNEUROSCI.3041-11.2011

Walton, J. P., Barsz, K., & Wilson, W. W. (2008). Sensorineural hearing loss and neural correlates of temporal acuity in the inferior colliculus of the C57bl/6 mouse. *Journal of the Association for Research in Otolaryngology*, *9*(1), 90–101. https://doi.org/10.1007/s10162-007-0101-z

Walton, J. P., Frisina, R. D., & O'Neill, W. E. (1998). Age-related alteration in processing of temporal sound features in the auditory midbrain of the CBA mouse. *Journal of Neuroscience, 18*(7), 2764–2776. https://doi.org/10.1523/JNEUROSCI.18-07-02764.1998

Walton, J. P., Simon, H., Frisina, R. D., & Giraudet, P. (2002). Age-related alterations in the neural coding of envelope periodicities. *Journal of Neurophysiology, 88*(2), 565–578. https://doi.org/10.1152/jn.2002.88.2.565

Weinstein, B. E., & Ventry, I. M. (1982). Hearing impairment and social isolation in the elderly. *Journal of Speech, Language, and Hearing Research, 25*(4), 593–599. https://doi.org/10.1044/jshr.2504.593

Wen, T. H., Binder, D. K., Ethell, I. M., & Razak, K. A. (2018). The perineuronal 'safety' net? perineuronal net abnormalities in neurological disorders. *Frontiers in Molecular Neuroscience, 11*, 270. https://doi.org/10.3389/fnmol.2018.00270

Willott, J. F., Aitkin, L. M., & McFadden, S. L. (1993). Plasticity of auditory cortex associated with sensorineural hearing loss in adult C57BL/6J mice. *The Journal of Comparative Neurology, 329*(3), 402–411. https://doi.org/10.1002/cne.903290310

Zhou, M., Liang, F., Xiong, X. R., Li, L., Li, H., Xiao, Z., Tao, H. W., & Zhang, L. I. (2014). Scaling down of balanced excitation and inhibition by active behavioral states in auditory cortex. *Nature Neuroscience, 17*(6), 841–850. https://doi.org/10.1038/nn.3701

Chapter 3

Nicotine partially reverses age-related changes in cortical neural oscillations

Abstract

Age-related changes to central auditory processing may lead to communication difficulties, putting older humans at greater risk of cognitive decline. Resting-state and stimulus-evoked neural oscillations at specific frequency bands are associated with sensorimotor and cognitive functions and can serve to identify abnormalities in cortical circuit dynamics. In this study, we analyzed epidural electroencephalogram (EEG) signals recorded from auditory and frontal cortex of awake and freely moving mice across young, middle and old ages, and found multiple robust and novel age-related changes in cortical oscillations. Most notably, resting, evoked, and induced gamma power diminished with age. Inter-trial phase coherence of responses to time-varying stimuli is reduced in old mice. We also show that movement of mice (compared to still) increased EEG power across multiple spectral bands at all ages, but the movement-related modulation of gamma power is specifically reduced in old mice. An acute injection of nicotine (i.p., 0.5 mg/kg), but not saline, in old mice significantly increased resting gamma power, movement-related modulation of gamma power, inter-trial phase coherence, and induced gamma power towards values seen in young mice, partially reversing age-related changes. The age-related changes in neural oscillations are consistent with models of abnormal activation of specific inhibitory interneuron subtypes. Importantly, our data suggest that the auditory circuits that can produce "young" responses to sounds are present in old mice, and can be activated by nicotine.

Significance Statement

In aging humans, the central auditory system undergoes changes that can lead to difficulties in communication, even in the absence of significant age-related hearing loss. To establish a preclinical model of age-related central processing deficits, we analyzed EEG signals recorded from a mouse model of normal auditory aging and found significant age-related changes. Resting, induced, and entrained gamma oscillations recorded from the auditory and frontal cortices show age-related declines. We show that it is feasible to activate circuits that generate cortical gamma oscillations in old mice with nicotine. Because gamma oscillations are associated with cortical activation, temporal specificity and attentional mechanisms, these data suggest that nicotine administration may be a potential avenue to improve central auditory processing in older individuals.

Introduction

Older adults can experience difficulties understanding speech in challenging environments, even in the absence of significant age-related peripheral hearing loss. This indicates deteriorated processing in the aging central auditory system that may lead to reduced communication and social activities. Epidemiological studies have demonstrated a link between the degradation of communication, social activities, and declining cognitive abilities (Cacioppo & Hawkley, 2009; Gates et al., 2002; Lin et al., 2014; Panza et al., 2018). To improve central auditory processing in aging humans, it may be necessary to use a combination of hearing aids, behavioral and pharmacological treatment approaches. Currently, no pharmacological approach exists to improve central auditory processing. This is partly due to the lack of a preclinical model with objective, functional,

and translation-relevant outcome measures associated with age-related central auditory processing. In this study, we show that acute nicotine administration rescues multiple electrophysiological phenotypes in aging mouse cortex including temporal processing and cortical activation in the gamma frequency band.

Frequency-based analyses of electroencephalogram (EEG) signals indicate strong associations between neural oscillations, cortical dynamics, and sensorimotor and cognitive functions (Salinas and Sejnowski, 2001; Ward 2003; Hermann et al., 2010). Modeling (Volman et al., 2011) and in vivo activity (Cardin et al., 2009; Chen et al., 2017; Sohal et al., 2009) manipulation studies show a strong link between specific oscillation frequencies and subtypes of cortical GABAergic neurons such as parvalbumin (PV) and somatostatin (SOM). Reduced inhibition (Burianova et al., 2009; Caspary et al., 2013) and decreases in PV and SOM cell densities occur in the aging auditory cortex (Brewton et al., 2016; Martin del Campo et al., 2012; Ouda et al., 2008; Ouellet & de Villers-Sidani, 2014; Rogalla & Hildebrandt, 2020). Nevertheless, literature regarding age-related changes in cortical oscillations in animal models is limited outside the context of sleep studies.

To establish markers of cortical electrophysiological changes associated with aging, we quantified resting and sound evoked epidural EEG responses in awake and freely moving mice at 3, 6, 12 and 20 months of age. Based on the evidence for age-related changes in inhibitory interneurons, we tested the hypothesis that power and phase locking of low (30-60 Hz) and high (60-100 Hz) frequency gamma oscillations will be diminished in older mice. Activity in the auditory cortex is modulated by movement,

through a pathway from secondary motor cortex (M2) to PV neurons in A1 (Nelson et al., 2013; Schneider et al., 2014; Schneider & Mooney, 2018). Given the age-related changes affecting PV neurons, we hypothesized that the modulation of gamma oscillations by movement will be diminished in older mice.

Manipulating cholinergic signaling via nicotine administration can enhance sensory acuity, reaction time, and attentional and cognitive performance (Askew et al., 2017; Barr et al., 2008; Bueno-Junior et al., 2017; Gil & Metherate, 2018; Lawrence et al., 2002; Levin et al., 2006; Newhouse et al., 2004; Rezvani & Levin, 2001; Warburton, 1992). Activity in the auditory system is modulated by nicotinic acetylcholine receptors (nAChRs) at multiple processing levels, including thalamocortical inputs and the cortex (Askew et al., 2019; Metherate, 2011). Cholinergic transmission is impaired in the aging auditory system (Ghimire et al., 2020; Sottile et al., 2017). Therefore, we hypothesized that nicotine administration would reduce age-related electrophysiological phenotypes of impaired cortical processing in old mice. We report a number of age-related EEG phenotypes including reduced power of gamma oscillations and its modulation by movement and reduced phase locking to time varying signals. We show that acute nicotine treatment reduces these phenotypes, reversing age-related changes in old mice. These data indicate that the circuits involved in generating cortical gamma oscillations can be reactivated in old mice with nicotine.

Methods

Mice and age groups

All animal procedures were approved by the University of California, Riverside Institutional Animal Care and Use Committee (IACUC). FVB strain mice (FVB.129P2−Pde6b^{+}Tyr$^{c\text{-}ch}$/AntJ) were obtained from Jackson Laboratories and bred in-house. All mice were housed in an accredited vivarium with 12:12 light/dark cycle and given standard lab chow and water *ad libitum*. The following age ranges and sample sizes were used in this study: 3 months (n=14, 10 females, mean = 3.4 ± 0.1 mo), 6 months (n=21, 9 females, mean = 6.2 ± 0.4 mo), 12 months (n=16, 9 females, mean = 12.7 ± 0.8 mo) and 20 months (n=23, 9 females, mean = 19 ± 1.2mo).

Surgical techniques

The aseptic surgical procedures used were similar to those described in a previous publication (Lovelace et al., 2018). Briefly, after anesthetizing the mouse with ketamine/xylazine/acepromazine (80/10/1 mg/kg, i.p.), 1 mm diameter holes were drilled in the skull overlying the right auditory cortex, right frontal cortex, and the left occipital cortex, using a Foredom dental drill (Foredom Electric Co., CT). The auditory cortex screw position was determined using skull landmarks which have been validated previously using single unit (Rotschafer & Razak, 2013; Wen et al., 2018), epidural EEG (Wen et al., 2019) and depth ERP (Lovelace et al., 2016) recordings in the FVB mice. The frontal screw was placed just caudal to the frontal sinus, and just lateral to the sagittal suture. The occipital screw was placed in the parietal bone, just lateral to the intersection of the sagittal suture and lambdoid suture. The wires extending from three-

channel posts (InVivo, Roanoke, VA) were stripped and wrapped around 1mm screws (InVivo, Roanoke, VA), which were then screwed into the pre-drilled holes. Dental cement (Kuraray Dental, New York, NY) was used to cover the exposed skull and screws. Recovering mice were injected (subcutaneous) with 0.1 mg/kg buprenorphine every 6-8 hours for 48 hours after surgery. The mice had at least 5 days to recover following surgery, and at least 3 days after the last buprenorphine injection, before the first recording.

Auditory brainstem responses

Unlike the C57bl/6 mice, which show accelerated presbycusis, the FVB mouse strain is similar to the CBA strain at least up to 8 months of age, showing no significant hearing loss (Zheng et al., 1999). However, hearing threshold data are not available past this age for the FVB strain. Therefore, we recorded Auditory brainstem responses (ABR) from young and old FVB mice anesthetized with a solution of ketamine, xylazine, and acepromazine (80/10/1 mg/kg i.p.). Once an anesthetic plane was reached, as determined by the absence of a toe-pinch reflex, the mice were placed in a Faraday cage in an anechoic sound-attenuating chamber. We used the implanted occipital screw as the recording electrode. Grass needle electrodes (Grass Technologies, RI) were used as the reference and ground, placed in the ear ipsilateral to the speaker and in the skin of the hindquarters, respectively. A TDT (Tucker Davis Technologies, FL) RA4LI/RA4PA headstage/pre-amp connected to a TDT RZ6 multi-I/O processor was used to record signals from the electrodes. TDT software BioSigRZ and the RZ6 were used to generate stimuli and drive a TDT MF-1 speaker, which was placed 10 cm from the mouse's ear,

perpendicular to the long axis of the mouse. The system was calibrated using a ¼" Bruel and Kjaer (Nærum, Denmark) microphone. Clicks were presented at 10 dB SPL steps, starting from 90 dB SPL and ending at 10 dB SPL, with 512 clicks presented per sound level at 21 Hz repetition rate. The averaged 10 ms waveform was examined to determine hearing threshold, based on the presence of waves I and/or III occurring before 7.5 ms.

EEG recordings from awake, freely-moving mice

Mice were briefly anesthetized with isoflurane inhalation, and a three-channel cable was plugged into the implanted post. This cable was connected *via* freely-rotating commutator (InVivo, Roanoke, VA) to a TDT (Tucker Davis Technologies, FL) RA4LI/RA4PA headstage/pre-amp, which was connected to a TDT RZ6 multi-I/O processor. The frontal and auditory cortical screw electrodes were referenced and grounded to the occipital screw electrode. The period of anesthesia with isoflurane lasted <30 seconds and was intended to decrease discomfort and maintain implant integrity while connecting the cable. The mouse was then given a minimum of 10 minutes to habituate to the plastic arena, which was filled with sterile bedding, before the recording began. The recording chamber was placed in a Faraday cage inside of an anechoic sound-attenuating chamber (Gretch-Ken Industries, OR). Motion detection was achieved using a 27 mm piezoelectric pressure sensor (AW-PZT27L; Audiowell; Guangdong, China) placed beneath the arena, in addition to an infrared video camera mounted above the arena. OpenEx (TDT) was used along with the RZ6 to record EEG signals, record pressure signals, operate the LED light used to synchronize the video and waveform data, produce and store digital pulses, and to produce auditory stimuli. The EEG signals were

captured at a sampling rate of 24.414 kHz and down-sampled to 1024 Hz. EEG recordings were visually examined for artifacts, which were characterized by a temporary loss of signal, or by vertical lines indicative of clipping. Any recordings that included artifacts would have been eliminated from the study, but none did, so no EEG data were rejected.

Spectral analysis of resting EEG data

To quantify age-related changes in EEG spectral power distribution and the influence of movement on EEG power at different ages, we measured resting EEG power spectral densities in both auditory and frontal cortex across the different age groups. The phrase 'resting EEG' is used to describe data collected when there was no specific auditory stimulation. After >10 minutes of habituation, 5 minutes of resting EEG was recorded. We visually examined each trace and excluded segments containing clipping artifacts. This data was then split into periods of movement (referred to as 'move') and non-movement (referred to as 'still'), based on analysis of the pressure signal from the piezoelectric sensor. The two conditions (still vs. move) were then analyzed separately to identify movement-state dependent differences in power spectral density of resting EEG. The traces from each condition were split into Hanning-windowed 1-second segments with 50% overlap, which were then transformed to the frequency domain *via* Fourier transform. The average power spectra for each condition were calculated by averaging the spectra from each of the 1-second segments. Each average power spectrum was then split into canonical EEG frequency bands (theta: 3-7 Hz, alpha: 8-13 Hz, beta: 14-29 Hz, low gamma: 30-59 Hz, high gamma: 61-100 Hz, and high-frequency oscillations: 101-

250 Hz). Delta band power was not analyzed because the TDT RA4PA pre-amp implements a high-pass filter at 2.2 Hz. The average power from each frequency band was calculated. To compare the age groups, Kruskal-Wallis H tests were run on each frequency band within each region SPSS (IBM, NY), and the resulting p-values were adjusted for multiple comparisons within each region. Dunn's tests were run on each frequency band (SPSS, IBM, NY), and the resulting p-values were adjusted for multiple comparisons (Bonferroni) within each region.

Analysis of Modulation of EEG Spectral Power by Movement Velocity

To correlate EEG power with movement, videos recorded during EEG recordings were analyzed for motion. A custom MATLAB script was used to determine the location of the mouse in each frame, which was used to calculate instantaneous velocity. During recordings, a red LED light controlled by the RZ6 system flashed briefly every 5 minutes, and a simultaneous TTL pulse was generated and recorded alongside the EEG signal. The video and EEG signals were synchronized via the on/off times of the LED. Only the videos from the 3-month-old and the 20-month-old mice were used (n=14, n=11, respectively). The LED signal was absent from the videos recorded during the EEG recording sessions of the 6- and 12-month-old mice, and some of the 20-month-old mice, so the EEG data could not be synchronized with the video to the degree of precision necessary for this analysis. The EEG signal was transformed using a complex Morlet wavelet transform, with a constant wavelet parameter of 7, to provide instantaneous spectral power at frequencies ranging from 1-250 Hz. For each frequency, this spectral power was correlated with the velocity calculated from the video, using Spearman's Rho.

These measurements will allow us to determine if there were changes to movement characteristics and the correlation of velocity with EEG power with age, and if there were correlations between these measures.

Acoustic Stimulation

All electrophysiological recordings of responses to acoustic stimulation were conducted in a sound-attenuating chamber lined with anechoic foam (Gretch-Ken Industries, OR), and used the same hardware and software (Tucker Davis Technologies, FL) described previously (Lovelace et al. 2018). We generated acoustic stimuli using custom-designed RPvdsEx scripts, which were run on a TDT RZ6 device and presented through an MF1 speaker suspended 0.5m above the arena. The stimulus level was calibrated by generating continuous broadband noise at a specific attenuation level and measuring the sound level with a ¼" Bruel and Kjaer microphone.

Event-related potentials (ERPs)

To analyze how ERP component amplitudes and latencies change with age, we recorded ERPs elicited by 70 dB SPL, 100 ms broadband noise pulses repeated 120 times at a non-habituating rate of 0.25 Hz (Lovelace et al., 2016).

Amplitude-Modulated Chirp Stimulus (swept-frequency AM noise)

To analyze how temporal fidelity of responses to dynamic stimuli changed with age, we used a 'chirp' stimulus, previously described (Ethridge et al., 2017; Lovelace et al., 2018; Purcell et al., 2004). The chirp stimulus provides a means to measure the fidelity with which neural generators can synchronize responses to a time varying auditory stimulus. The stimulus consists of sinusoidally amplitude modulated broadband

noise, for which the frequency of modulation was increased from 1 to 100 Hz over the course of 2 seconds. A one-second-long broadband noise ramp was presented immediately before the chirp stimulus onset to avoid confounding the chirp response with an onset response. The stimulus was repeated 300 times, with an inter-stimulus interval of one second, from the end of a chirp to the beginning of the next broadband noise ramp.

Analysis of Auditory Responses

For ERP component analysis, we averaged 120 responses to the stimulus, and measured the latencies and amplitudes (from baseline) of P1 (P20), N1 (N40), P2 (P80), and N2 components. For each mouse, the responses were baseline-corrected, de-trended, and averaged. Peaks were located by finding either the minimum or maximum amplitude within a specific time window for each expected peak, i.e. the P20 peak was the maximum value within a window of 10-30 ms following the stimulus onset, the N40 peak was the minimum value within a window of 25-60 ms post-stimulus onset, the P80 peak was the maximum value within 50-90 ms post-stimulus onset, and N2 was the minimum value between 150 and 250 ms post-stimulus onset. The amplitude of each peak was calculated as the difference from 0 mV (baseline) to the voltage at the peak.

For time-frequency analysis of responses to acoustic stimuli, we implemented a dynamic complex Morlet wavelet transform with Gabor normalization, in which the wavelet parameter was set for each frequency to optimize time-frequency resolution (Cohen, 2014). We measured baseline-normalized power by averaging the time-frequency power matrix for each presentation of the stimulus, measuring mean baseline power (from -500ms to -50ms) for each frequency, and calculating the dB change from

baseline during the stimulus. We measured inter-trial phase clustering (phase-locking factor) (Cohen, 2014; Tallon-Baudry et al., 1996), which quantifies the consistency of the responses across trials, by extracting the phase time-series for each frequency during each stimulus presentation, and calculating the average vector, plotted on the unit circle, at each time-frequency point.

Statistical Analysis of Auditory Responses

To compare the responses across age-groups, we implemented a non-parametric permutation test approach, which shows significant differences in time-frequency matrices across age groups (Carlson et al., 2011; Cohen, 2014; Lee et al., 2014; Liao et al., 2012; Maris & Oostenveld, 2007). First, a t-test was run on each time-frequency point for the two groups being compared, yielding the T-values for each TF point. T-values corresponding to $p<0.025$ were considered significant. Clusters of significant T-values were found and their area was measured. Next, the group assignments were shuffled randomly, and the t-tests and cluster-measurements were run again on the surrogate groups. This was performed 2000 times to generate a distribution of cluster sizes that we would expect to find by chance. In the original group comparison, clusters that were larger than 95% of the surrogate clusters were considered to be significant. This method allows for the discovery of significant differences between groups while accounting for multiple comparisons, and without making assumptions about normality or homogeneity of variance between groups.

Recordings with acute nicotine injections

Responses to auditory stimuli were measured following an i.p. injection of 0.5 mg/kg (freebase) nicotine ditartrate dihydrate (ACROS Organics) dissolved in saline. This dose does not cause significant changes in heart rate or body temperature, and is much lower than the dosage required to induce clonic seizures, as measured in other strains of mice (Matta et al., 2007). In other studies of the effects of nicotine on the murine auditory system, a higher dose is commonly used (2.1 mg/kg in Askew et al., 2017; 1.0 mg/kg in Featherstone et al., 2012; 1.05 mg/kg in Metzger et al., 2007; 1.0 mg/kg in Phillips, et al., 2007).

The mouse was weighed, injected with the nicotine solution, and connected to the recording apparatus. EEG signals were recorded for 5 minutes in silence and then recorded while acoustic stimuli were presented. Because the effects of nicotine on auditory responses only last up to 30 minutes in FVB mice (Intskirveli & Metherate, 2012), we recorded responses to one type of acoustic stimulus per recording session. In separate sessions, we recorded responses to broadband noise and chirp stimuli. We also recorded responses to these stimuli after injecting the mice with sterile saline. These saline-injection recordings were counterbalanced with the nicotine injections, and the recordings for each stimulus were performed on consecutive days, with a week separating the ERP and chirp recording sessions. The responses to chirp and noise stimuli were recorded a week apart, to minimize order effects or multiple injection effects. The relatively low dose, along with the separation of nicotine injections by a week, reduces

the possibility of the sensitization effects shown in studies of rats (Bueno-Junior et al., 2017).

Results

The first main goal of this study was to use EEG recordings to quantify age-related changes in resting and sound-evoked neural oscillations in the auditory and frontal cortices (henceforth, AC and FC) of mice. Because we analyzed movement while recording EEGs, the second main goal was to quantify how movement changed spectral power of oscillations and how movement-related modulation of oscillations changed with age. The third main aim was to determine the effects of acute nicotine injection on resting and sound-evoked neural oscillations.

Hearing thresholds show moderate increase from 3- to 20-months in the FVB strain mice

To identify changes in hearing thresholds with age, click ABRs were measured from 3-month-old mice (n=7) and from 20-month-old mice (n=15). Figure 3.1A and 3.1B show examples of typical ABR traces recorded from a 3-month-old and a 20-month-old

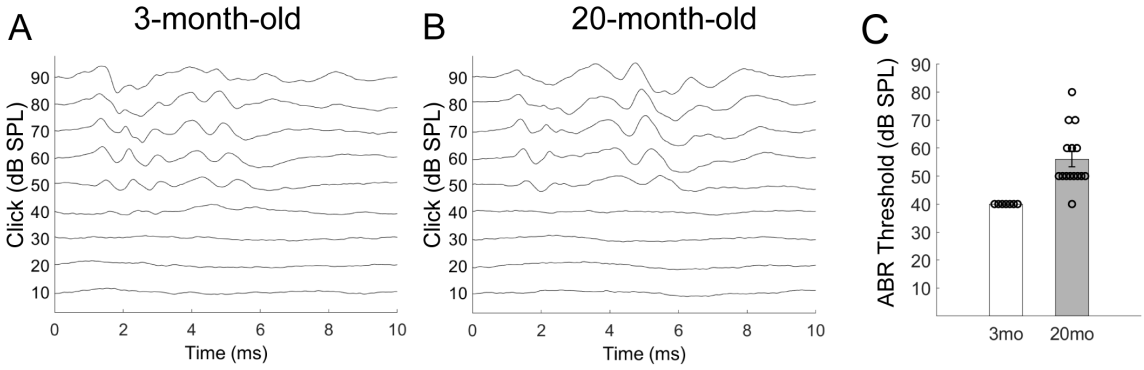

Figure 3.1. FVB mice show moderate hearing loss with age. Example ABR traces from a 3-month-old mouse (A) and a 20-month-old mouse (B). 20-month-old mice (n=15) have significantly increased hearing thresholds (C) compared to 3-month-old mice (n=7); χ^2 (1, N=22) = 14.83, $p < 0.001$.

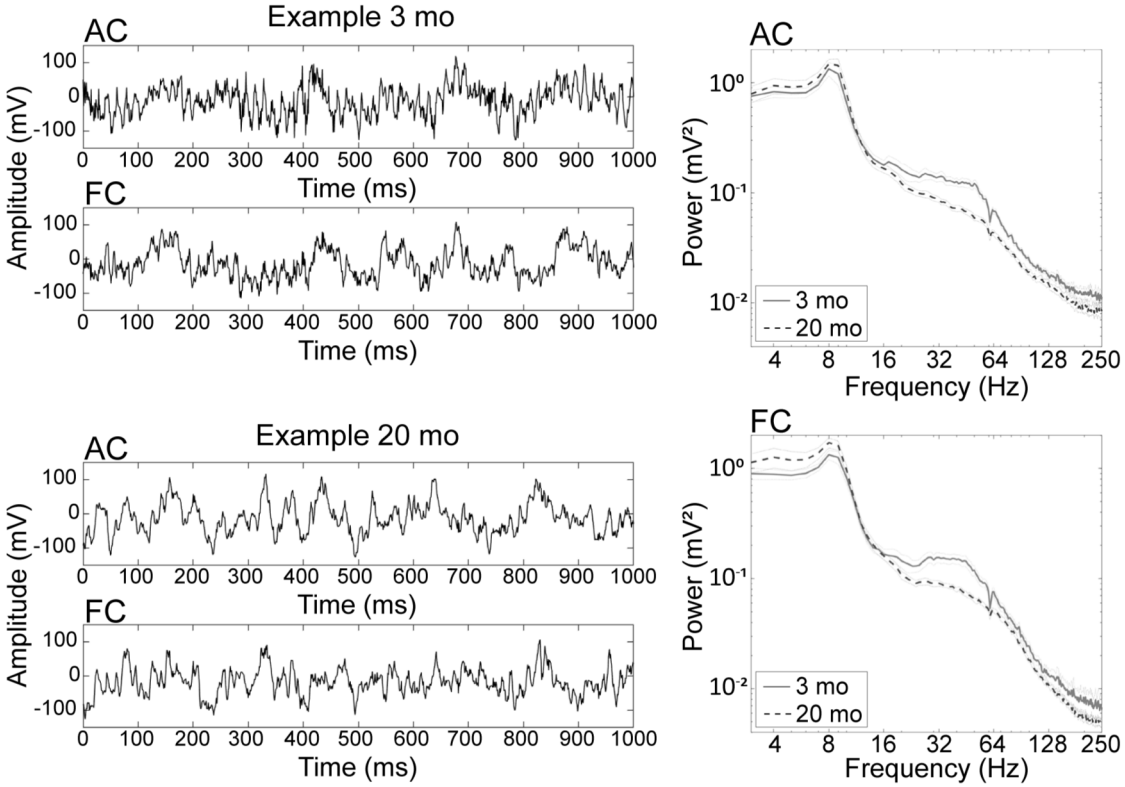

Figure 3.2. Characterization of age-related frequency-specific changes in EEG power. (A) Example traces from 3-month-old (top two traces, AC and FC) and 20-month-old mice (bottom two traces AC and FC) show a decrease in high-frequency activity. (B) Power spectral density plots from resting EEG exhibit frequency-specific decreases, quantified in Figure 3.3. PSDs from 3-month-old mice are shown as solid lines, and PSDs from 20-month-old mice are shown as dashed lines.

mouse, respectively. Thresholds were determined by visual confirmation of the appearance of wave I and/or III before 7.5ms. All of the 3-month-old mice tested had thresholds of 40 dB SPL, which is similar to previously reported thresholds for 13-week-old FVB/NJ mice (38 dB SPL; Zheng et al., 1999). The 20-month-old mice had thresholds of 56 dB ± 10 dB SPL (Figure 3.1C). The click ABR thresholds of the old mice were significantly higher than those of the young mice, χ^2 (1, N=22) = 14.83, $p < 0.001$. CBA/CaJ mice show an increase in threshold of ~10-15 dB SPL from 4-5 months to 19 months (Hunter & Willott, 1987). Thus, in terms of hearing thresholds, the FVB

mice are comparable to the CBA mice, a strain commonly used to study auditory aging without accelerated hearing loss.

Movement-, frequency- and age-specific changes in resting EEG spectral power

Resting EEG power was analyzed in AC and FC of 3-mo, 6-mo, 12-mo, and 20-mo old mice. Figure 3.2A shows example one-second EEG traces from a young (3-mo) mouse and an old (20-mo) mouse recorded from the AC and FC. Figure 3.2B shows the mean power spectra for the duration of the recording for the 3 and 20-mo groups. The age-related reduction of higher frequency power can be qualitatively observed in the raw traces as well as the power spectral density plots. Recordings such as these obtained over 5 minutes were then separately analyzed depending on whether the mouse was moving or still. Because movement and motor cortex stimulation affects neural activity in the AC and inferior colliculus (Schneider & Mooney, 2018; Yang et al., 2020), we analyzed how resting EEG spectral power distribution in AC and FC changed with movement, and how such changes were affected by age (Figures 3.3-3.4).

During EEG recordings, a piezoelectric sensor was placed beneath the arena floor to record the movements of the mouse. There was no difference in the average percentage of time that the different age groups spent moving within the 5 minutes of recording time (one-way ANOVA, $p>0.05$, Table 3.1). EEG recordings during periods of movement were segmented into Hanning-windowed one-second segments with 50% overlap. Fourier transforms were performed on the EEG data from these windows, and the resulting power spectra were averaged. The average spectra were then split into canonical frequency bands, and the mean power within each band was calculated. The bar charts in

Figure 3.3 show the power of each age group as a ratio of the 3-mo group mean. Theta and HFO showed no age-related differences in power during move or still states (data not shown). Because not all of the data were normally distributed, Kruskal-Wallis H-tests were run on each frequency band in each region, with pairwise comparisons assessed

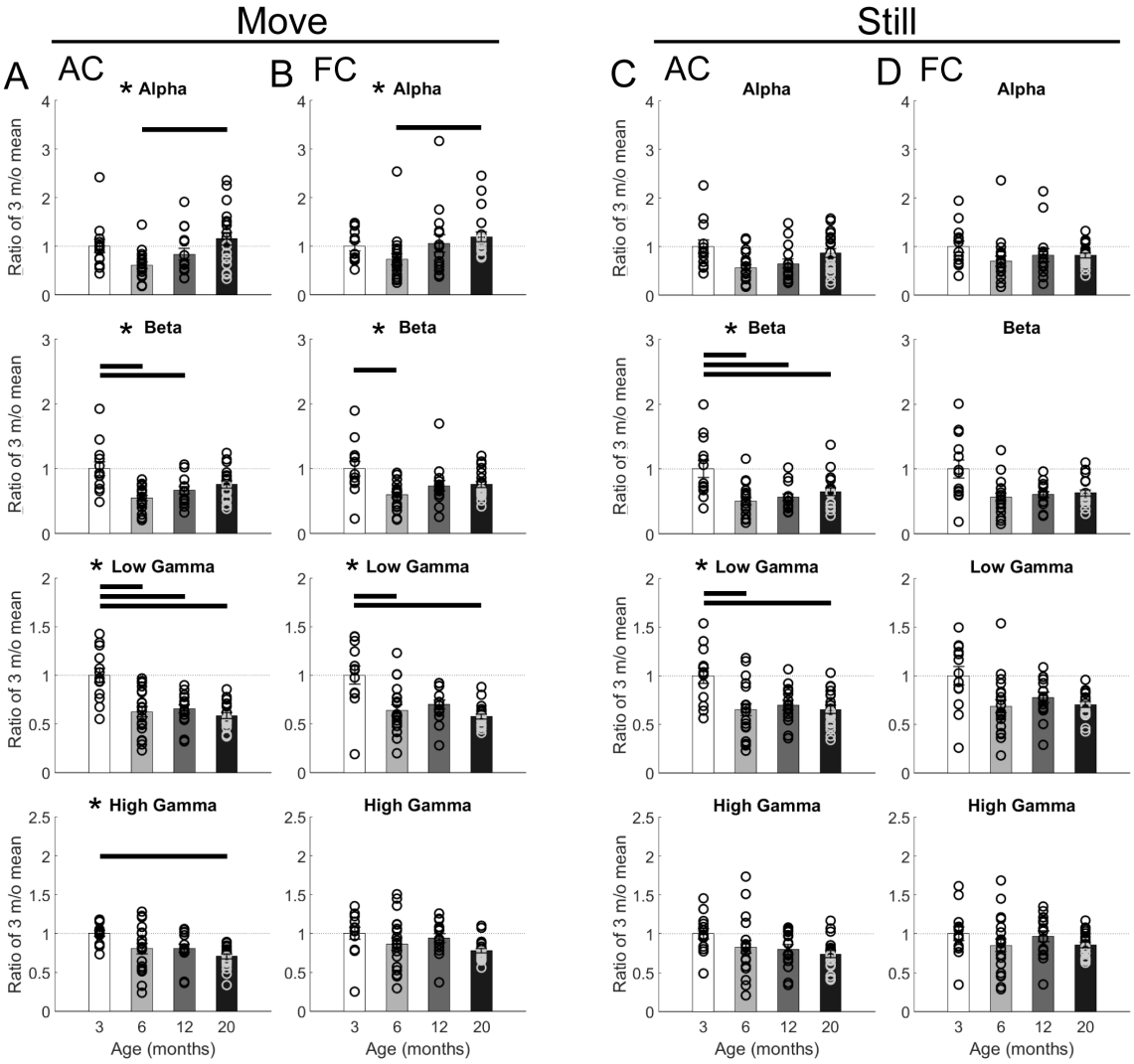

Figure 3.3. Age and movement related changes in EEG spectral power. Older mice exhibit lower beta, low-gamma, and high-gamma power during movement (A and B) and lower beta and low-gamma power during the 'still' condition (C and D), compared to younger mice. During movement, old mice showed higher power in the alpha band in both AC and FC. Significant differences are shown with lines spanning the pairs of groups. Significant results from Kruskal-Wallis tests (Bonferroni-corrected $p<0.05$) are indicated by asterisks (*) next to the name of the frequency band.

with Dunn's nonparametric test. The p-values for the K-W-H tests were Bonferroni corrected for each region, and the results from the pairwise Dunn's tests were Bonferroni corrected for multiple comparisons. In Figure 3.3, significant results from the K-W-H tests are denoted with asterisks (*), and significant pairwise comparisons are marked with horizontal lines. Complete results from the K-W-H tests and post-hoc Dunn's tests are shown in Table 3.2 to identify statistical differences in EEG power with age, region, and spectral band.

During movement, EEG power in the AC in alpha (8-13 Hz; H=13.4, p=0.023), beta (14-30 Hz; H=17.0, p=0.004), low-gamma (30-59 Hz; H=19.9, p=0.001), and high-gamma (60-100 Hz; H=16.0, p=0.007) bands change as mice age (Fig. 3A-B). EEG power in the FC in the alpha (H=15.9, p=0.007), beta (H=13.9, p=0.018) and low-gamma (H=20.1, p=0.001) bands change with age (Figure 3.3B). Notably, low gamma power decreases from 3 to 6 months and then remains low through 20 months in both regions, whereas high gamma shows a decrease in the 3- and 20-month comparisons in the AC. In both regions, beta power decreases from 3 to 6 months and then remains low at 12 and 20 mo while alpha power shows a significant increase from 6-months to 20-months. There were relatively less age-related changes in EEG while the mice were still. EEG power in the AC in the beta (H=15.8, p=0.008) band and in the low-gamma band (H=13.2, p=0.025) showed age related reduction (Figure 3.3C-D). There were no significant age-related differences in the FC during the still condition. Together, these data indicate considerable frequency-, movement- and age-dependent changes in spectral power of EEG signals.

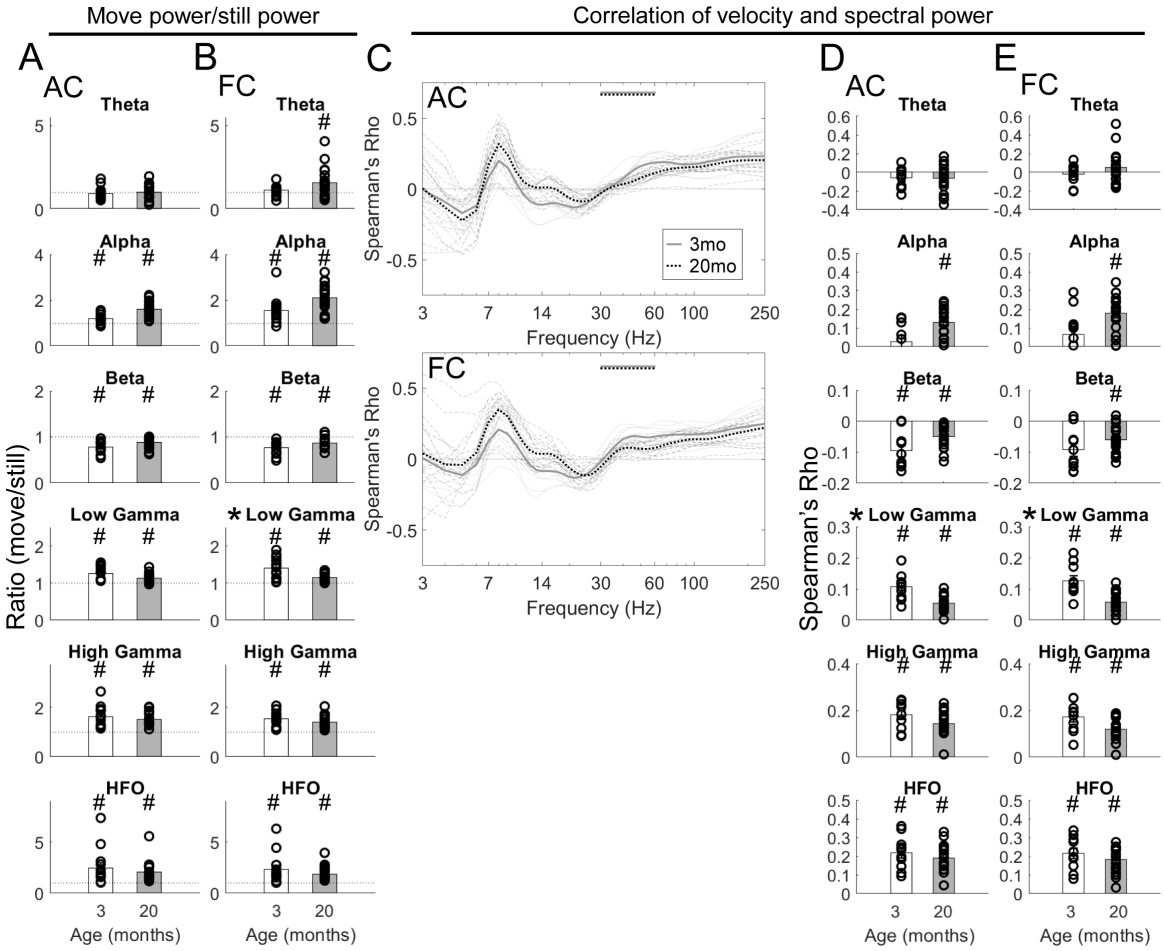

Figure 3.4. The effect of movement on gamma band power shows an age-related decrease. Movement related modulation is quantified in (A and B) as ratios of EEG power (move power/still power) for each frequency band. One sample t-tests, comparing each distribution of ratios to 1 (in which case, move power is equal to still power), were used to determine whether or not the power in each frequency band was modulated by movement. The distributions with Bonferroni corrected p-values (p*2) less than 0.05 are marked with '#' characters. For the age group comparisons, t-tests with unequal variance were used. Bonferroni corrected (p*6) p-values < 0.05 are marked with stars. In this measure of movement related modulation of power, only low gamma in the frontal cortex shows age-related differences. Spearman correlations of spectral power with movement velocity (C-E) show frequency-specific modulation of power by movement. (C) The correlation of velocity with spectral power at each frequency is shown for each mouse (thin lines), and group averages are shown with thicker lines (3-month-old: solid gray line; 20-month-old: dashed black line). This line plot shows that the correlation of velocity with power is frequency-specific, where alpha power is positively correlated with velocity, beta power is negatively correlated with velocity, and gamma power is positively correlated with velocity. The correlation of low gamma power with velocity shows a significant age-related decrease, as denoted by the stacked horizontal lines spanning the low gamma range. In the auditory (D) and frontal (E) cortices, the modulation of low gamma power by movement is significantly diminished in 20-month-old mice compared to 3-month-old mice, as measured by Bonferroni corrected t-tests with unequal variance. The results of one-sample t-tests, indicating movement-related modulation, are marked with '#' characters, as in (A and B).

Figure 3.4 shows quantification of the movement related modulation of EEG power through two different analysis techniques. First, EEG power in each spectral band during movement is divided by the corresponding power when the mouse was still, yielding a move:still ratio in AC (Figure 3.4A) and FC (Figure 3.4B). Second, continuous spectral power is correlated with movement velocity (Figure 3.4C-E). Figure 3.4A-B shows the frequency and age-related changes in the ratio of EEG power between movement and still states across 3-mo-old and 20-mo-old age groups. One-sample t-tests were performed on the ratios of move/still power for each frequency band in each group and Bonferroni corrected for multiple comparisons. Significant differences, denoted with '#' signs, indicate that EEG power in that frequency band is significantly modulated by movement, because the move:still ratio of power is significantly different from 1. For both age groups and cortical regions, movement significantly modulates EEG power in a frequency-specific manner (Figure 3.4A-B). Beta power decreased and gamma power increased with movement in both AC and FC. Theta was affected by movement only in the FC.

Age-related differences in move:still ratio were calculated with Kruskal-Wallis H tests and the significant results from subsequent pairwise comparisons are shown with an asterisk (Figure 3.4). In the AC, there are no significant age effects on the ratio of power between move and still recordings (Figure 3.4A). In the FC, the move:still ratio of low gamma power is significantly different across ages (*p= 0.018, Figure 3.4B). In younger mice, low-gamma power in the FC increases more during movement, compared to old mice, wherein movement has less of a modulatory effect on low-gamma power.

In addition to the binary movement/still approach, we also used a motion-capture script to measure velocity, and we calculated correlations of velocity with EEG spectral power. As shown in Table 3.1, the young (3mo) and old (20mo) mice moved for a similar percentage of the time. The average movement velocity of the old mice was higher than that of the young mice ($p=0.039$, Table 3.1). Figure 3.4C shows that the correlation of power with velocity for the young and old mice follow a similar frequency-specific pattern. Alpha, low and high gamma, and HFO show increase in power with increasing velocity. Beta power shows a negative correlation with velocity. The mean Spearman's Rho values shown in Figure 3.4D-E quantify these correlations within each frequency band. The significance of the correlation of velocity with power was determined for each band for both age groups using a one sample t-test, comparing the distribution of Rho values to a normal distribution with a mean of zero (significant correlations are marked with '#' signs). When 3-mo and 20-mo mice are compared, the young group shows a significantly higher correlation of velocity with low gamma power in the AC (*Kruskal-Wallis $H=10.02$, $p=0.009$, Figure 3.4C) and FC (*$H=12.16$, $p=0.003$, Figure 3.4D) compared to the old group. This indicates that both young and old mice increase low-gamma power with increasing velocities of movement, but this modulation is reduced with age. As seen with the binary move/still measurements, the reduced modulation with age was specific for the low-gamma band and not a non-specific effect across multiple frequency bands.

Taken together, the resting EEG data show age-related changes in power and age-related changes in the modulation of EEG power by movement. Lower frequency power

is elevated in older animals, and higher frequency power is reduced in older animals. EEG power is modulated by movement, and the degree of modulation changes with age, where low gamma power is increased during movement to a lesser degree in older mice, compared to 3-month old mice.

Age related changes in auditory event related potentials and spectral perturbations

We compared amplitudes and latencies of ERP components across the four age groups. A 100 ms, 70 dB SPL broadband noise stimulus was repeated 120 times (0.25 Hz rate). Table 3.3 shows results from the statistical analysis of standard ERP amplitude and latency parameters for P1, N1, P2, and N2, which appear at approximately 20 ms, 40 ms, 80 ms, and 200 ms post-stimulus, respectively (Figure 3.5 shows group average ERP waveforms for 3-mo and 20-mo mice as inset in panels A, B, D, and E). Krukal-Wallis H tests were calculated for each ERP component in each brain region. After correcting for multiple comparisons (Bonferroni; p*8), only the N2 component in the FC appeared to show any effect of age ($H=12.593$, $p=0.048$). The N2 component, which occurs ~200 ms post-stimulus, is larger in magnitude in the FC of 3-mo old mice compared to 20-mo old mice (Bonferroni corrected pairwise Dunn's z test; $p=0.003$).

Standard analysis of positive and negative peaks in averaged traces ignores frequency-specific changes in brain activity following the stimulus. To further investigate the responses to broadband noise, we examined the time-frequency transform of the responses, in an approach known as event-related desynchronization (ERD; Pfurtscheller & Lopes da Silva, 1999), event-related spectral perturbations (ERSP; Makeig, 1993), or event-related oscillations (ERO; Başar, et al, 2001).

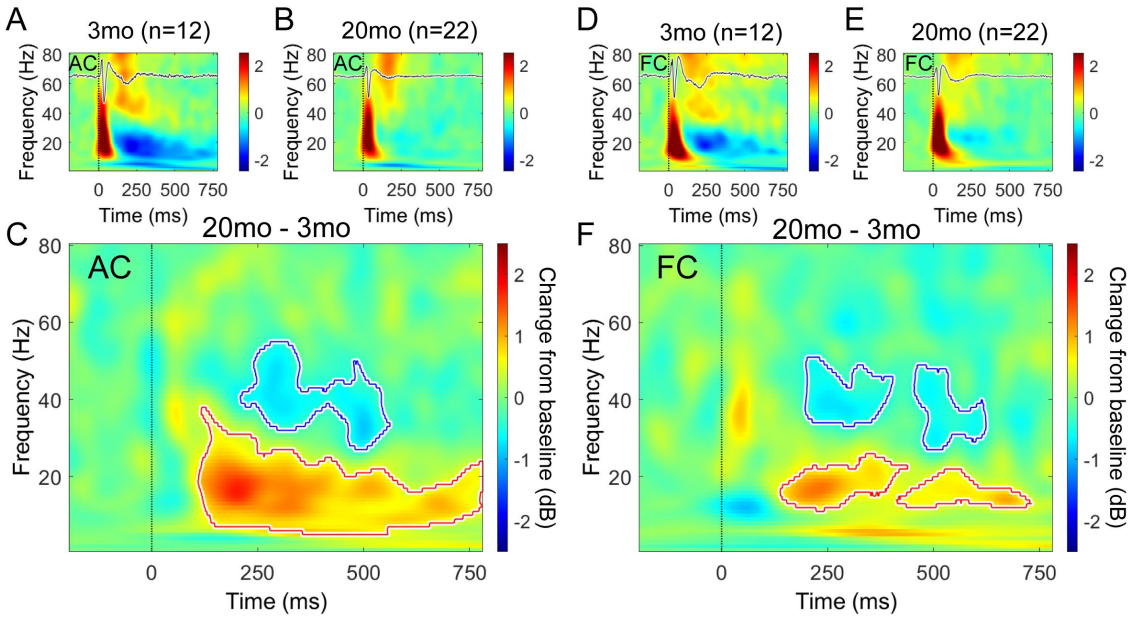

Figure 3.5. Long-latency time-frequency ERP components show significant changes from 3mo to 20mo. Group averages of baseline-normalized power in response to 100 ms broadband noise pulses are shown for 3- and 20-month-old mice for the auditory cortex (A-B) and frontal cortex (D-E). Red pixels represent an increase in power compared to baseline at that time for that frequency, and blue pixels represent a decrease in power. Group differences are shown in the larger heatmaps (C and F). Significant differences, as determined by a non-parametric permutation test (see methods), are illustrated as dotted lines surrounding clusters of time-frequency points. The young animals show an increase in long-latency gamma and a decrease in long-latency beta, whereas the old animals show a significantly attenuated version of these changes.

For each mouse, every ERP response was transformed using an adaptive Morlet wavelet transform, which uses a dynamic wavelet parameter that increases with frequency, for optimal time-frequency resolution (Cohen, 2014; Ethridge et al., 2017). The total power of each animal's responses was calculated by taking the average of the spectral power (voltage squared) across trials. Baseline-normalized power was calculated by first averaging across the pre-stimulus period (with a 50ms buffer), to find the baseline. The entire time-frequency transform was then divided by the baseline power for each frequency, and dB-transformed to calculate the dB-change from baseline, which is

shown for the young AC, FC (Figure 3.5A, D) and old AC, FC (Figure 3.5B, E). Red signifies an increase in power relative to baseline, and blue signifies a decrease in power relative to baseline. The larger heatmap below the group averages shows differences between the two age groups.

In the group averages (shown in the upper panels), the pattern of activity shows a broadband beta/gamma power onset response, followed by an increase in gamma-power and decrease in beta-power, relative to baseline. These longer-latency responses quantify oscillatory neural dynamics that extend beyond the onset response, and have been demonstrated in other mammals (Brosch et al., 2002; Franowicz & Barth, 1995; Jeschke et al., 2008). To statistically compare groups, a nonparametric permutation method was implemented (see methods). Significant differences are demarcated in Figure 3.5C (AC) and Figure 3.5F (FC) with colored lines. The clusters outlined in red show values that are higher in the 20-month-old mice, compared to the 3-month-old mice, whereas clusters outlined in blue show values that are lower in the old mice, compared to the young. The 20-mo group exhibited attenuated changes to gamma and beta power compared to the young (3-month-old) mice, indicating an age-related decline in event-related spectral perturbations in the gamma and beta bands.

Age-related changes in inter-trial phase clustering to time varying stimuli

A 2-second amplitude-modulated noise stimulus, during which the modulation frequency increases linearly from 1-100 Hz (Figure 3.6A; hereafter, “chirp”), was presented while EEG signals were recorded from the AC and FC. This stimulus allows a quantification of the temporal fidelity of evoked responses to a time varying stimulus and

facilitates identification of changes in temporal processing using EEG recordings. A dynamic complex Morlet transform (Cohen, 2014) was applied to calculate the complex

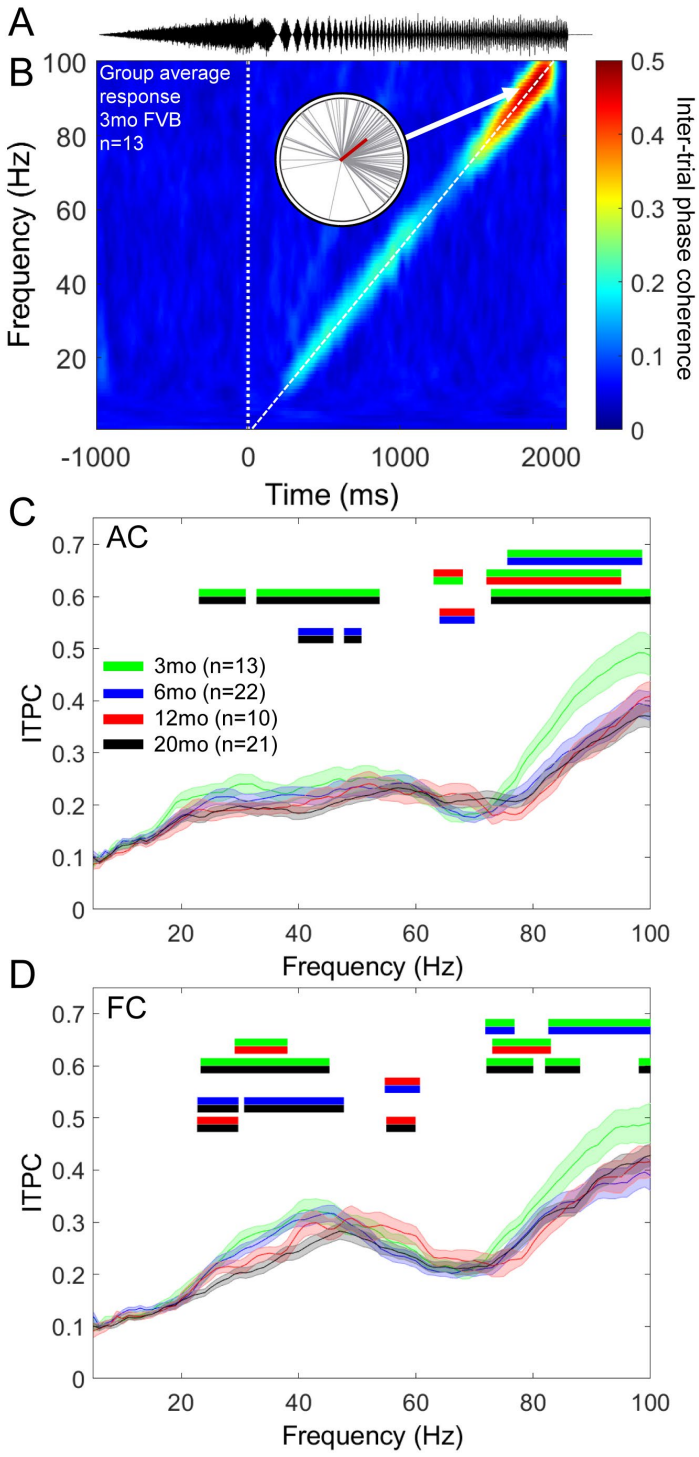

Figure 3.6. Temporal fidelity of responses to an amplitude-modulated chirp stimulus declines with age. An amplitude-modulated broadband noise chirp was presented 300 times to groups of 3-, 6-, 12-, and 20-month-old mice. The consistency of the EEG responses of the mice to these stimuli was measured as inter-trial phase clustering (ITPC). The oscillogram (A) shows an example of the auditory stimulus and the 2D heatmap (B) shows the group average ITPC values of 3-month-old mice in response to the stimulus. The inset polar plot shows a schematic example of the calculation of ITPC: the phases for the response at a particular frequency at a particular time are plotted on a unit circle. The length of the average vector is the ITPC value for that time-frequency point. The shaded line graphs (C and D) were generated by finding the maximum ITPC value at each frequency for each mouse. The shaded lines depict age group averages +/- SEM. Significant differences were found by performing pairwise non-parametric permutation cluster-based tests on the 2D ITPC heatmaps (see methods), and these clusters were converted to 1-dimensional frequency ranges. Differences are shown as stacked bars, spanning the frequencies for which two groups being compared are different. The group represented by the color on top has significantly higher ITPC than the group represented by the color on the bottom. Older mice show less consistent responses to the stimulus across a broad range of frequencies, compared to younger mice.

time-frequency representation of the responses to the chirp stimulus. The inter-trial phase clustering (ITPC; also referred to as 'phase-locking factor'), was calculated using the phase derived from the complex transform (see inset, Figure 3.6B) (Cohen, 2014). The ITPC measures the consistency of responses to the chirp stimulus across trials. The 2D ITPC heatmap shows a diagonal response (Figure 3.6B), meaning that the oscillations in brain activity recorded with the EEG electrodes recapitulate the instantaneous amplitude-modulation frequency of the auditory stimulus. We then used a pairwise nonparametric permutation testing approach to find ranges of frequencies that were significantly different between age groups (see methods). To flatten the response into one dimension, we extracted the maximal ITPC value for each frequency, which occurred along the diagonal (highlighted with a dotted white line in Figure 3.6B), at the instantaneous modulation frequency of the stimulus.

The complete results of the pairwise comparisons between age groups are represented in Figure 3.6C-D. In the signals recorded from AC and FC, 3-mo old mice had more consistent responses at lower frequencies (~20-50 Hz) and higher frequencies (~75-100 Hz), compared to 20-mo old mice. Additionally, in the FC, the 6- and 12-mo old mice had more consistent responses at 22-28 Hz, compared to the 20-mo old mice. In the AC, the 3-mo old mice had more consistent responses at higher frequencies (~75-100 Hz) compared to 6-, 12-, and 20-mo old mice. These results show an age-related increase in the trial-to-trial variability in temporal consistency of responses to time varying stimuli across a range of modulation frequencies, mostly within the gamma frequency range.

Acute nicotine injections reverse age-related changes in resting and sound evoked EEG components in 20-mo old mice

Nicotine and other AChR modulators improve cognitive and sensory measures in aged subjects (Askew et al., 2017; Barr et al., 2008; Bueno-Junior et al., 2017; Lawrence et al., 2002; Levin et al., 2006; Newhouse et al., 2004). In the auditory system, systemic administration of nicotine sharpens tuning by increasing gain and narrowing receptive fields (Askew et al., 2017). This effect is mediated in part by the actions of nicotinic agonists at nAChRs on thalamocortical inputs to the auditory cortex, which decrease in density with age (Sottile et al., 2017). We hypothesized that an acute injection of nicotine will reverse age-related auditory phenotypes identified in previous sections. Specifically, we tested the hypotheses that nicotine (compared to saline) would increase resting EEG gamma power, normalize event-related desynchronization, and increase the ITPC to chirp responses in 20-mo old mice.

We injected 20-month-old mice with 0.5 mg/kg (freebase) nicotine dihydrate ditartrate dissolved in sterile saline and immediately recorded resting EEG for 5 minutes, followed by responses to auditory stimuli. These acute nicotine injections were counterbalanced with injections of sterile saline, to control for order and injection effects. Figure 3.7 demonstrates the partial reversal of age-related changes in EEG power and the modulation of power by movement. Previously we showed that gamma power decreases with age in mice (Figure 3.3). Here we demonstrate that an acute injection of nicotine increases low-gamma power in the AC and FC of mice during movement (Figure 3.7A and 7B), partially reversing age-related changes (paired t-test; AC: $p=0.0228$; FC:

p=0.0041). Significant p-values (after correcting for multiple comparisons using the Holm procedure) are marked with asterisks (*). The power values in Figure 3.7A-D are displayed as ratios of average 3-month-old values to show the reversal of age-related changes. The modulation of gamma power by movement is diminished in older mice (Figure 3.4). Following an injection of nicotine in the old mice, low-gamma power in the AC and FC is modulated by movement to a greater degree. In the FC, high-gamma power is increased during movement following nicotine administration, and movement-related

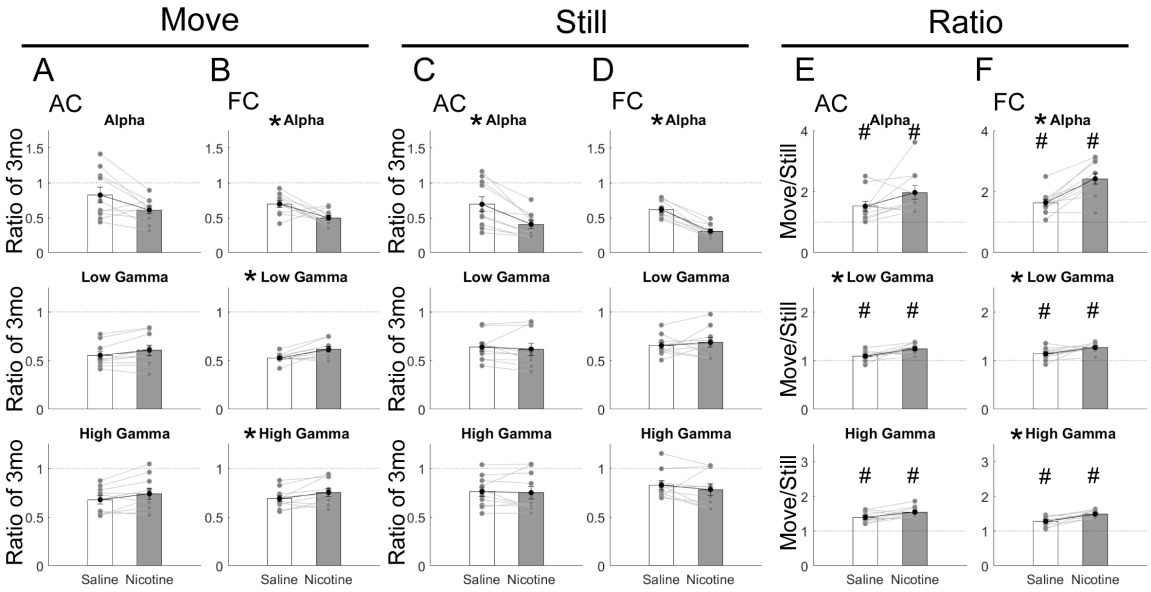

Figure 3.7. An acute injection of nicotine increases movement related modulation of EEG power. In old mice, an acute injection of nicotine causes movement- and frequency-specific changes in EEG power. Significant differences between saline-injection and nicotine-injection conditions are shown with asterisks (paired t-tests, Holm procedure corrected for multiple comparisons). During movement, alpha, low gamma, and high gamma power is increased in the frontal cortex (B) following an injection of nicotine. During the 'still' condition, alpha power is decreased in the auditory (C) and frontal (D) cortices. A-D are displayed as a ratio of the mean power in the 3-month-old mice. The movement related modulation (move:still ratio) of low gamma power is increased in the auditory cortex following an injection of nicotine (E), while the movement related modulation in all frequency bands is increased in the frontal cortex (F). Significant movement-related modulation of power is denoted for each condition and each frequency band with a '#' character.

modulation of high-gamma power is likewise increased. Acute nicotine decreases alpha power during still and move conditions in the AC and FC (Figure 3.7A-D), and increases the modulation of alpha power by movement in the FC (Figure 3.7F). Complete results from statistical analyses can be found in Table 3.4.

Twenty-month old mice show attenuated long-latency beta and gamma changes in the ERSP (Figure 3.5). The increase in long-latency gamma and the decrease in long-latency beta are both smaller in magnitude in old mice compared to young (3-mo old) mice. Here we injected 20-month-old mice with nicotine and, following a 5-minute rest

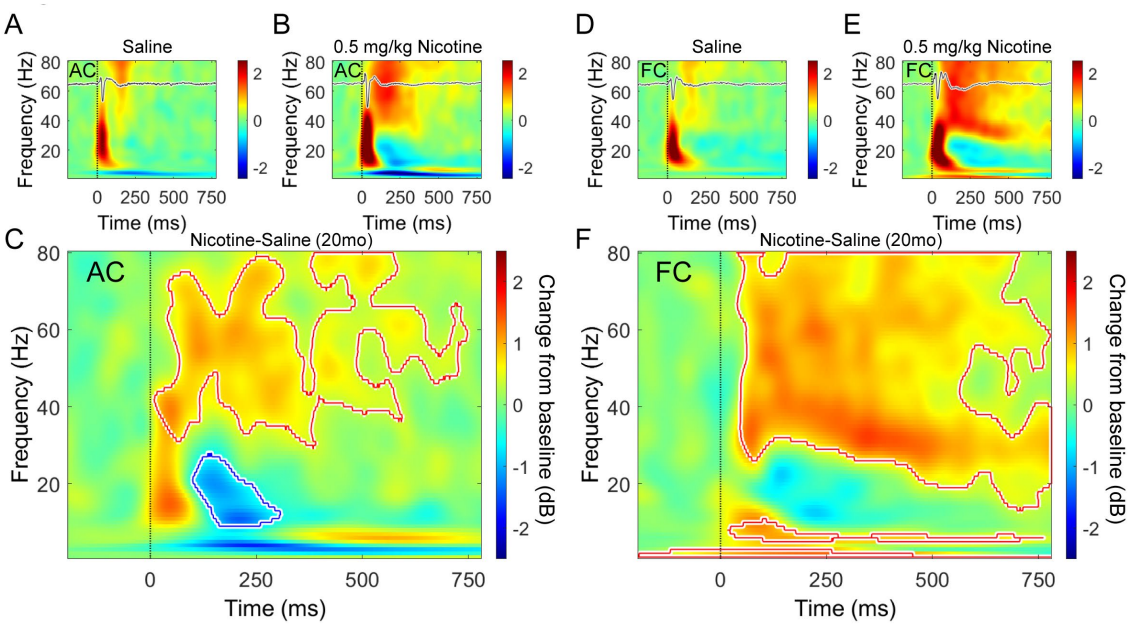

Figure 3.8. Acute injections of nicotine reverse age-related changes in event-related long-latency induced gamma and beta power. Group average ERSPs are shown for saline (A and D) and nicotine (B and E) conditions for auditory and frontal cortex. Mice injected with nicotine showed increases in long-latency gamma in both the auditory (C) and frontal (F) cortices, and decreased long-latency beta in the auditory cortex, compared to mice injected with saline, suggesting that nicotine reverses age-related changes in long-latency induced power in response to sound.

period, recorded their responses to 100 ms broadband noise pulses (0.25 Hz, 70 dB SPL). Figure 3.8, which displays baseline-normalized power for each injection condition, and

the difference between them, shows that nicotine has a pronounced effect on long-latency gamma and beta. In the AC, long-latency gamma is increased, while long-latency beta is decreased, reversing the age-related attenuation of these frequency-specific responses. In the FC, long-latency gamma is increased for over 700 ms post-stimulus, although long-latency beta power is not significantly decreased as seen in the AC.

We recorded responses to the chirp stimulus following an injection of nicotine. This experiment was performed a week after the ERP recordings, to mitigate effects of repeated injections. Figure 3.9 shows a rescue of chirp ITPC in 20-month-old mice by nicotine. Responses from nicotine-injected mice are shown in purple, with saline-injected shown in black and young in green. We consider a full rescue to include frequency ranges where response ITPC in the nicotine-injected mice is significantly higher than saline-injected, and not different from the young responses. In the AC, this includes the 25-35 Hz and 75-90 Hz ranges, which were both decreased in the old mice compared to the young. Partial rescues, which include the frequencies at which the response in the nicotine-injected response was not significantly different from either saline-injected or young, occurred in the AC from 15-25 Hz and 35-50 Hz. In the FC, a partial rescue occurred around 40-50 Hz, and 75-90 Hz. These data indicate that acute nicotine increases trial-by-trial temporal fidelity of responses in the gamma-band of old mice suggesting improvement in auditory temporal processing.

Discussion

We report multiple novel age-related electrophysiological changes in cortical neural oscillations and show that acute nicotine administration in old mice can reverse

these changes. There is an overall increase in low frequency power and a decrease in high frequency power with age (Figure 3.3). Both resting EEG gamma power and the movement-related modulation of resting EEG gamma power decline with age (Figures

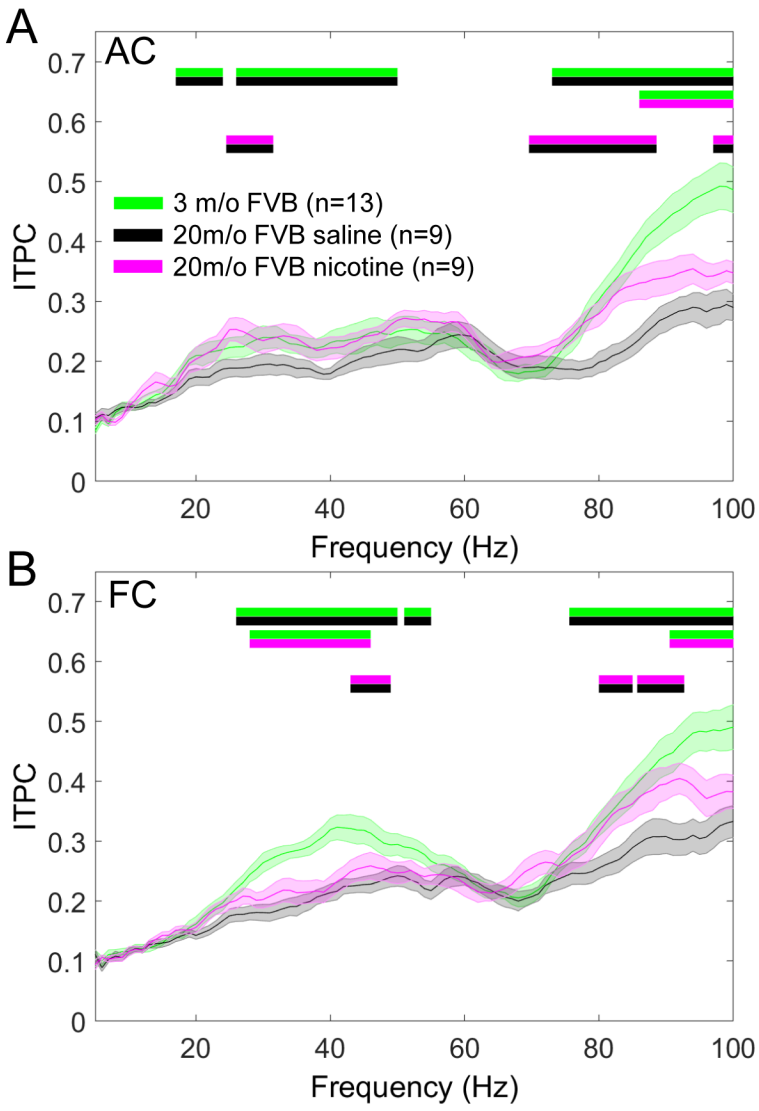

Figure 3.9. An acute injection of nicotine reverses age-related temporal fidelity deficits in response to amplitude modulated chirps. The line plots and significant differences were calculated as in Figure 3.6. Differences are shown as stacked bars, spanning the frequencies for which two groups being compared are different. The group represented by the color on top has significantly higher ITPC than the group represented by the color on the bottom. Whereas the responses from saline-injected old mice were less consistent than the young mice, the responses recorded from the auditory cortex (A) of the same old mice injected with nicotine were not significantly different from responses recorded from young mice at beta, low gamma, and high gamma frequency ranges. The responses from nicotine-injected old mice are significantly more consistent than responses from saline-injected old mice at a subset of these frequency ranges. The responses recorded from the frontal cortex (B) were more consistent in old animals following an injection of nicotine, though the consistency of responses was still significantly lower than those of young mice across the low gamma and high gamma frequency ranges.

3.3, 3.4). The ERP component amplitudes and latencies do not show considerable change with age, but a significant decline in event-related spectral perturbations occurs in old mice (Figure 3.5). Responses to time varying amplitude modulated stimuli (chirp) reveals a decline in ITPC with age (Figure 3.6C-D). Acute nicotine increased resting EEG gamma power, movement-related modulation of gamma power, event-related spectral perturbation and ITPC to time varying stimuli (Figures 3.7-3.9). We recorded EEG signals from both the AC and FC, because the FC may compensate for age-related declines in auditory processing (Grossman et al., 2002; Martins et al., 2015; Peelle & Wingfield, 2016; Tyler et al., 2010). However, AC and FC show mostly similar directions of change in age-related EEG phenotypes and nicotine-induced recovery.

Movement related modulation of gamma power decreases with age

Movement modulates cortical EEG power, with beta power decreasing and alpha and gamma power increasing with movement across all age groups. We present the novel finding that the movement related modulation of gamma power decreases with age (Figure 3.4). Correlating movement data with EEG power shows that, in young mice, gamma power is higher at high velocities compared to the same correlation in old mice. Activation of secondary motor cortex enhances inhibition in A1 via activation of local PV neurons (Nelson et al., 2013; Schneider et al., 2014; Zhou et al., 2014). Increasing PV neuronal activity enhances power in the gamma band (Cardin et al., 2009; Sohal et al., 2009). The observed movement related increase in gamma power in our study, which is consistent with previous findings (Zhou et al., 2014), may occur from activation of PV neurons by projections from the motor cortex. The behavioral relevance of movement

related modulation of auditory cortex remains speculative, but the efferent copy-like timing effects (Schneider et al., 2014) suggest that this may function to reduce sensitivity to self-generated sounds, including vocalizations (Curio et al., 2000; Saoud et al., 2012). Reduction of such modulation with age may be detrimental for audio-vocal feedback control (Li et al., 2018; Liu et al., 2011).

Induced neural oscillations in response to sound change with age

Our data shows that aging is associated with altered ERSPs. Time frequency analyses of EEGs recorded in response to auditory stimuli reveal two types of gamma oscillations: evoked and induced (Galambos, 1992; Pantev, 1995; Pfurtscheller & Lopes da Silva, 1999). Evoked gamma is phase locked to the stimulus and occurs within 100 msec of stimulus onset. Induced gamma, occurs in the 150-400 msec window, is not phase locked to the stimulus and is characterized as ERSP (Brosch et al., 2002; Crone et al., 2001; Franowicz & Barth, 1995). ERSPs in response to auditory stimuli have been measured in humans (Cervenka et al., 2011; Christov & Dushanova, 2016; Edwards et al., 2005; Flinker et al., 2010; Ray et al., 2008; Sinai et al., 2005, 2009) and several animal models, including rats (Franowicz & Barth, 1995; Macdonald et al., 1996; MacDonald et al., 1998; Sukov & Barth, 2001), gerbils (Jeschke et al., 2008), mice (Ehlers & Criado, 2009) and macaques (Brosch et al., 2002), but how aging affects auditory ERSPs is unclear. We observed increased induced gamma power and decreased beta power, compared to baseline, across young and old mice with the same time course observed in the macaque and rat cortex (Brosch et al., 2002; Franowicz & Barth, 1995).

However, the event-related modulation of induced power was significantly reduced in the old mice.

The ERSP quantifies stimulus induced dynamics of neural oscillations and has been associated with cortical activation and attention in somatic (Tallon-Baudry et al., 1996), visual (Desmedt & Tomberg, 1994), and auditory cortex (Jokeit & Makeig, 1994). Metherate & Cruikshank (1999) showed that thalamic stimulation caused an early glutamatergic potential in the input layer of auditory cortex. This was followed by gamma-band fluctuations driven by polysynaptic activity mainly in the middle and superficial layers and propagated intracortically. This may facilitate formation of transient neural assemblies by synchronizing activity across rapidly changing pools of neurons. Taken together, the reduced gamma band induced power with age suggests a general reduction in such corticocortical functional assemblies and reduction of cortical activation by stimuli which may have implications for processing sequential stimuli (Lisman & Idiart, 1995; Metherate & Cruikshank, 1999). Future research with task-related measurements of ERSPs in old mice is required to address if reduced gamma power is associated with attentional demands in specific auditory tasks.

Aging is associated with a decline in the ITPC at gamma band frequencies when tested with time varying amplitude modulated signals. This is consistent with a degradation of precise timing in the aging auditory system, as has been shown in humans (Anderson et al., 2012; Chen & Glover, 2015; Harris & Dubno, 2017) and rats (Herrmann et al., 2017; Parthasarathy & Bartlett, 2011; Parthasarathy et al., 2019). Studies of macaques have also shown an age-related decrease in the number of A1 neurons that

follow AM signals (Overton & Recanzone, 2016) and decreased phase-locking precision to stimulus envelopes (Ng & Recanzone, 2018). Accuracy in temporal processing is important in fundamental functions of the auditory system including sound localization and discrimination of amplitude and frequency modulations. Age-related decline in speech processing may arise from changes in temporal processing (Gordon-Salant et al., 2011; Mazelová et al., 2003; Tremblay et al., 2002).

Potential mechanisms of age-related decline in gamma oscillations

The 20mo old mice in this study showed elevated ABR thresholds than the 3mo old mice (Figure 3.1). The altered EEG responses may partially be related to this threshold shift. However, the P1 and N1 amplitudes of the ERPs did not differ between the young and old mice when presented with a 70dB stimuli, indicating that the evoked response synchrony or amplitude was similar across age. Therefore, the altered gamma responses are unlikely to be related to hearing threshold differences. The reversal of EEG phenotypes in old mice with acute nicotine also indicates that the reduced gamma was unlikely to be due to increased hearing thresholds, and the effects reflect central changes.

Over the lifespan, the balance of excitation and inhibition shifts in the central auditory system (Caspary et al., 2008). The density of PV+ neurons decreases with age in the murine auditory cortex, and perineuronal nets (PNN) are degraded (Brewton et al., 2016; Martin del Campo et al., 2012; Rogalla & Hildebrandt, 2020). PNNs are thought to increase excitability of PV neurons (Balmer, 2016) and to protect them from oxidative stress (Cabungcal et al., 2013). Loss of both PV expression and PNNs with age may explain the decreased gamma band power and its movement related modulation. The

frequency-specific changes in oscillations may also be related to life-span changes in $GABA_AR$ $\gamma 1$ subunit composition in the auditory neuraxis (Robinson et al., 2019). Because gamma oscillations shape sensory processing, particularly in relation to consistency of timing of responses (Cardin et al., 2009), these data suggest that age-related decline in ITPC may be due to reduced activation of PV neurons and gamma power in the auditory cortex.

Potential mechanisms of nicotine effects on EEG phenotypes in aging

An acute injection of nicotine significantly reverses age-related reduction in resting, induced, and evoked gamma power. Previous work has shown that nicotine administration increased gamma power in rat PFC, and this increase was associated with improved visual attention (Bueno-Junior et al., 2017). Cholinergic modulation influences signaling throughout the auditory system, from the cochlea to the cortex (Askew et al., 2017; Schofield et al., 2011), and age-related changes have been demonstrated at many of these sites of cholinergic modulation (Sottile et al., 2017; Raza et al., 1994) and likely contribute to age-related auditory processing deficits.

Changes in inhibitory control and cholinergic modulation in the auditory system may account for the system-level age-related changes we observe with EEG analysis. Vasoactive intestinal peptide-expressing (VIP) inhibitory interneurons express nicotinic acetylcholine receptors, and are responsive to nicotinic agonists (Gulledge et al., 2007). VIP neurons inhibit somatostatin-positive and PV interneurons, both of which inhibit pyramidal cells (Askew et al., 2019; Lee et al., 2013; Pfeffer et al., 2013). Ultimately, activation of VIP neurons leads to disinhibition of cortical activity (Pi et al. 2013, Lee et

al. 2013). Nicotine excites VIP neurons and facilitates a sharpening of auditory tuning (Askew et al., 2017). Whether VIP neuron density declines in auditory cortex with age is debated (Cha et al., 1997, Ouellet and de Villers-Sidani, 2014) and whether nicotinic receptor density of VIP neurons declines is unknown. Future studies of aged animals are needed to test if nicotine enhances auditory processing by boosting the signal of the nicotinic receptors on VIP neurons.

Conclusions

We demonstrate robust age-related electrophysiological changes in the murine auditory system, including a reduction in resting, movement-related, induced and evoked gamma power. Similar EEG/MEG measures can be relatively easily obtained in humans with non-invasive scalp recordings. The observed reduction in power and fidelity of gamma oscillations is consistent with age related declines in markers of PV and SOM inhibitory neurons in the rodent cortex. The acute nicotine effect suggests that these cells can be activated towards normal (young) level and indicates that at least some age-related brain changes can be reversed with pharmacological approaches. Future studies are needed to identify the effects of chronic nicotine treatment as well as treatments given in the middle age groups. If studies in humans show similar results to what we have observed in mice, then nicotine or other nicotinic agonists may be profoundly beneficial for aging adults with central auditory processing disruptions in the absence of pathological hearing loss.

	3mo	6mo	12mo	20mo
Percent movement	36% (12%)	39% (11%)	37% (11%)	40% (10%)
Mean velocity (cm/s)	5.4 (0.8)	n/a	n/a	6.3 (1.0)

Table 3.1: Movement properties across age. Mice in the four age groups moved for approximately the same amount of time during the recording sessions. On average, 20-month-old mice moved faster than 3-month-old mice.

AC	p-value	K-W H	p-value	K-W H	p-value	K-W H	p-value	K-W H	p-value	K-W H	p-value	K-W H	p-value	K-W H
Move	Main Effect of Age		**3mo-6mo**		**3mo-12mo**		**3mo-20mo**		**6mo-12mo**		**6mo-20mo**		**12mo-20mo**	
Theta (3-7 Hz)	0.152	9.3												
Alpha (8-13 Hz)	**0.023**	13.4	0.089	17.2	1.000	8.3	1.000	-4.5	1.000	-8.8	**0.003**	-21.7	0.346	-12.8
Beta (14-29 Hz)	**0.004**	17.0	**0.000**	28.0	**0.036**	20.6	0.365	13.2	1.000	-7.3	0.110	-14.8	1.000	-7.4
Low Gamma (30-59 Hz)	**0.001**	19.9	**0.002**	25.5	**0.022**	21.7	**0.000**	30.0	1.000	-3.7	1.000	4.6	1.000	8.3
High Gamma (60-100 Hz)	**0.007**	16.0	0.105	16.7	0.158	16.7	**0.000**	28.2	1.000	-0.1	0.402	11.5	0.526	11.5
HFO (101-250 Hz)	2.633	2.7												
Still	Main Effect of Age		**3mo-6mo**		**3mo-12mo**		**3mo-20mo**		**6mo-12mo**		**6mo-20mo**		**12mo-20mo**	
Theta	0.108	10.1												
Alpha	0.062	11.3												
Beta	**0.008**	15.8	**0.001**	26.6	**0.016**	22.5	0.220	14.7	1.000	-4.1	0.342	-11.9	1.000	-7.8
Low Gamma	**0.025**	13.2	**0.007**	23.0	0.093	18.1	**0.007**	23.0	1.000	-4.8	1.000	0.0	1.000	4.8
High Gamma	0.191	8.8												
HFO	4.874	1.0												
Ratio	Main Effect of Age		**3mo-6mo**		**3mo-12mo**		**3mo-20mo**		**6mo-12mo**		**6mo-20mo**		**12mo-20mo**	
Theta	5.696	0.4												
Alpha	0.092	10.4												
Beta	0.891	5.3												
Low Gamma	0.175	9.0												
High Gamma	4.000	1.6												
HFO	4.373	1.3												
FC														
Move	Main Effect of Age		**3mo-6mo**		**3mo-12mo**		**3mo-20mo**		**6mo-12mo**		**6mo-20mo**		**12mo-20mo**	
Theta	0.453	6.9												
Alpha	**0.007**	15.9	0.106	16.7	1.000	3.6	1.000	-7.8	0.311	-13.1	**0.001**	-24.5	0.554	-11.4
Beta	**0.018**	13.9	**0.001**	26.2	0.158	16.6	0.195	15.1	0.940	-9.6	0.447	-11.2	1.000	-1.6
Low Gamma	**0.001**	20.1	**0.003**	24.4	0.162	16.6	**0.000**	30.3	1.000	-7.8	1.000	5.9	0.254	13.7
High Gamma	0.076	10.8												
HFO	1.160	4.7												
Still	Main Effect of Age		**3mo-6mo**		**3mo-12mo**		**3mo-20mo**		**6mo-12mo**		**6mo-20mo**		**12mo-20mo**	
Theta	0.073	10.9												
Alpha	0.320	7.7												
Beta	0.087	10.5												
Low Gamma	0.059	11.4												
High Gamma	1.396	4.3												
HFO	5.871	0.2												
Ratio	Main Effect of Age		**3mo-6mo**		**3mo-12mo**		**3mo-20mo**		**6mo-12mo**		**6mo-20mo**		**12mo-20mo**	
Theta	2.083	3.3												
Alpha	0.068	11.1												
Beta	1.754	3.7												
Low Gamma	**0.018**	14.0	1.000	1.7	1.000	7.1	**0.012**	21.9	1.000	5.4	**0.008**	20.2	0.176	14.7
High Gamma	1.241	4.6												
HFO	2.358	3.0												

Table 3.2. Age and movement related changes in EEG power

Raw results from Kruskal-Wallis H tests and pairwise Dunn's nonparametric tests. The first two columns of data show the results from the Kruskal-Wallis H tests, Bonferroni corrected for multiple comparisons (p-values were multiplied by 6, and the significance threshold was set to 0.05). Post-hoc pairwise Dunn's nonparametric tests were performed only if the corrected p-value for a frequency band was significant. The Dunn's nonparametric tests were Bonferroni corrected for multiple comparisons. Non-significant rows are gray, and significant p-values are bolded.

AC	**Main effect of age**		**3mo-20mo**	
	Bonferroni-corrected p-value	K-W H	Adj. p-value	Dunn's Test z
P1 Amplitude	0.928	5.912		
N1 Amplitude	2.552	3.515		
P2 Amplitude	0.064	11.759		
N2 Amplitude	0.536	7.168		
P1 Latency	5.280	1.599		
N1 Latency	1.424	4.914		
P2 Latency	0.080	11.314		
N2 Latency	7.576	0.367		
FC	**Main effect of age**		**3mo-20mo**	
	Bonferroni-corrected p-value	K-W H	Adj. p-value	Dunn's Test z
P1 Amplitude	0.712	6.518		
N1 Amplitude	6.368	1.022		
P2 Amplitude	0.584	6.952		
N2 Amplitude	**0.048**	**12.593**	**0.003**	**-22.750**
P1 Latency	0.120	10.395		
N1 Latency	3.312	2.859		
P2 Latency	3.208	2.939		
N2 Latency	0.368	8.024		

Table 3.3. Group average ERP waveforms show few age-related differences.
A 100 ms broadband noise stimulus was presented to the 3mo, 6mo, 12mo, and 20mo mice 120 times at a rate of 0.25 Hz at 70 dB SPL. The trials were averaged to yield individual ERP waveforms for each age group. The ERP components (P1, N1, P2, and N2) were quantified from each individual animal, and group comparisons are presented in this table. Kruskal-Wallis H tests were used to test for age-related changes in amplitude and latency across all age groups. The p-values from the K-W H tests were Bonferroni corrected for multiple comparisons (p*8), and the significance threshold was set at 0.05. For measures that showed significant age-related effects, Dunn's nonparametric tests were used to compare age groups in a pairwise manner. Only the 3mo-20mo comparison is shown here for simplicity. The magnitude of N2 is higher in the FC of young mice compared to older mice.

p-values from t-tests with unequal variance, Holm-corrected			
	Move	Still	Ratio
AC	p-value	p-value	p-value
Alpha	0.0391	**0.0018**	0.1015
Low Gamma	0.0228	0.5714	**0.0148**
High Gamma	0.062	0.7497	0.0203
FC			
Alpha	0.0201	**<0.0001**	**0.0005**
Low Gamma	**0.0041**	0.4764	**0.0293**
High Gamma	0.0429	0.3523	**0.0049**

p-values from t-tests with unequal variance, Holm-corrected			
	Move	Still	Ratio
AC	p-value	p-value	p-value
Alpha	0.0391	**0.0018**	0.1015
Low Gamma	0.0228	0.5714	**0.0148**
High Gamma	0.062	0.7497	0.0203
FC			
Alpha	0.0201	**<0.0001**	**0.0005**
Low Gamma	**0.0041**	0.4764	**0.0293**
High Gamma	0.0429	0.3523	**0.0049**

Table 3.4. Nicotine effects on movement related EEG

An acute injection of 0.5 mg/kg nicotine changes resting EEG power in 20mo mice, significantly reversing some age-related changes. This table contains p-values from t-tests with unequal variance, comparing resting power and movement related modulation of power in 20mo mice injected with either saline or nicotine. The p-values that are significant after correcting for multiple comparisons (Holm procedure) are in bold. The data for these comparisons is shown in Figure 3.7.

References

Anderson, S., Parbery-Clark, A., White-Schwoch, T., & Kraus, N. (2012). Aging affects neural precision of speech encoding. *The Journal of Neuroscience*, *32*(41), 14156–14164. https://doi.org/10.1523/JNEUROSCI.2176-12.2012

Askew, C. E., Lopez, A. J., Wood, M. A., & Metherate, R. (2019). Nicotine excites VIP interneurons to disinhibit pyramidal neurons in auditory cortex. *Synapse*, *73*(9), 1–12. https://doi.org/10.1002/syn.22116

Askew, C., Intskirveli, I., & Metherate, R. (2017). Systemic nicotine increases gain and narrows receptive fields in a1 via integrated cortical and subcortical actions. *ENeuro*, *4*(3). https://doi.org/10.1523/ENEURO.0192-17.2017

Balmer, T. S. (2016). Perineuronal nets enhance the excitability of fast-spiking neurons. *ENeuro*, *3*(4), 745–751. https://doi.org/10.1523/ENEURO.0112-16.2016

Barr, R. S., Culhane, M. A., Jubelt, L. E., Mufti, R. S., Dyer, M. A., Weiss, A. P., Deckersbach, T., Kelly, J. F., Freudenreich, O., Goff, D. C., & Evins, A. E. (2008). The effects of transdermal nicotine on cognition in nonsmokers with schizophrenia and nonpsychiatric controls. *Neuropsychopharmacology*, *33*(3), 480–490. https://doi.org/10.1038/sj.npp.1301423

Başar, E., Schürmann, M., Demiralp, T., Baar-Eroglu, C., & Ademoglu, A. (2001). Event-related oscillations are “real brain responses” - wavelet analysis and new strategies. *International Journal of Psychophysiology*, *39*(2–3), 91–127. https://doi.org/10.1016/S0167-8760(00)00135-5

Brewton, D. H., Kokash, J., Jimenez, O., Pena, E. R., & Razak, K. A. (2016). Age-related deterioration of perineuronal nets in the primary auditory cortex of mice. *Frontiers in Aging Neuroscience*, *8*, 270. https://doi.org/10.3389/fnagi.2016.00270

Brosch, M., Budinger, E., & Scheich, H. (2002). Stimulus-related gamma oscillations in primate auditory cortex. *Journal of Neurophysiology*, *87*(6), 2715–2725. https://doi.org/10.1152/jn.00583.2001

Bueno-Junior, L. S., Simon, N. W., Wegener, M. A., & Moghaddam, B. (2017). Repeated nicotine strengthens gamma oscillations in the prefrontal cortex and improves visual attention. *Neuropsychopharmacology*, *42*(8), 1590–1598. https://doi.org/10.1038/npp.2017.15

Burianova, J., Ouda, L., Profant, O., & Syka, J. (2009). Age-related changes in GAD levels in the central auditory system of the rat. *Experimental Gerontology*, *44*(3), 161–169. https://doi.org/10.1016/j.exger.2008.09.012

Cabungcal, J. H., Steullet, P., Morishita, H., Kraftsik, R., Cuenod, M., Hensch, T. K., & Do, K. Q. (2013). Perineuronal nets protect fast-spiking interneurons against oxidative stress. *Proceedings of the National Academy of Sciences of the United States of America*, *110*(22), 9130–9135. https://doi.org/10.1073/pnas.1300454110

Cacioppo, J. T., & Hawkley, L. C. (2009). Perceived social isolation and cognition. *Trends in Cognitive Sciences 13*(10), 447–454. https://doi.org/10.1016/j.tics.2009.06.005

Cardin, J. A., Carlén, M., Meletis, K., Knoblich, U., Zhang, F., Deisseroth, K., Tsai, L. H., & Moore, C. I. (2009). Driving fast-spiking cells induces gamma rhythm and controls sensory responses. *Nature*, *459*(7247), 663–667. https://doi.org/10.1038/nature08002

Carlson, G. C., Talbot, K., Halene, T. B., Gandal, M. J., Kazi, H. A., Schlosser, L., Phung, Q. H., Gur, R. E., Arnold, S. E., & Siegel, S. J. (2011). Dysbindin-1 mutant mice implicate reduced fast-phasic inhibition as a final common disease mechanism in schizophrenia. *Proceedings of the National Academy of Sciences of the United States of America*, *108*(43). https://doi.org/10.1073/pnas.1109625108

Caspary, D. M., Hughes, L. F., & Ling, L. L. (2013). Age-related GABAA receptor changes in rat auditory cortex. *Neurobiology of Aging*, *34*(5), 1486–1496. https://doi.org/10.1016/j.neurobiolaging.2012.11.009

Caspary, D. M., Ling, L., Turner, J. G., & Hughes, L. F. (2008). Inhibitory neurotransmission, plasticity and aging in the mammalian central auditory system. *Journal of Experimental Biology*, *211*(11), 1781–1791. https://doi.org/10.1242/jeb.013581

Cervenka, M. C., Nagleb, S., & Boatman-Reich, D. (2011). Cortical high-gamma responses in auditory processing. *American Journal of Audiology*, *20*(2). https://doi.org/10.1038/jid.2014.371

Chen, G., Zhang, Y., Li, X., Zhao, X., Ye, Q., Lin, Y., Tao, H. W., Rasch, M. J., & Zhang, X. (2017). Distinct inhibitory circuits orchestrate cortical beta and gamma band oscillations. *Neuron*, *96*(6), 1403-1418. https://doi.org/10.1016/j.neuron.2017.11.033

Chen, J. E., & Glover, G. H. (2015). Functional magnetic resonance imaging methods. *Neuropsychology Review*, *25*(3), 289–313. https://doi.org/10.1007/s11065-015-9294-9

Christov, M., & Dushanova, J. (2016). Functional correlates of brain aging: beta and gamma components of event-related band responses. *Acta Neurobiologiae Experimentalis*, *76*(2), 98–109. https://doi.org/10.21307/ane-2017-009

Cohen, M. X. (2014). Analyzing neural time series data: theory and practice. *MIT press*.

Crone, N., Boatman, D., Gordon, B., & Hao, L. (2001). Induced electrocorticographic gamma activity during auditory perception. *Clinical Neurophysiology*, *112*, 565–582. https://doi.org/10.1016/S1388-2457(00)00545-9

Curio, G., Neuloh, G., Numminen, J., Jousmäki, V., & Hari, R. (2000). Speaking modifies utterance-related activity of the human auditory cortex. *Human Brain Mapping*, *9*, 183–191. https://doi.org/10.1016/s1053-8119(18)30881-4

Desmedt, J. E., & Tomberg, C. (1994). Transient phase-locking of 40 Hz electrical oscillations in prefrontal and parietal human cortex reflects the process of conscious somatic perception. *Neuroscience Letters*, *168*, 126–129. https://doi.org/10.1016/0304-3940(94)90432-4

Edwards, E., Soltani, M., Deouell, L. Y., Berger, M. S., & Knight, R. T. (2005). High gamma activity in response to deviant auditory stimuli recorded directly from human cortex. *Journal of Neurophysiology*, *94*(6), 4269–4280. https://doi.org/10.1152/jn.00324.2005

Ehlers, C. L., & Criado, J. R. (2009). Event-related oscillations in mice: effects of stimulus characteristics. *Journal of Neuroscience Methods*, *181*(1), 52–57. https://doi.org/10.1016/j.jneumeth.2009.04.015

Ethridge, L. E., White, S. P., Mosconi, M. W., Wang, J., Pedapati, E. V., Erickson, C. A., Byerly, M. J., & Sweeney, J. A. (2017). Neural synchronization deficits linked to cortical hyper-excitability and auditory hypersensitivity in fragile X syndrome. *Molecular Autism*, *8*(1), 1–11. https://doi.org/10.1186/s13229-017-0140-1

Featherstone, R. E., Phillips, J. M., Thieu, T., Ehrlichman, R. S., Halene, T. B., Leiser, S. C., Christian, E., Johnson, E., Lerman, C., & Siegel, S. J. (2012). Nicotine receptor subtype-specific effects on auditory evoked oscillations and potentials. *PLoS ONE*, *7*(7). https://doi.org/10.1371/journal.pone.0039775

Flinker, A., Chang, E. F., Kirsch, H. E., Barbaro, N. M., Crone, N. E., & Knight, R. T. (2010). Single-trial speech suppression of auditory cortex activity in humans.

Journal of Neuroscience, *30*(49), 16643–16650. https://doi.org/10.1523/JNEUROSCI.1809-10.2010

Franowicz, M. N., & Barth, D. S. (1995). Comparison of evoked potentials and high-frequency (gamma-band) oscillating potentials in rat auditory cortex. Journal of *Neurophysiology*, *74*(1), 96–112. https://doi.org/10.1152/jn.1995.74.1.96

Galambos, R. (1992). A comparison of certain gamma band (40-Hz) brain rhythms in cat and man. In E. Baar & T. H. Bullock (Eds.), Induced Rhythms in the Brain, 201–216. *Birkhäuser Boston*. https://doi.org/10.1007/978-1-4757-1281-0_11

Gates, G. A., Beiser, A., Rees, T. S., D'Agostino, R. B., & Wolf, P. A. (2002). Central auditory dysfunction may precede the onset of clinical dementia in people with probable Alzheimer's disease. *Journal of the American Geriatrics Society, 50*(3), 482–488. https://doi.org/10.1046/j.1532-5415.2002.50114.x

Ghimire, M., Cai, R., Ling, L., Hackett, T. A., & Caspary, D. M. (2020). Nicotinic receptor subunit distribution in auditory cortex: impact of aging on receptor number and function. *The Journal of Neuroscience*, *40*(30). https://doi.org/10.1523/jneurosci.0093-20.2020

Gil, S. M., & Metherate, R. (2018). Enhanced sensory–cognitive processing by activation of nicotinic acetylcholine receptors. *Nicotine & Tobacco Research*, *21*(3), 377-382. https://doi.org/10.1093/ntr/nty134

Gordon-Salant, S., Fitzgibbons, P. J., & Yeni-Komshian, G. H. (2011). Auditory temporal processing and aging: implications for speech understanding of older people. *Audiology Research*, *1*(1), 9–15. https://doi.org/10.4081/audiores.2011.e4

Grossman, M., Cooke, A., DeVita, C., Alsop, D., Detre, J., Chen, W., & Gee, J. (2002). Age-related changes in working memory during sentence comprehension: an fMRI study. *NeuroImage*, *15*(2), 302–317. https://doi.org/10.1006/nimg.2001.0971

Gulledge, A. T., Park, S. B., Kawaguchi, Y., & Stuart, G. J. (2007). Heterogeneity of phasic cholinergic signaling in neocortical neurons. *Journal of Neurophysiology*, *97*(3), 2215–2229. https://doi.org/10.1152/jn.00493.2006

Harris, K. C., & Dubno, J. R. (2017). Age-related deficits in auditory temporal processing: unique contributions of neural dyssynchrony and slowed neuronal processing. *Neurobiology of Aging*, *53*, 150–158. https://doi.org/10.1016/j.neurobiolaging.2017.01.008

Herrmann, B., Parthasarathy, A., & Bartlett, E. L. (2017). Ageing affects dual encoding of periodicity and envelope shape in rat inferior colliculus neurons. *European Journal of Neuroscience*, *45*(2), 299-311. https://doi.org/10.1111/ejn.13463

Hunter, K. P., & Willott, J. F. (1987). Aging and the auditory brainstem response in mice with severe or minimal presbycusis. *Hearing Research*, *30*(2–3), 207–218. https://doi.org/10.1016/0378-5955(87)90137-7

Intskirveli, I., & Metherate, R. (2012). Nicotinic neuromodulation in auditory cortex requires MAPK activation in thalamocortical and intracortical circuits. Journal of *Neurophysiology*, *107*(10), 2782–2793. https://doi.org/10.1152/jn.01129.2011

Jeschke, M., Lenz, D., Budinger, E., Herrmann, C. S., & Ohl, F. W. (2008). Gamma oscillations in gerbil auditory cortex during a target-discrimination task reflect matches with short-term memory. *Brain Research*, *1220*, 70-80. https://doi.org/10.1016/j.brainres.2007.10.047

Jokeit, H., & Makeig, S. (1994). Different event-related patterns of gamma-band power in brain waves of fast- and slow-reacting subjects. *Proceedings of the National Academy of Sciences of the United States of America*, *91*(14), 6339–6343. https://doi.org/10.1073/pnas.91.14.6339

Lawrence, N. S., Ross, T. J., & Stein, E. A. (2002). Cognitive mechanisms of nicotine on visual attention. *Neuron, 36*(3), 539–548. https://doi.org/10.1016/S0896-6273(02)01004-8

Lee, G. T., Lee, C., Kim, K. H., & Jung, K. Y. (2014). Regional and inter-regional theta oscillation during episodic novelty processing. *Brain and Cognition, 90*, 70–75. https://doi.org/10.1016/j.bandc.2014.06.009

Lee, S., Kruglikov, I., Huang, Z. J., Fishell, G., & Rudy, B. (2013). A disinhibitory circuit mediates motor integration in the somatosensory cortex. *Nature Neuroscience, 16*(11), 1662–1670. https://doi.org/10.1038/nn.3544

Levin, E. D., McClernon, F. J., & Rezvani, A. H. (2006). Nicotinic effects on cognitive function: behavioral characterization, pharmacological specification, and anatomic localization. *Psychopharmacology, 184*(3–4), 523–539. https://doi.org/10.1007/s00213-005-0164-7

Li, J., Hu, H., Chen, N., Jones, J. A., Wu, D., Liu, P., & Liu, H. (2018). Aging and sex influence cortical auditory-motor integration for speech control. *Frontiers in Neuroscience, 12*, 749. https://doi.org/10.3389/fnins.2018.00749

Liao, W., Gandal, M. J., Ehrlichman, R. S., Siegel, S. J., & Carlson, G. C. (2012). MeCP2+/- mouse model of RTT reproduces auditory phenotypes associated with Rett syndrome and replicate select EEG endophenotypes of autism spectrum disorder. *Neurobiology of Disease, 46*(1), 88–92. https://doi.org/10.1016/j.nbd.2011.12.048

Lin, F. R., Ferrucci, L., An, Y., Goh, J. O., Doshi, J., Metter, E. J., Davatzikos, C., Kraut, M. A., & Resnick, S. M. (2014). Association of hearing impairment with brain volume changes in older adults. *NeuroImage, 90*, 84-92. https://doi.org/10.1016/j.neuroimage.2013.12.059

Lisman, J. E., & Idiart, M. A. P. (1995). Storage of 7 +/- 2 short-term memories in oscillatory subcycles. *Science, 267*(5203), 1512–1515.

Liu, P., Chen, Z., Jones, J. A., Huang, D., & Liu, H. (2011). Auditory feedback control of vocal pitch during sustained vocalization: a cross-sectional study of adult aging. *PLoS ONE, 6*(7). https://doi.org/10.1371/journal.pone.0022791

Lovelace, J. W., Ethell, I. M., Binder, D. K., & Razak, K. A. (2018). Translation-relevant EEG phenotypes in a mouse model of Fragile X Syndrome. *Neurobiology of Disease, 115*, 39–48. https://doi.org/10.1016/j.nbd.2018.03.012

Lovelace, J. W., Wen, T. H., Reinhard, S., Hsu, M. S., Sidhu, H., Ethell, I. M., Binder, D. K., & Razak, K. A. (2016). Matrix metalloproteinase-9 deletion rescues auditory evoked potential habituation deficit in a mouse model of Fragile X Syndrome. *Neurobiology of Disease, 89*, 126–135. https://doi.org/10.1016/j.nbd.2016.02.002

MacDonald, K. D., Brett, B., & Barth, D. S. (1996). Inter- and intra-hemispheric spatiotemporal organization of spontaneous electrocortical oscillations. *Journal of Neurophysiology, 76*(1), 423–437. https://doi.org/10.1152/jn.1996.76.1.423

MacDonald, K. D., Fifkova, E., Jones, M. S., & Barth, D. S. (1998). Focal stimulation of the thalamic reticular nucleus induces focal gamma waves in cortex. *Somatosensory and Motor Research, 15*(1), 76.

Makeig, S. (1993). Auditory event-related dynamics of the EEG spectrum and effects of exposure to tones. *Electroencephalography and Clinical Neurophysiology, 86*(4), 283–293. https://doi.org/10.1016/0013-4694(93)90110-H

Maris, E., & Oostenveld, R. (2007). Nonparametric statistical testing of EEG- and MEG-data. *Journal of Neuroscience Methods, 164*(1), 177–190. https://doi.org/10.1016/j.jneumeth.2007.03.024

Martin del Campo, H. N., Measor, K. R., & Razak, K. A. (2012). Parvalbumin immunoreactivity in the auditory cortex of a mouse model of presbycusis. *Hearing Research, 294*(1–2), 31–39. https://doi.org/10.1016/j.heares.2012.08.017

Martins, R., Joanette, Y., & Monchi, O. (2015). The implications of age-related neurofunctional compensatory mechanisms in executive function and language processing including the new temporal hypothesis for compensation. *Frontiers in Human Neuroscience, 9*, 221. https://doi.org/10.3389/fnhum.2015.00221

Matta, S. G., Balfour, D. J., Benowitz, N. L., Boyd, R. T., Buccafusco, J. J., Caggiula, A. R., Craig, C. R., Collins, A. C., Damaj, M. I., Donny, E. C., Gardiner, P. S., Grady, S. R., Heberlein, U., Leonard, S. S., Levin, E. D., Lukas, R. J., Markou, A., Marks, M. J., McCallum, S. E., … Zirger, J. M. (2007). Guidelines on nicotine dose selection for in vivo research. *Psychopharmacology, 190*(3), 269–319. https://doi.org/10.1007/s00213-006-0441-0

Mazelová, J., Popelar, J., & Syka, J. (2003). Auditory function in presbycusis: peripheral vs. central changes. *Experimental Gerontology, 38*(1), 87–94. https://doi.org/https://doi.org/10.1016/S0531-5565(02)00155-9

Metherate, R. (2011). Functional connectivity and cholinergic modulation in auditory cortex. *Neuroscience and Biobehavioral Reviews, 35*(10), 2058–2063. https://doi.org/10.1016/j.neubiorev.2010.11.010

Metherate, R., & Cruikshank, S. J. (1999). Thalamocortical inputs trigger a propagating envelope of gamma-band activity in auditory cortex in vitro. *Experimental Brain Research, 126*(2), 160–174. https://doi.org/10.1007/s002210050726

Metzger, K. L., Maxwell, C. R., Liang, Y., & Siegel, S. J. (2007). Effects of nicotine vary across two auditory evoked potentials in the mouse. Biological *Psychiatry, 61*(1), 23–30. https://doi.org/10.1016/j.biopsych.2005.12.011

Nelson, A., Schneider, D. M., Takatoh, J., Sakurai, K., Wang, F., & Mooney, R. (2013). A circuit for motor cortical modulation of auditory cortical activity. *Journal of Neuroscience, 33*(36), 14342–14353. https://doi.org/10.1523/JNEUROSCI.2275-13.2013

Newhouse, P. A., Potter, A., & Singh, A. (2004). Effects of nicotinic stimulation on cognitive performance. *Current Opinion in Pharmacology, 4*(1), 36–46. https://doi.org/10.1016/j.coph.2003.11.001

Ng, C. W., & Recanzone, G. H. (2018). Age-related changes in temporal processing of rapidly-presented sound sequences in the macaque auditory cortex. *Cerebral Cortex, 28*(11), 3775–3796. https://doi.org/10.1093/cercor/bhx240

Ouda, L., Druga, R., & Syka, J. (2008). Changes in parvalbumin immunoreactivity with aging in the central auditory system of the rat. *Experimental Gerontology, 43*(8), 782–789. https://doi.org/10.1016/j.exger.2008.04.001

Ouellet, L., & de Villers-Sidani, E. (2014). Trajectory of the main GABAergic interneuron populations from early development to old age in the rat primary auditory cortex. *Frontiers in Neuroanatomy, 8*, 40. https://doi.org/10.3389/fnana.2014.00040

Overton, J. A., & Recanzone, G. H. (2016). Effects of aging on the response of single neurons to amplitude-modulated noise in primary auditory cortex of rhesus macaque. *Journal of Neurophysiology, 115*(6), 2911–2923. https://doi.org/10.1152/jn.01098.2015

Pantev, C. (1995). Evoked and induced gamma-band activity of the human cortex. *Brain Topography, 7*(4), 321–330. https://doi.org/10.1007/BF01195258

Panza, F., Lozupone, M., Sardone, R., Battista, P., Piccininni, M., Dibello, V., La Montagna, M., Stallone, R., Venezia, P., Liguori, A., Giannelli, G., Bellomo, A., Greco, A., Daniele, A., Seripa, D., Quaranta, N., & Logroscino, G. (2018). Sensorial frailty: age-related hearing loss and the risk of cognitive impairment and dementia in later life. *Therapeutic Advances in Chronic Disease*, *10*. https://doi.org/10.1177/2040622318811000

Parthasarathy, A, & Bartlett, E. L. (2011). Age-related auditory deficits in temporal processing in F-344 rats. *Neuroscience, 192*, 619–630. https://doi.org/https://doi.org/10.1016/j.neuroscience.2011.06.042

Parthasarathy, A., Herrmann, B., & Bartlett, E. L. (2019). Aging alters envelope representations of speech-like sounds in the inferior colliculus. *Neurobiology of Aging, 73*, 30–40. https://doi.org/10.1016/j.neurobiolaging.2018.08.023

Peelle, J. E., & Wingfield, A. (2016). The neural consequences of age-related hearing loss. *Trends in neurosciences, 39*(7), 486-497. https://doi.org/10.1016/j.tins.2016.05.001

Pfeffer, C. K., Xue, M., He, M., Huang, Z. J., & Scanziani, M. (2013). Inhibition of inhibition in visual cortex: the logic of connections between molecularly distinct interneurons. *Nature Neuroscience, 16*(8), 1068–1076. https://doi.org/10.1038/nn.3446.Inhibition

Pfurtscheller, G., & Lopes da Silva, F. H. (1999). Event-related EEG/MEG synchronization and desynchronization: basic principles. *Clinical*

Neurophysiology, 110, 1842–1857. https://doi.org/10.1016/S1388-2457(99)00141-8

Phillips, J. M., Ehrlichman, R. S., & Siegel, S. J. (2007). Mecamylamine blocks nicotine-induced enhancement of the P20 auditory event-related potential and evoked gamma. *Neuroscience, 144*(4), 1314–1323. https://doi.org/10.1016/j.neuroscience.2006.11.003

Purcell, D. W., John, S. M., Schneider, B. A., & Picton, T. W. (2004). Human temporal auditory acuity as assessed by envelope following responses. *The Journal of the Acoustical Society of America, 116*(6), 3581–3593. https://doi.org/10.1121/1.1798354

Ray, S., Niebur, E., Hsiao, S. S., Sinai, A., & Crone, N. E. (2008). High-frequency gamma activity (80-150 Hz) is increased in human cortex during selective attention. *Clinical Neurophysiology, 119*(1), 116–133. https://doi.org/10.1016/j.clinph.2007.09.136

Raza, A., Milbrandt, J. C., Arneric, S. P., & Caspary, D. M. (1994). Age-related changes in brainstem auditory neurotransmitters: measures of GABA and acetylcholine function. *Hearing Research, 77*(1–2), 221–230. https://doi.org/10.1016/0378-5955(94)90270-4

Rezvani, A., & Levin, E. (2001). Cognitive effects of nicotine. *Biological Psychiatry, 49*(3), 258–267. https://doi.org/10.1016/S0006-3223(00)01094-5

Robinson, L. C., Barat, O., & Mellott, J. G. (2019). GABAergic and glutamatergic cells in the inferior colliculus dynamically express the GABAAR 1 subunit during aging. *Neurobiology of Aging, 80*, 99–110. https://doi.org/10.1016/j.neurobiolaging.2019.04.007

Rogalla, M. M., & Hildebrandt, J. K. (2020). Aging but not age-related hearing loss dominates the decrease of parvalbumin immunoreactivity in the primary auditory cortex of mice. *ENeuro, 7*(3). https://doi.org/ENEURO.0511-19.2020

Rotschafer, S., & Razak, K. (2013). Altered auditory processing in a mouse model of fragile X syndrome. *Brain Research, 1506*, 12–24. https://doi.org/10.1016/j.brainres.2013.02.038

Saoud, H., Josse, G., Bertasi, E., Truy, E., Chait, M., & Giraud, A. L. (2012). Brain-speech alignment enhances auditory cortical responses and speech perception. *Journal of Neuroscience, 32*(1), 275–281. https://doi.org/10.1523/JNEUROSCI.3970-11.2012

Schneider, D. M., & Mooney, R. (2018). How movement modulates hearing. *Annual Review of Neuroscience, 41*, 553–572. https://doi.org/10.1146/annurev-neuro-072116-031215

Schneider, D. M., Nelson, A., & Mooney, R. (2014). A synaptic and circuit basis for corollary discharge in the auditory cortex. *Nature, 513*(7517), 189–194. https://doi.org/10.1038/nature13724

Schofield, B. R., Motts, S. D., & Mellott, J. G. (2011). Cholinergic cells of the pontomesencephalic tegmentum: connections with auditory structures from cochlear nucleus to cortex. *Hearing Research, 279*(1–2), 85–95. https://doi.org/10.1016/j.heares.2010.12.019

Sinai, A., Crone, N. E., Wied, H. M., Franaszczuk, P. J., Miglioretti, D., & Boatman-Reich, D. (2009). Intracranial mapping of auditory perception: event-related responses and electrocortical stimulation. *Clinical Neurophysiology, 120*(1), 140–149. https://doi.org/10.1016/j.clinph.2008.10.152

Sinai, Alon, Bowers, C. W., Crainiceanu, C. M., Boatman, D., Gordon, B., Lesser, R. P., Lenz, F. A., & Crone, N. E. (2005). Electrocorticographic high gamma activity versus electrical cortical stimulation mapping of naming. *Brain, 128*(7), 1556–1570. https://doi.org/10.1093/brain/awh491

Sohal, V. S., Zhang, F., Yizhar, O., & Deisseroth, K. (2009). Parvalbumin neurons and gamma rhythms enhance cortical circuit performance. *Nature, 459*(7247), 698–702. https://doi.org/10.1038/nature07991

Sottile, S. Y., Ling, L., Cox, B. C., & Caspary, D. M. (2017). Impact of ageing on postsynaptic neuronal nicotinic neurotransmission in auditory thalamus. *Journal of Physiology, 595*(15), 5375–5385. https://doi.org/10.1113/JP274467

Sukov, W., & Barth, D. S. (2001). Cellular mechanisms of thalamically evoked gamma oscillations in auditory cortex. *Journal of Neurophysiology, 85*(3), 1235–1245. https://doi.org/10.1152/jn.2001.85.3.1235

Tallon-Baudry, C., Bertrand, O., Delpuech, C., & Pernier, J. (1996). Stimulus specificity of phase-locked and non-phase-locked 40 Hz visual responses in human. *Journal of Neuroscience, 16*(13), 4240–4249. https://doi.org/10.1523/jneurosci.16-13-04240.1996

Tremblay, K. L., Piskosz, M., & Souza, P. (2002). Aging alters the neural representation of speech cues. *NeuroReport, 13*(15), 1865–1870. https://doi.org/10.1097/00001756-200210280-00007

Tyler, L. K., Shafto, M. A., Randall, B., Wright, P., Marslen-Wilson, W. D., & Stamatakis, E. A. (2010). Preserving syntactic processing across the adult life span: the modulation of the frontotemporal language system in the context of age-related atrophy. *Cerebral Cortex, 20*(2), 352–364. https://doi.org/10.1093/cercor/bhp105

Volman, V., Behrens, M. M., & Sejnowski, T. J. (2011). Downregulation of parvalbumin at cortical GABA synapses reduces network gamma oscillatory activity. *Journal of Neuroscience, 31*(49), 18137–18148. https://doi.org/10.1523/JNEUROSCI.3041-11.2011

Warburton, D. M. (1992). Nicotine as a cognitive enhancer. *Progress in Neuropsychopharmacology and Biological Psychiatry, 16*(2), 181–192. https://doi.org/10.1016/0278-5846(92)90069-Q

Wen, T. H., Afroz, S., Reinhard, S. M., Palacios, A. R., Tapia, K., Binder, D. K., Razak, K. A., & Ethell, I. M. (2018). Genetic reduction of matrix metalloproteinase-9 promotes formation of perineuronal nets around parvalbumin-expressing interneurons and normalizes auditory cortex responses in developing Fmr1 knock-out mice. *Cerebral Cortex, 28*(11), 3951–3964. https://doi.org/10.1093/cercor/bhx258

Wen, T. H., Lovelace, J. W., Ethell, I. M., Binder, D. K., & Razak, K. A. (2019). Developmental changes in EEG phenotypes in a mouse model of Fragile X Syndrome. *Neuroscience, 398*, 126–143. https://doi.org/10.1016/j.neuroscience.2018.11.047

Yang, Y., Lee, J., & Kim, G. (2020). Integration of locomotion and auditory signals in the mouse inferior colliculus. *ELife, 9*, e52228. https://doi.org/10.7554/eLife.52228

Zheng, Q. Y., Johnson, K. R., & Erway, L. C. (1999). Assessment of hearing in 80 inbred strains of mice by ABR threshold analyses. *Hearing Research, 130*(1–2), 94–107. https://doi.org/10.1016/S0378-5955(99)00003-9

Zhou, M., Liang, F., Xiong, X. R., Li, L., Li, H., Xiao, Z., Tao, H. W., & Zhang, L. I. (2014). Scaling down of balanced excitation and inhibition by active behavioral states in auditory cortex. *Nature Neuroscience, 17*(6), 841–850. https://doi.org/10.1038/nn.3701

Chapter 4

Age-Related Changes to Gap-Evoked Auditory Steady State Responses in Mice with and without Pathological Hearing Loss

Abstract

Age-related changes to hearing affect older adults with and without severe increases in audiometric thresholds. To differentiate between the effects of sensorineural hearing loss and aging, we measured responses to auditory stimuli from two strains of mice, one with a genetic mutation causing early onset of severe presbycusis (C57), and one which ages without considerable hearing loss (FVB). Young and old mice from each strain were recorded, using epidural screw electrodes, while freely moving and passively listening to broadband noise stimuli. We measured event related potentials (ERP) and auditory steady-state responses (ASSR) to assess auditory cortical processing. ASSRs were measured as the consistency of phases across trials (inter-trial phase clustering; ITPC). We used a novel stimulus, termed the gap-ASSR stimulus, which elicits an ASSR by rapidly presenting short gaps in continuous noise. By varying the gap widths and depths, we probed the limits of temporal processing in young and old mice. We recorded robust ERP from mice in all of the age groups. The old C57 mice showed significantly diminished ASSRs. The FVB mice showed robust ASSRs, regardless of age or stimulus level. The old FVB mice showed decreased gap-ASSR responses compared to young mice. When the stimulus level was increased, the FVB mice still showed deficits at modulation depths < 100%. While the pulse-ASSR did not differentiate the young from old FVB mice, the gap-ASSR showed a significant age-related difference. This work

contributes to the evidence suggesting that the auditory temporal processing deficits in aging are subtle, and it provides a tool to measure differences in auditory temporal processing fidelity, which may inform translational research and testing in preclinical models.

Introduction

High-fidelity auditory temporal processing is vital for speech processing. Older adults show deficits in speech processing that are linked, at least in part, to auditory temporal processing deficits (Dimitrijevic et al., 2004, 2016; Leigh-Paffenroth D.E. & Fowler, 2006). Recent studies have suggested that in animal models with noise induced hearing loss, there may be increased central gain to compensate for reduced peripheral input (Chambers et al., 2016). Interestingly, even though response magnitudes in auditory cortex and inferior colliculus increase, even in the absence of an auditory brainstem responses, plasticity occurs without a concomitant improvement in temporal processing. Whether age-related hearing loss, a process that occurs over a longer trajectory compared to noise-induced hearing loss, also produces increased gain with reduced temporal acuity is unclear in animal models.

To determine if age-related hearing loss is associated with increased cortical response magnitudes with reduced temporal acuity, we recorded auditory evoked responses from two different strains of mice across two age groups. The C57bl6/J (C57) mice show accelerated age-related hearing loss, with very high (>90 dB SPL) auditory brainstem response (ABR) thresholds in mice older than 20 mo of age. This strain is often used as a model to study central effects of age-related hearing loss. The FVB strain, on

the other hand, shows only between 10-15 dB increase in ABR hearing thresholds at ages >20 mo, and is suitable to study aging without considerable hearing loss. In this study, we recorded epidural EEG signals from awake, freely moving mice at young (~3 mo) and advanced age (~20-24 mo) and quantified ERPs, 40 Hz auditory steady state response (ASSR) and a novel 40 Hz gap-ASSR to quantify response magnitudes, latencies and temporal fidelity of evoked responses.

Auditory event-related potentials (ERPs) are the result of population-level activity in the auditory cortex in response to an acoustic stimulus, and they are reviewed thoroughly in Key et al. (2005). Each characteristic peak represents a step in auditory signal transmission. The first positive deflection in the ERP, P1, which occurs around 20 ms in mice reflects inputs into the cortex. P1 is followed by N1, a negative deflection occurring around 40 ms in mice and reflects cortical processing. P2 is associated with sensory arousal and attention, while N2 is associated with target detection (Čeponiene et al., 2008; reviewed in Harris et al., 2012). Studies of aging humans have shown age-related increases in P1 and N1 amplitudes, and age-related decreases in P2 and N2 amplitudes (reviewed in Čeponiene et al., 2008). The increases in P1 and N1 amplitudes are interpreted as a decrease in top-down control of sensory input (Friedman, 2008; Stothart & Kazanina, 2016). The decrease in P2 amplitude may be related to altered attentional processing, and the decrease in N2 is thought to be a result of decreased inhibitory control of irrelevant stimuli (Stothart & Kazanina, 2016). Given apparent similarities between human and mouse ERPs (Umbricht et al., 2004), we expect to see similar age-related changes in mice, including increases in P1 and N1 amplitudes, and

decreases in P2 and N2 amplitudes. We expected the increase in N1 amplitude to be most prominent in the C57 strain, due to increased central gain as a compensatory mechanism for peripheral hearing loss.

The ASSR demonstrates the capacity of the auditory system to accurately code rapidly fluctuating amplitude modulations in sound. The ASSR detects altered temporal processing in conditions such as schizophrenia (Uhlhaas & Singer, 2010) and autism spectrum disorders (Lovelace et al., 2020; Wilson et al., 2007). Other studies have shown a relationship between the ASSR and age-related changes to speech in noise understanding (Leigh-Paffenroth D.E. & Fowler, 2006; McClaskey et al., 2019). The ASSR can be characterized using multiple measurements, including the amplitude of the oscillation frequency in the frequency transform (FFT) of the signal (Parthasarathy et al., 2010), the amplitude of the Hilbert transform of the filtered signal, the vector strength of the signal with the original oscillatory stimulus, the phase-locking of FFTs (PLI) (Yokota & Naruse, 2015), or the inter-trial phase clustering (ITPC) at the oscillation frequency (Lovelace et al., 2020). ASSR amplitudes have not shown consistent age-related differences in previous studies (Dimitrijevic et al., 2016; McClaskey et al., 2019). Vector strength is most applicable to a SAM stimulus, which has a continuously changing phase, as opposed to a click/pulse train, which does not have an explicit phase. ITPC provides both time and frequency information, and it is a direct measure of the degree of response consistency across trials, so it was used to assess ASSRs in this study. Given that previous studies in humans do not show evidence of age-related changes to click-evoked ASSRs in the absence of presbycusis, we hypothesized that we would see no age-related

changes to the ASSR in FVB mice. Older adults with hearing loss show decreased ASSR amplitudes (Dimitrijevic et al., 2004), so we hypothesized that the C57 mice would show decreased ASSR consistency.

We presented a novel stimulus (gap-ASSR), which uses gaps in noise to evoke an ASSR, with the premise that if all of the gaps in a block of noise are consistently registered by the auditory system, then we will see a response that fluctuates at 40 Hz. By changing gap widths and modulation depths, this stimulus is intended to measure the limits of auditory temporal processing, where aging auditory systems should show deficits. A previous study, which tested the effects of gap depth and lead time on gap-related inhibition of the auditory startle response, suggests that decreases in ASR inhibition in older mice could be explained by central processing deficits (Ison et al., 1998). Older mice and humans show decreased gap detection abilities (Barsz et al., 2002). Within-channel gaps are lower than 10 ms in mice, rats, gerbils, and humans (Barsz et al., 2002; Gleich & Strutz, 2011; He et al., 1999; Snell, 1997; Snell & Frisina, 2000; Walton et al., 1998; Zhao et al., 2015). Behavioral and multiunit measures of gap detection both appear to show similar limits (Eggermont, 2000). We suggest that the novel gap-ASSR stimulus is suited to detect subtle temporal processing deficits. If some of the gaps are not reliably coded, then the stimulus should not elicit an ASSR at 40 Hz. To produce an ASSR for a given gap-ASSR stimulus, the auditory system must (1) be capable of responding to a gap in noise, (2) overcome forward masking to respond to subsequent gaps, and (3) be capable of synchronizing activity to a periodic stimulus. We hypothesized that the gap-ASSR in old C57 mice would be severely diminished, similarly

to the pulse-ASSR. Older humans show temporal processing deficits under challenging listening conditions. Therefore, we hypothesized that the FVB mice will show age-related deficits with shorter gaps and shallow modulation depths.

Methods

All procedures were approved by the Institutional Animal Care and Use Committee at the University of California, Riverside. C57 (C57bl6/J) mice were obtained from an in-house breeding colony that originated from Jackson Laboratory (Bar Harbor, ME). FVB (FVB.129P2−Pde6b+Tyrc-ch/AntJ) were obtained from Jackson Laboratories and bred in-house. One to four mice were housed in each cage under a 12:12-h light-dark cycle and fed *ad libitum*. The following age ranges and sample sizes were used in this study: young C57 (n=10, 5 females, mean = 3.0 mo), old C57bl/6 (n=17, 9 females, mean = 24.2 mo), young FVB (n=14, 10 females, mean = 3.4 mo), and old FVB (n=23, 9 females, mean = 19 mo). The ERP data from the young and old C57 mice was previously published (J. A. Rumschlag et al., 2020). These datasets are included here to demonstrate the existence of auditory responses in the old C57 mice and to compare with the FVB mouse. The rest of the data has not been previously published. The aging FVB mice were recorded at a younger age than the aging C57 mice due to higher attrition. The aseptic procedures used for surgery have been previously described in Rumschlag et al. (2020). Mice were first anesthetized with ketamine/xylazine/acepromazine (80/10/1 mg/kg, i.p.). After exposing the skull, we drilled 1 mm diameter holes in the skull above the right auditory cortex, right frontal cortex, and left occipital cortex, using a dental drill (Foredom Electric Co., CT). Screws attached to wires on a 3-channel post (P1

Technologies, Roanoke, VA) were then screwed into these holes. Auditory screw placement was guided by landmarks which have been previously validated using single unit (Rotschafer & Razak, 2013; Wen et al., 2018), epidural EEG (Wen et al., 2019), and depth ERP (Lovelace et al., 2016) recordings in the FVB mice, and using single unit recordings (Trujillo et al., 2011; Willott et al., 1993) and epidural EEG recordings (Lovelace et al., 2018) in the C57 mice (~AP 2.2-.2.3 mm relative to Bregma and ~ML 4.3-4.4 mm). The frontal screw was implanted lateral to the sagittal suture and caudal to the frontal sinus. The occipital screw, which served as the reference and ground, was implanted in the parietal bone, lateral to the intersection of the sagittal and lambdoid sutures. The screws and skull were covered with dental cement (Kuraray Dental, New York, NY). During the initial 48-hour postoperative recovery period, mice were injected (subcutaneous) with 0.1 mg/kg buprenorphine HCl every 6-8 hours. The mice recovered for at least 5 days following surgery, and at least 3 days after the last buprenorphine injection, before being recorded.

EEG recording

EEG signals were recorded from freely moving mice placed in a plastic arena, with clean bedding covering the floor. The mice were tethered to a freely rotating commutator by a cable connected to the implant. The cable was connected to a Tucker-Davis Technologies (TDT) RA4LI/PA headstage/preamplifier, which was connected via optic fiber to a TDT RZ6 input/output device. The setup was contained in a wire mesh Faraday cage, grounded to an external building pipe. The Faraday cage was placed on a

metal table in a sound-attenuating chamber lined with anechoic foam (Gretch-Ken Industries, OR).

Auditory stimulus presentation

Broadband noise stimuli generated with a TDT RZ6 with a sampling rate of 24.414 kHz were presented to freely moving mice through a TDT MF1 speaker placed 20 cm above the arena. Sound levels were calibrated using a ¼" Bruel and Kjaer (Nærum, Denmark) microphone. For C57 mice, the stimuli were presented at 70 dB SPL to young mice (3 mo) and 90 dB SPL to old mice (24 mo), to account for age-related hearing loss (Hunter & Willott, 1987; Johnson et al., 1997). For FVB mice, stimuli were presented at 70 dB to all young mice (3 mo), and at 70 dB to all older mice (20 mo). Additionally, the stimuli were presented at 80 dB to 8 of the older FVB mice, to account for the ~10 dB threshold shift measured with ABR. TTL pulses marking stimulus onsets were recorded on a separate channel in the EEG data.

Broadband noise pulses (120 repetitions, 100 ms, 5ms r/f, 0.25 Hz; Figure 4.1A) were used to evoke event-related potentials (ERPs). In this study, the ERP is mainly used to quantify magnitude and latency of cortical responses to sounds. The C57 ERP data shown here was analyzed in greater detail in a previous publication (Rumschlag et al., 2020). A pulsed broadband noise stimulus (200 repetitions, 8ms, 2ms r/f, 40 Hz, 1-2 s random ISI; Figure 4.1B) was used to evoke an auditory steady state response at 40 Hz.

The gap-ASSR stimulus used in this study uses gaps in continuous noise to elicit an ASSR. The stimuli consisted of continuous broadband noise periodically interrupted by 10 gaps placed 25 ms apart from onset to onset (for a presentation frequency of 40

Hz). A single stimulus began with 250 ms of noise, followed by 250 ms of gap-interrupted noise, followed by continuous noise, and so on, for a total of 10 presentations of the gap-interrupted noise. The stimulus ended with 250 ms of continuous noise, followed by a silent ISI of 500 ms. For each 250 ms segment, the gap width and modulation depth were randomly selected from a parameter space, consisting of 1-10 ms gaps (1 ms intervals), and modulation depths of 100%, 75%, 50%, and 25%, for a total of 40 possible combinations of gap width and modulation depth. Each stimulus was presented at least 200 times over the 1-hour presentation period. Figure 4.1C shows the gap widths in order from 1 ms to 10 ms with 100% modulation.

Auditory response analyses

All responses were measured using custom MATLAB (MathWorks, Natick, MA) scripts. The EEG signals were recorded at 24.414 kHz and downsampled to 1024 Hz using linear interpolation. All analyses were performed on signals collected from both the AC and the FC.

ERP analysis

To measure ERPs, the EEG trace was split into trials, using the TTL pulses marking the sound onset. Each trial was baseline corrected, such that for each trial, the mean of the 250 ms baseline period was subtracted from the trial trace. Each trial was then detrended (MATLAB detrend function). To extract the ERP, all of the trials were averaged together. ERPs recorded from mice have distinct peaks, which are analogous to those seen in human ERPs (Umbricht et al., 2004). For each mouse, the peak magnitudes and latencies were measured as the local minimum or maximum within a physiologically

relevant range, e.g. the P1 component was the local maximum between 15 ms and 30 ms following stimulus onset.

The age groups were compared via multiple 3-way ANOVAs (SPSS), one each for P1 amplitude, P1 latency, N1 amplitude, and N1 latency. With age, mouse strain, and region (AC or FC), we tested for main effects and interactions.

***Pulse-ASSR* analysis**

The pulse-ASSR was analyzed by calculating the average consistency of the 40 Hz response during the last 1000 ms of the 2000 ms stimulus. This was done to capture the steady-state response while avoiding the onset response. To that end, the trace was transformed to the time-frequency domain via dynamic complex Morlet wavelet transform. Then, inter-trial phase clustering (ITPC) was calculated for each time-frequency point as the average vector of phase unit vectors across trials. If the phase response is consistent at a particular time-frequency point, it will have a high ITPC value. The ITPC calculations showed a high degree of phase consistency at 40 Hz during the pulse-ASSR stimulus. The ITPC values at 40 Hz over the second half of the stimulus were averaged to extract one value for each mouse, representing the consistency of the 40 Hz ASSR. A 3-way ANOVA was used to examine interactions and main effects of age, mouse strain, and region. A separate ANOVA was used to compare the responses of old mice to 70 dB and 80 dB SPL stimuli.

Gap-ASSR analysis

The gap-ASSR was analyzed similarly to the pulse-ASSR, in which the consistency of the 40 Hz response was calculated. For the gap-ASSR, the consistency

was calculated for each of the 40 stimuli (4 modulation depths x 10 gap widths). The EEG trace was transformed using a dynamic complex Morlet wavelet transform. The trials corresponding to each stimulus were grouped together, and the ITPC was calculated. A band of high ITPC appears at 40 Hz, which is clearly visible in the responses from all of the FVB mice and the young C57 mice. The average ITPC value at 40 Hz during the stimulus was extracted for each stimulus for each mouse. These values were used to run a 2-way, 2-level repeated measures ANOVA (SPSS) for each region, to evaluate the effects of age and strain. To evaluate the effect of stimulus presentation level on the responses in the old FVB mice, separate 2-way rmANOVAs were used, one for each region, with factors of age and presentation level.

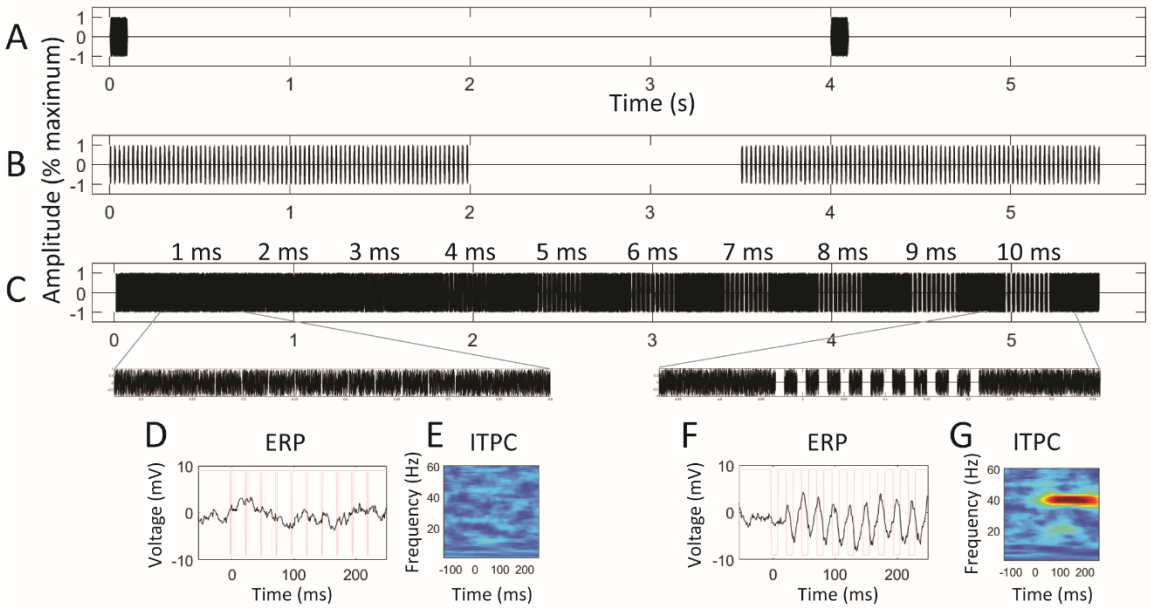

Figure 4.1. Schematics of broadband noise stimuli presented to mice. 100 ms broadband noise bursts were presented at 0.25 Hz (A) to elicit ERPs. 2-second-long trains of 8 ms noise bursts presented at 40 Hz (B) were used to elicit ASSRs. A novel gap-in-noise stimulus (C) was used to elicit ASSRs.

Results

To measure age-related changes to auditory temporal processing with and without hearing loss, we recorded auditory responses from young and old mice from two strains: C57bl/6J mice, which serve as a model for age-related sensorineural hearing loss, and the FVB mice, which show <~15 dB hearing level shifts in auditory brainstem responses up to 24 months. Three distinct auditory stimuli were presented to freely moving mice, which were implanted with epidural screw electrodes to obtain EEG recordings from auditory and frontal cortices (AC, FC), with a screw in the occipital cortex serving as reference. Responses to broadband noise bursts (100 ms, 0.25 Hz repetition) were used to measure event related potential (ERP) amplitude and latency. 40 Hz pulse trains were used to measure the auditory steady state response (ASSR, 8 ms each pulse, 2-second train length, random inter-train interval of between 1-2 sec). Lastly a novel stimulus, here termed gap-ASSR, was used to measure how consistently the auditory system is able to register brief gaps in noise.

The magnitudes and latencies of ERP components show interactions between strain and age

Freely moving mice in each of the four groups (3-month-old C57bl/6Js, 3-month-old FVBs, 24-month-old C57s, and 20-month-old FVBs) were presented with broadband noise stimuli (100 ms bursts, 5 ms rise/fall, 0.25 Hz repetition rate, 120 presentations, 70 dB SPL except for 24-month-old C57, which were presented with 90 dB SPL stimuli), while EEG signals were recorded. Individual responses to noise stimuli were extracted from the EEG traces, baseline-corrected, and averaged. The group average responses are

shown in Figure 4.2**.** Figures 4.2A-2B show the C57 group average ERP (+/- s.e.) in the AC and FC, respectively, and 4.2C-4.2D show the FVB ERPs. Latencies and magnitudes of ERP components were extracted from each mouse's recording.

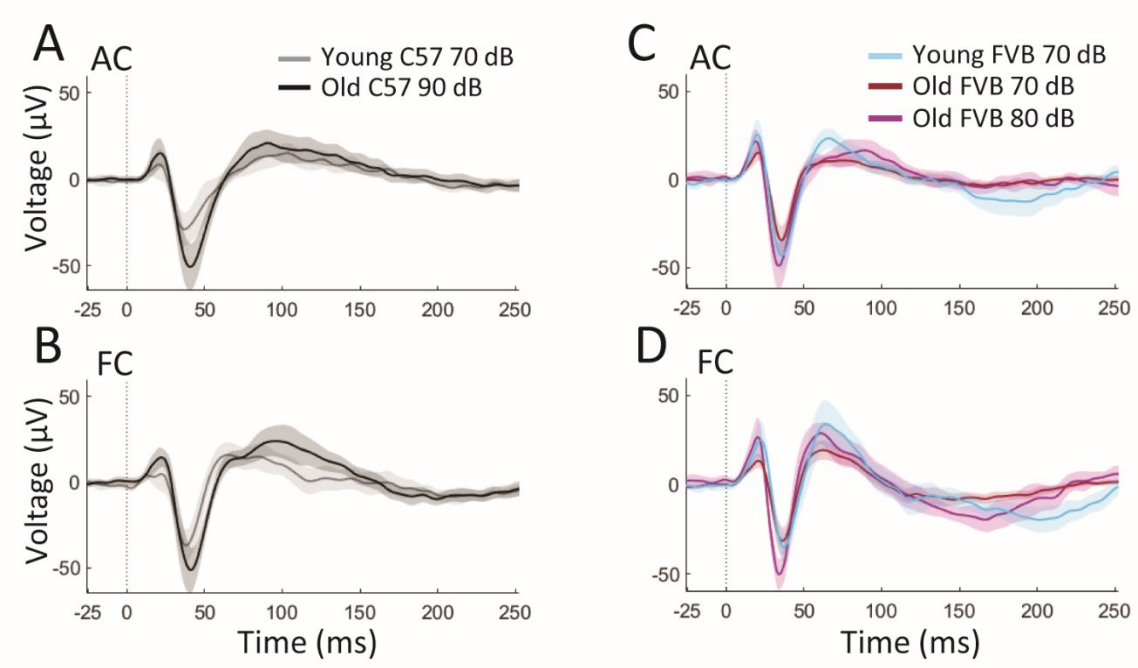

Figure 4.2. Event-related potentials in C57 and FVB mice. Event related potentials were recorded from C57 (A-B) and FVB (C-D) mice, from the AC (A & C), and FC (B & D). Smoothed average ERPs are shown with transparent patches representing +/- 2*SEM.

We tested for interactions and main effects of age and strain on ERP component magnitudes and latencies with a two-way ANOVA for each ERP component. We found statistically significant interactions of age and strain on P1 amplitude, P2, and N2 amplitude recorded from the AC and FC, and on N1 in the AC (see Table 4.1 for full results). We found statistically significant main effects of strain on N1 and N2 latencies in both regions, and an effect of strain on P2 latency in the FC. No other statistically significant results survived correcting for multiple comparisons (Bonferroni, n=4). These

results suggest that age has a differential impact on ERP components in the two strains. In FVB mice, the P2 and N2 amplitudes are significantly decreased, which mirrors findings in older humans (Čeponiene et al., 2008). In the C57 mice, N1 amplitude is larger, suggesting increased central gain.

Pulse-ASSR

We presented mice with a 40 Hz broadband noise pulse stimulus to elicit an ASSR. To measure the consistency of response timing, we calculated inter-trial phase clustering (ITPC) at 40 Hz during the presentation period. We extracted the mean 40 Hz ITPC for each mouse to compare ASSR between ages and strains. The mean +/- standard error are shown in Figure 4.3. ASSR ITPC values are stronger in the FC overall compared to the AC. ITPC values are significantly lower in the older C57 group, compared to the younger C57 group. ITPC values for the FVB mice are not significantly altered with age. Performing a 3-way ANOVA on this data using strain, age, and region as factors and mean ITPC as the dependent variable, we found statistically significant interactions of strain and age, strain and region, as well as statistically significant main effects of strain, age, and region (see Table 4.2 for full results). We also observed a marginally significant 3-way interaction of strain, age, and region. Post-hoc analysis shows that ASSR consistency, as measured by ITPC at 40 Hz, decreases with age in the AC and FC in C57bl/6J mice. ASSR consistency shows no age-related decrease in old FVB mice. These results show that in the absence of age-related hearing loss, temporal processing of highly salient stimuli measured using the ASSR is robust to age-related

changes. But with hearing loss (C57), the ASSR ITPC is almost entirely absent, suggesting severe deficits in temporal processing.

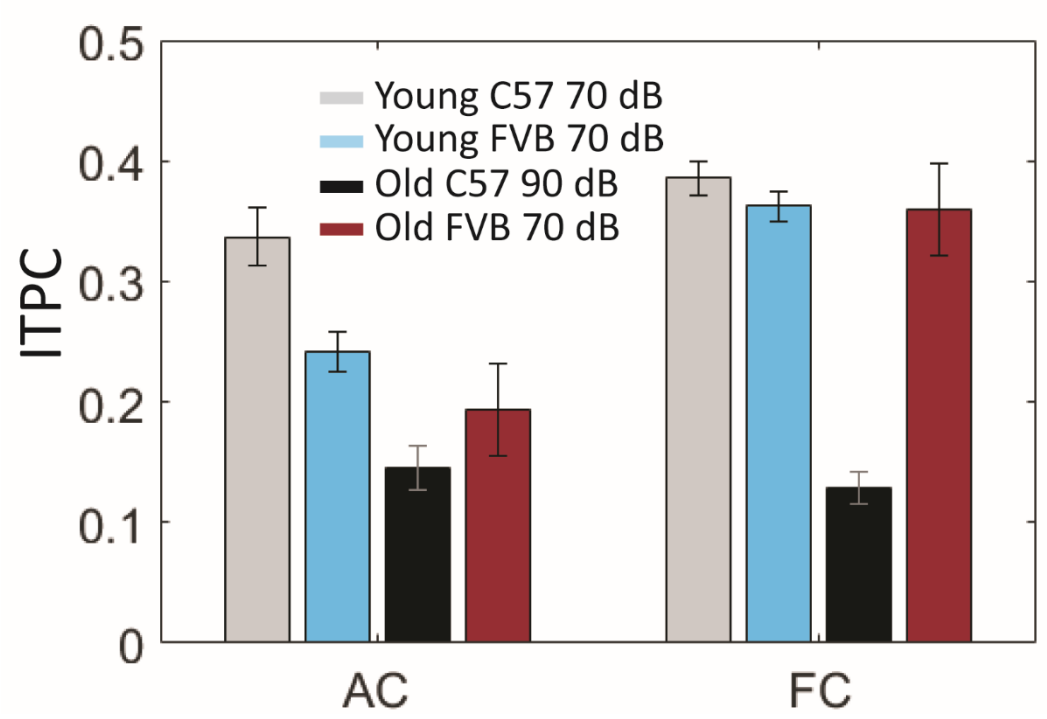

Figure 4.3. ASSR consistency (ITPC) in C57 and FVB mice. The 40 Hz ITPC during the last second of the 2-s ASSR was averaged for each mouse. Group averages are shown +/- SEM. ITPC values in FC are higher for the FVB mice. Older C57s show significantly lower ITPC than the young C57s.

Gap-ASSR

The gap-ASSR stimulus, shown in Figure 4.1C, consisted of 5.75-second trains of noise, alternating between 250 ms of noise and 250 ms of noise interrupted by gaps spaced 25 ms apart, from onset to onset. These 250 ms periods of noise interrupted by gaps elicit an ASSR at 40 Hz, shown in Figure 4.1D-G, the strength of which varies with gap width and modulation depth. If each gap in a 250 ms stimulus elicits a measurable response, then the recording will show a robust 40 Hz oscillatory signal, as seen in Figure

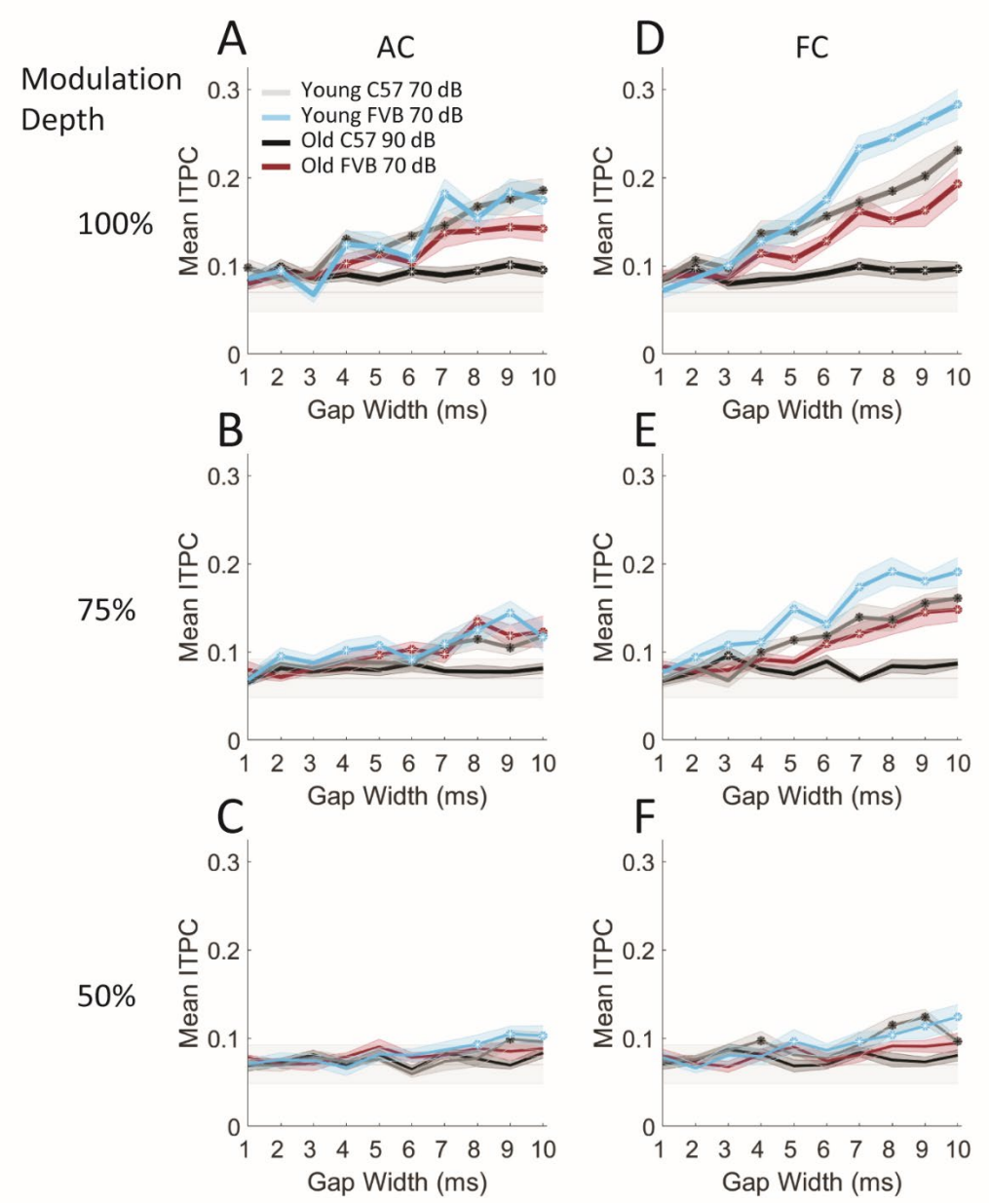

Figure 4.4. Gap-ASSR responses across gap widths and modulation depths. Each line represents the group average ITPC values at each gap width, with the transparent patch representing +/- SEM. A circle with a '*' on a vertex represents a measurable response (ITPC value significantly higher than the noise floor, $p<0.001$).

4.1F, and this response will be consistent across trials, yielding a high ITPC value, as in Figure 4.1G. If some gaps in a stimulus fail to produce a response, as in Figure 4.1D, then the ITPC value will be significantly lower (Figure 4.1E). The gap-ASSR is a

measurement of the ability of the cortex to consistently respond to rapid short gaps in noise. By reducing gap duration and modulation depth, the ability of the auditory system to detect gaps in increasingly more difficult signal conditions can be quantified. This measure can then be compared across ages and level of hearing loss.

For each stimulus presentation within a 5.75-second stimulus train, the gap width was randomly chosen from 1 ms to 10 ms, in 1 ms increments (0.1 ms r/f), and the modulation depth was randomly assigned to be 100%, 75%, 50%, or 25%. There were no detectable responses to any of the gap widths at the 25% modulation depth for any of the mice, so these values were excluded, aside from the 1 ms, 25% modulation depth condition, which was used as the noise floor for comparison. Figure 4.4 shows the group average ITPC values at 40 Hz during the presentation of each stimulus type. For each group, the values for each stimulus combination are compared via 2-sample t-test to the values of the 1 ms, 25% modulation depth condition (which are not significantly different from baseline 40 Hz ITPC), pooled from all groups. Because there are 10 gap widths for each modulation depth, we used a conservative p-value significance threshold of 0.001 to indicate a response significantly higher than the noise floor. Significant group responses are marked with asterisks. The responses in the FC have higher ITPC values in almost every case, consistent with topographical studies of 40 Hz responses in mice (Hwang et al., 2020). The young FVB mice clearly show more consistent responses compared to the old FVB mice, except for the 75% condition in the AC. In every case, the young C57bl/6J mice exhibit stronger responses than the old C57bl/6J mice. To statistically test

these observations, we performed a repeated measures ANOVA for each region individually.

For each region, we performed a repeated measures ANOVA with 3 levels of modulation depth (100%, 75%, and 50%) and 10 levels of gap width (1-10ms), with factors of age and strain. For both regions, Mauchly's Test of Sphericity indicated that the assumption of sphericity had been violated for the interaction of modulation depth and gap width and therefore, a Greenhouse-Geisser correction was used. Full statistical results are shown in Table 4.3. In both the AC and FC measures, we found interactions of modulation depth, gap width, and age, gap width and strain, gap width and age, and modulation depth and age. Though we did not observe a significant 4-way interaction, we observed a statistically significant 3-way interaction of modulation depth, gap width, and strain in the FC. The statistically significant main effects of modulation depth and gap width demonstrate that the responses recorded from the mice were higher when the modulation depth was deeper and when the gap width was wider, such that a stimulus that contained 10 ms silent gaps (100% modulation depth) elicited a more consistent oscillatory response compared to a stimulus with 1 ms gaps that were half as loud as the rest of the stimulus (50% modulation depth). This result demonstrates that the gap-ASSR can show more subtle auditory temporal processing deficits than the pulse-ASSR. While the pulse-ASSR and gap-ASSR show similar age-related differences for the C57 mice, these two measures show divergent results in FVB mice. In the FVB mice, the pulse-ASSR shows no age-related change. In contrast, the gap-ASSR ITPC is significantly

lower in older FVB mice, suggesting an age-related deficit in auditory temporal processing in the absence of severe age-related hearing loss.

Stimulus level increased for old FVB mice

To determine whether the reduction in auditory temporal processing in the older FVB mice was due to the observed ~10 dB hearing threshold increase, as measured by ABR, we also presented the three stimuli at 80 dB SPL to 8 of the old FVB mice. Although the 70 dB SPL stimulus was within the hearing range of the old mice, this was done to examine the effect of increasing signal gain on temporal processing.

To test the effect of increasing stimulus level on ERP components (Figure 4.2C-D), we tested for main effects of age and stimulus presentation level using a 2-way ANOVA for each ERP component, and found statistically significant main effects of both age and presentation level for P1, N1, P2, and N2 amplitudes (full statistics in Table 4.4). We also observed a statistically significant main effect of age on P1 latency, a significant effect of presentation level on N1 latency, and an effect of region on N1 and P2 latencies as well as P2 and N2 amplitudes. Lastly there was a statistically significant interaction of age and region on P1 and P2 latencies. This shows that sound presentation level and age significantly affect timing and population activation level of the cortical auditory impulse response.

In the case of the pulse-ASSR (Figure 4.5), a 2-way ANOVA with age and sound level as factors found no statistically significant differences between mean ITPC values for either AC or FC. This means that the consistency of 40 Hz responses was not

dependent on sound presentation level in the older mice, and the younger and older mice had the same degree of consistency in their responses.

The gap-ASSR shows auditory processing deficits in older mice, even with increased stimulus level. Figure 4.6 shows the 70 dB and 80 dB SPL gap-ASSR results for the old FVB compared to the young mice (70 dB SPL). At 100% modulation depth,

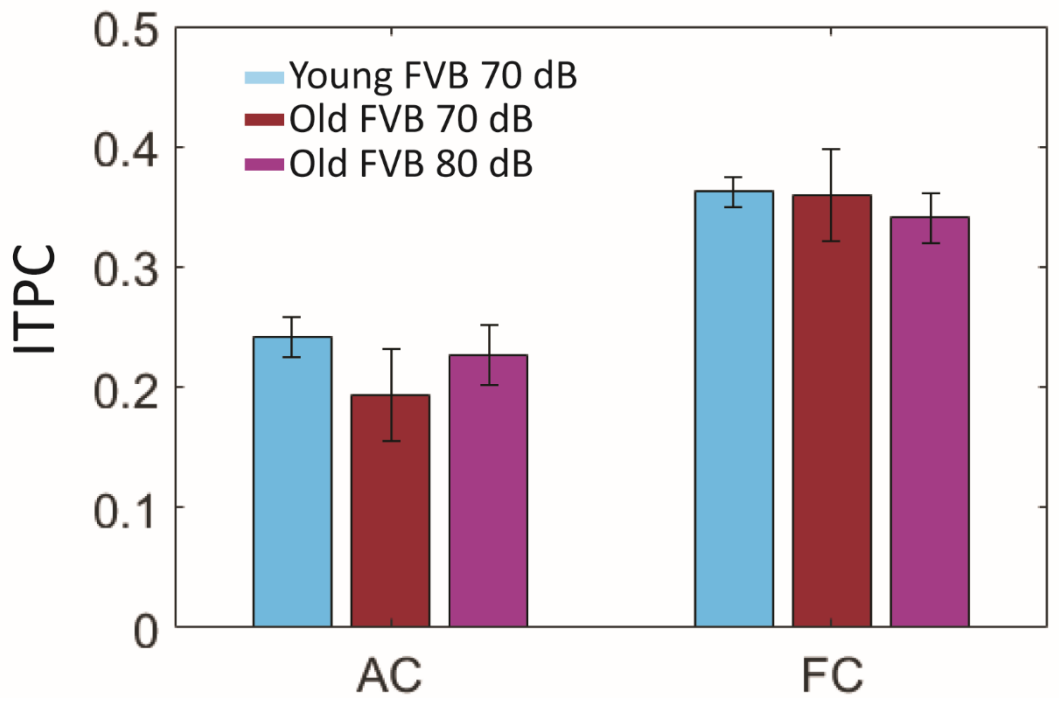

Figure 4.5. ASSR consistency (ITPC) in FVB mice with stimulus level compensation. The 40 Hz ITPC group average values +/- SEM are shown, as in Figure 4.3. There are no differences with age or with stimulus presentation level.

the response consistency is not significantly lower in the level-compensated old mice. However, at 75% modulation depth, the level compensated old mice have significantly lower ITPC values in the FC compared to the young mice, demonstrating an age-related deficit in auditory temporal processing, even with boosted signal gain. This difference is more subtle at 50% modulation, though the young mice have 5 responses that are

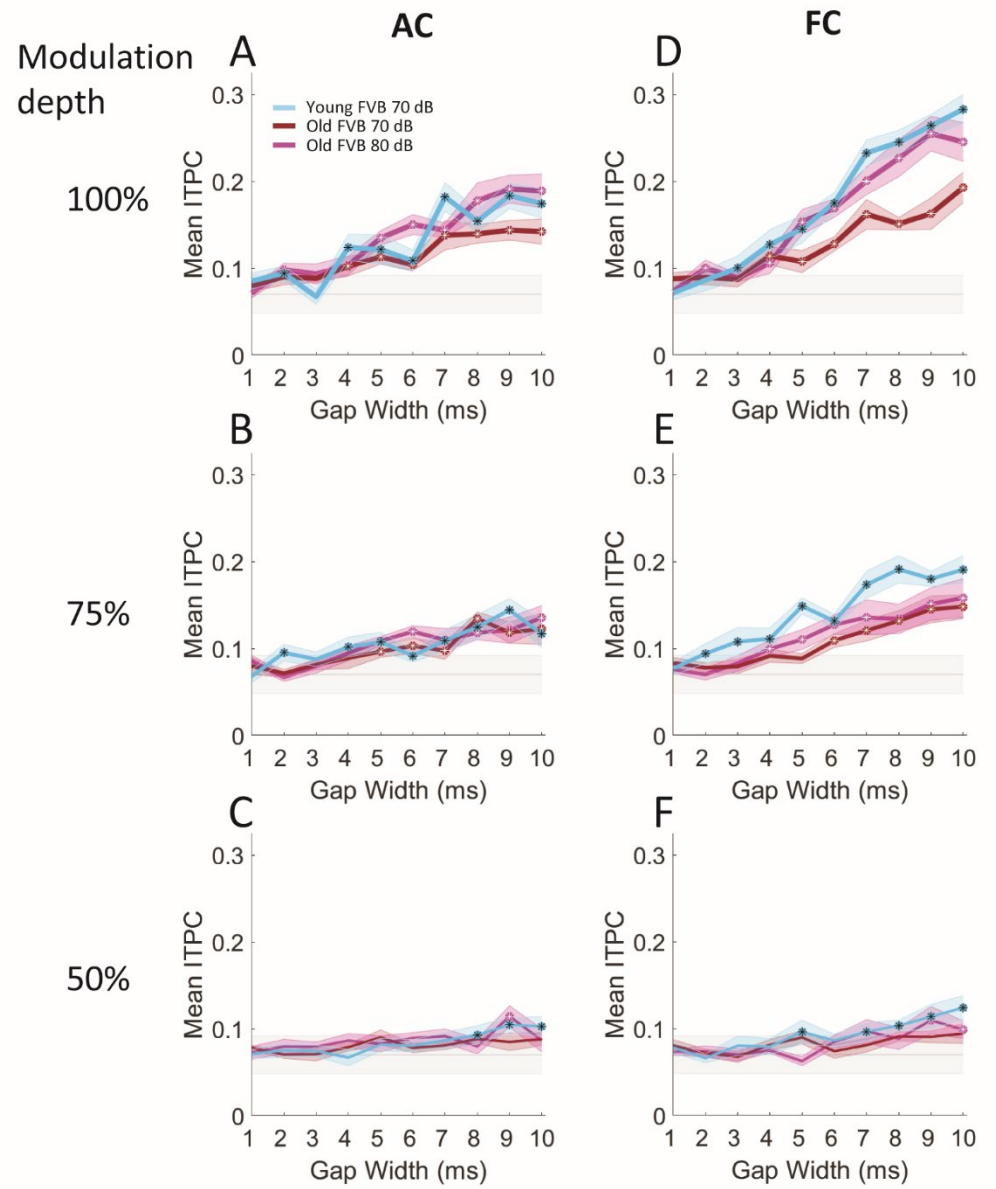

Figure 4.6 Gap-ASSR responses in FVB mice with stimulus level compensation. Increasing the presentation level of the gap-ASSR stimulus improves old response consistency at 100% modulation depth. As modulation depth decreases, the benefit conferred by increased signal gain diminishes.

significantly above baseline, while the level compensated old FVBs have 2, and the non-compensated old FVBs have none. A 2-way, 2-level repeated-measures ANOVA shows a statistically significant interaction of modulation depth and age in the FC (F(1.93,

36.71)=3.946, p=0.029, η_p^2=0.172. In the AC, the repeated-measures ANOVA shows a marginally significant interaction of modulation depth, gap width, and age (F(7.88, 149.72)=1.791, p=0.084, η_p^2=0.086). Even when the sound level is increased by 10 dB, the old FVB show temporal processing deficits, as measured by the gap-ASSR, which contrasts with the findings from the pulse-ASSR, which showed no differences with age.

Discussion

The data presented in this study provide a number of electrophysiological biomarkers of age- and presbycusis-related changes in the auditory system, particularly relevant to temporal processing. The ERP results demonstrate that broadband noise bursts evoke cortical activity in all mice tested. Consistent with prior research (Dias et al., 2019; Tremblay et al., 2003; Woods & Clayworth, 1986), the ERPs were stronger in the older mice, when the sound level was adjusted for hearing loss. The cortical response to a sequence of broadband noise pulses at 40 Hz showed no age-related change in the healthy-aging model mice but was severely diminished in the older age-related hearing loss model mice.

Our results show that auditory temporal processing, as measured by the gap-ASSR, declines with age in mice with and without hearing loss. The gap-ASSR is deficient in older mice without severe hearing loss, even when the sound level is increased, and it is almost completely absent in older mice with severe hearing loss.

In the FVB mice, a model for healthy auditory aging, auditory temporal processing deficits were only observed when the mice were presented with challenging stimuli. Mice with significant age-related hearing loss showed severe deficits in temporal

processing for both types of ASSR-evoking stimuli tested. Together, these data show that aging in the absence of pathological age-related hearing loss negatively impacts auditory temporal processing under challenging stimulus conditions, while aging with presbycusis reduces auditory temporal processing capabilities even with highly salient stimuli.

The duration of gaps in the gap-ASSR results that show significant age-related differences in mice are remarkably similar to the gap detection results from a previous study in humans (6 and 9 ms), in which participants were presented with a continuous noise stimulus occasionally interrupted by gaps (Harris et al., 2012). In addition to finding an age-related deficit in gap detection, they found a significant relationship between gap detection and processing speed, as measured by the Purdue Pegboard and Connections tests (Harris et al., 2012). These results also closely match with a psychometric function of gap detection in mice (He et al., 1999).

The decrease in gap response reliability with age may be related to a similar age-related effect of a short leading marker in gap detection tasks in older adults. In the gap-ASSR stimulus, if the auditory system responds to a gap, then the following noise pulse preceding the next gap will serve as the leading marker. In studies of mice (He et al., 1999) and humans (Schneider & Hamstra, 1999), older subjects demonstrated higher gap detection thresholds than young subjects when the leading marker was short, suggesting a longer temporal integration window. In the context of the gap-ASSR, the 10 ms gaps would be preceded by a 15 ms marker, while the 1 ms gaps would be preceded by a 24 ms marker. The perceptual benefit of the longer gap widths may be offset by the added challenge of a shorter leading marker.

The gap-ASSR appears to measure multiple aspects of auditory temporal processing without requiring any behavioral training, and analogous responses could theoretically be measured in humans using a simple EEG recording setup. Future studies will determine the utility of the gap-ASSR as a preclinical biomarker of auditory temporal processing to test interventions, such as auditory training, therapeutics, or cochlear gene therapy.

Our finding that C57 mice showed significant temporal processing deficits despite showing increased ERP N1 amplitudes supports the hypothesis that age-related hearing loss results in increased central gain, along with a decrease in temporal processing acuity. Previous studies have found decreases in inhibitory transmission at all levels of the central auditory system (see Caspary et al., 2008 for a review of the topic). Inhibitory signaling is important for shaping temporal responses (Donald M. Caspary et al., 2002; Gleich et al., 2003; K. A. Razak & Fuzessery, 2007; Khaleel A Razak & Fuzessery, 2013), so age-related loss of inhibition is thought to result in deficient temporal processing (D. M. Caspary et al., 2008).

Tables

Factor	ERP Components	(p-value corrected for 4 comparisons)
Age	AC P1 Amplitude	$F(1,48)=0$, $p=1$, $\eta_p^2=0$
	FC P1 Amplitude	$F(1,48)=0.289$, $p=1$, $\eta_p^2=0.006$
	AC N1 Amplitude	$F(1,48)=0.302$, $p=1$, $\eta_p^2=0.006$
	FC N1 Amplitude	$F(1,48)=0.304$, $p=1$, $\eta_p^2=0.006$
	AC P2 Amplitude	$F(1,48)=0.272$, $p=1$, $\eta_p^2=0.006$
	FC P2 Amplitude	$F(1,48)=4.695$, $p=0.14$, $\eta_p^2=0.089$
	AC N2 Amplitude	$F(1,48)=4.924$, $p=0.124$, $\eta_p^2=0.093$
	FC N2 Amplitude	$F(1,48)=3.683$, $p=0.244$, $\eta_p^2=0.071$
	AC P1 Latency	$F(1,48)=4.063$, $p=0.196$, $\eta_p^2=0.078$
	FC P1 Latency	$F(1,48)=0.492$, $p=1$, $\eta_p^2=0.01$
	AC N1 Latency	$F(1,48)=2.629$, $p=0.444$, $\eta_p^2=0.052$
	FC N1 Latency	$F(1,48)=4.261$, $p=0.176$, $\eta_p^2=0.082$
	AC P2 Latency	$F(1,48)=5.146$, $p=0.112$, $\eta_p^2=0.097$
	FC P2 Latency	$F(1,48)=0.814$, $p=1$, $\eta_p^2=0.017$
	AC N2 Latency	$F(1,48)=0.469$, $p=1$, $\eta_p^2=0.01$
	FC N2 Latency	$F(1,48)=0.436$, $p=1$, $\eta_p^2=0.009$
Strain	AC P1 Amplitude	$F(1,48)=0.235$, $p=1$, $\eta_p^2=0.005$
	FC P1 Amplitude	$F(1,48)=0.41$, $p=1$, $\eta_p^2=0.008$
	AC N1 Amplitude	$F(1,48)=0.67$, $p=1$, $\eta_p^2=0.014$
	FC N1 Amplitude	$F(1,48)=6.349$, $p=0.06$, $\eta_p^2=0.117$
	AC P2 Amplitude	$F(1,48)=0.043$, $p=1$, $\eta_p^2=0.001$
	FC P2 Amplitude	$F(1,48)=0.966$, $p=1$, $\eta_p^2=0.02$
	AC N2 Amplitude	$F(1,48)=4.018$, $p=0.204$, $\eta_p^2=0.077$
	FC N2 Amplitude	$F(1,48)=0.985$, $p=1$, $\eta_p^2=0.02$
	AC P1 Latency	$F(1,48)=0.286$, $p=1$, $\eta_p^2=0.006$
	FC P1 Latency	$F(1,48)=1.445$, $p=0.94$, $\eta_p^2=0.029$
	AC N1 Latency	**$F(1,48)=12.494$, $p=0.004$, $\eta_p^2=0.207$**
	FC N1 Latency	**$F(1,48)=10.758$, $p=0.008$, $\eta_p^2=0.183$**
	AC P2 Latency	$F(1,48)=6.584$, $p=0.052$, $\eta_p^2=0.121$
	FC P2 Latency	**$F(1,48)=9.228$, $p=0.016$, $\eta_p^2=0.161$**
	AC N2 Latency	**$F(1,48)=13.701$, $p=0.004$, $\eta_p^2=0.222$**
	FC N2 Latency	**$F(1,48)=6.898$, $p=0.048$, $\eta_p^2=0.126$**
Age * Strain	**AC P1 Amplitude**	**$F(1,48)=7.164$, $p=0.04$, $\eta_p^2=0.13$**
	FC P1 Amplitude	**$F(1,48)=7.392$, $p=0.036$, $\eta_p^2=0.133$**
	AC N1 Amplitude	**$F(1,48)=10.95$, $p=0.008$, $\eta_p^2=0.186$**
	FC N1 Amplitude	$F(1,48)=4.995$, $p=0.12$, pEs=0.094

	AC P2 Amplitude	**$F(1,48)=9.815$, $p=0.012$, $\eta_p^2=0.17$**
	FC P2 Amplitude	**$F(1,48)=7.471$, $p=0.036$, $\eta_p^2=0.135$**
	AC N2 Amplitude	**$F(1,48)=8.767$, $p=0.02$, $\eta_p^2=0.154$**
	FC N2 Amplitude	**$F(1,48)=8.979$, $p=0.016$, $\eta p2=0.158$**
	AC P1 Latency	$F(1,48)=5.308$, $p=0.104$, $\eta_p^2=0.1$
	FC P1 Latency	$F(1,48)=4.486$, $p=0.156$, $\eta_p^2=0.085$
	AC N1 Latency	$F(1,48)=0.749$, $p=1$, $\eta_p^2=0.015$
	FC N1 Latency	$F(1,48)=4.607$, $p=0.148$, $\eta_p^2=0.088$
	AC P2 Latency	$F(1,48)=1.334$, $p=1$, $\eta_p^2=0.027$
	FC P2 Latency	$F(1,48)=4.09$, $p=0.196$, $\eta_p^2=0.079$
	AC N2 Latency	$F(1,48)=0.212$, $p=1$, $\eta p2=0.004$
	FC N2 Latency	$F(1,48)=0.099$, $p=1$, $\eta_p^2=0.002$

Table 4.1. Full statistical results from ANOVAs, testing group differences in ERP component amplitudes and latencies

Factor	Dependent Variable	(p-value corrected for 2 comparisons)
strain	ITPC AC 40Hz	$F(1,40)=0.791$, $p=0.758$, $\eta_p^2=0.019$
	ITPC FC 40Hz	**$F(1,40)=23.216$, $p<0.001$, $\eta_p^2=0.367$**
age	**ITPC AC 40Hz**	**$F(1,40)=31.66$, $p<0.001$, $\eta_p^2=0.442$**
	ITPC FC 40Hz	**$F(1,40)=47.797$, $p<0.001$, $\eta_p^2=0.544$**
strain * age	**ITPC AC 40Hz**	**$F(1,40)=10.041$, $p=0.006$, $\eta_p^2=0.201$**
	ITPC FC 40Hz	**$F(1,40)=39.404$, $p<0.001$, $\eta_p^2=0.496$**

Table 4.2. Full statistical results from ANOVAs, testing group differences in pulse-ASSR consistency

Measure: AC mean ITPC	
Mauchly's Test of Sphericity	$\chi2(170) = 235.174$, $p = 0.001$
Greenhouse-Geisser Correction applied	
Modulation Depth (MD)	$F(1.825,69.353)=92.555$, $p<0.001$, $\eta_p^2=0.709$
MD * age	$F(1.825,69.353)=11.224$, $p<0.001$, $\eta_p^2=0.228$
MD * strain	
MD * age * strain	$F(1.825,69.353)=2.926$, $p=0.065$, $\eta_p^2=0.071$
Gap Width (GW)	$F(5.517,209.644)=27.157$, $p<0.001$, $\eta_p^2=0.417$
GW * age	$F(5.517,209.644)=4.725$, $p<0.001$, $\eta_p^2=0.111$
GW * strain	$F(5.517,209.644)=2.862$, $p=0.013$, $\eta_p^2=0.07$
GW * age * strain	
MD * GW	$F(10.509,399.334)=6.444$, $p<0.001$, $\eta_p^2=0.145$
MD * GW * age	$F(10.509,399.334)=2.2$, $p=0.015$, $\eta_p^2=0.055$
MD * GW * strain	
Measure: FC mean ITPC	
Mauchly's Test of Sphericity	$\chi2(170) =223.807$, $p = 0.006$
Greenhouse-Geisser Correction applied	
MD	$F(1.626,60.178)=213.383$, $p<0.001$, $\eta_p^2=0.852$
MD * age	$F(1.626,60.178)=33.436$, $p<0.001$, $\eta_p^2=0.475$
MD * strain	$F(1.626,60.178)=18.212$, $p<0.001$, $\eta_p^2=0.33$
MD * age * strain	
GW	$F(6.3,233.098)=59.015$, $p<0.001$, $\eta_p^2=0.615$
GW * age	$F(6.3,233.098)=15.054$, $p<0.001$, $\eta_p^2=0.289$
GW * strain	$F(6.3,233.098)=7.759$, $p<0.001$, $\eta_p^2=0.173$
GW * age * strain	
MD * GW	
MD * GW * age	$F(10.478,387.671)=3.115$, $p=0.001$, $\eta_p^2=0.078$
MD * GW * strain	$F(10.478,387.671)=2.525$, $p=0.005$, $\eta_p^2=0.064$

Table 4.3. Statistical results from repeated measures ANOVA, testing for age- and strain-dependent differences in gap-ASSR consistency.

Factor	Measure	(p-values corrected for 4 comparisons)
Age	AC P1 amplitude	$F(1,31)=5.671$, $p=0.096$, $\eta_p^2=0.155$
	FC P1 amplitude	$F(1,31)=6.366$, $p=0.068$, $\eta_p^2=0.17$
	AC N1 amplitude	$F(1,31)=5.662$, $p=0.096$, $\eta_p^2=0.154$
	FC N1 amplitude	$F(1,31)=2.317$, $p=0.552$, $\eta_p^2=0.07$
	AC P2 amplitude	$F(1,31)=17.689$, $p<0.001$, $\eta_p^2=0.363$
	FC P2 amplitude	$F(1,31)=14.089$, $p=0.004$, $\eta_p^2=0.312$
	AC N2 amplitude	$F(1,31)=11.035$, $p=0.008$, $\eta_p^2=0.263$
	FC N2 amplitude	$F(1,31)=10.182$, $p=0.012$, $\eta_p^2=0.247$
	AC P1 Latency	$F(1,31)=0.078$, $p=1$, $\eta_p^2=0.003$
	FC P1 Latency	$F(1,31)=7.612$, $p=0.04$, $\eta_p^2=0.197$
	AC N1 Latency	$F(1,31)=0.56$, $p=1$, $\eta_p^2=0.018$
	FC N1 Latency	$F(1,31)=0.01$, $p=1$, $\eta_p^2=0$
	AC P2 Latency	$F(1,31)=5.458$, $p=0.104$, $\eta_p^2=0.15$
	FC P2 Latency	$F(1,31)=0.645$, $p=1$, $\eta_p^2=0.02$
	AC N2 Latency	$F(1,31)=0.021$, $p=1$, $\eta_p^2=0.001$
	FC N2 Latency	$F(1,31)=0.588$, $p=1$, $\eta_p^2=0.019$
SPL	AC P1 amplitude	$F(1,31)=4.556$, $p=0.164$, $\eta_p^2=0.128$
	FC P1 amplitude	$F(1,31)=4.475$, $p=0.172$, $\eta_p^2=0.126$
	AC N1 amplitude	$F(1,31)=10.337$, $p=0.012$, $\eta_p^2=0.25$
	FC N1 amplitude	$F(1,31)=18.545$, $p<0.001$, $\eta_p^2=0.374$
	AC P2 amplitude	$F(1,31)=7.399$, $p=0.044$, $\eta_p^2=0.193$
	FC P2 amplitude	$F(1,31)=5.865$, $p=0.084$, $\eta_p^2=0.159$
	AC N2 amplitude	$F(1,31)=1.235$, $p=1$, $\eta_p^2=0.038$
	FC N2 amplitude	$F(1,31)=7.214$, $p=0.048$, $\eta_p^2=0.189$
	AC P1 Latency	$F(1,31)=2.579$, $p=0.472$, $\eta_p^2=0.077$
	FC P1 Latency	$F(1,31)=0.519$, $p=1$, $\eta_p^2=0.016$
	AC N1 Latency	$F(1,31)=7.821$, $p=0.036$, $\eta_p^2=0.201$
	FC N1 Latency	$F(1,31)=17.704$, $p<0.001$, $\eta_p^2=0.364$
	AC P2 Latency	$F(1,31)=0.228$, $p=1$, $\eta_p^2=0.007$
	FC P2 Latency	$F(1,31)=0.057$, $p=1$, $\eta_p^2=0.002$
	AC N2 Latency	$F(1,31)=0.18$, $p=1$, $\eta_p^2=0.006$
	FC N2 Latency	$F(1,31)=2.503$, $p=0.496$, $\eta_p^2=0.075$

Table 4.4. Statistical results from ANOVAs testing differences in young (70 dB) and old (70 & 80 dB) FVB mouse ERP components.

References

Barsz, K., Ison, J. R., Snell, K. B., & Walton, J. P. (2002). Behavioral and neural measures of auditory temporal acuity in aging humans and mice. *Neurobiology of Aging*, *23*(4), 565–578. https://doi.org/10.1016/S0197-4580(02)00008-8

Caspary, D. M., Ling, L., Turner, J. G., & Hughes, L. F. (2008). Inhibitory neurotransmission, plasticity and aging in the mammalian central auditory system. *Journal of Experimental Biology*, *211*(11), 1781–1791. https://doi.org/10.1242/jeb.013581

Caspary, Donald M., Palombi, P. S., & Hughes, L. F. (2002). GABAergic inputs shape responses to amplitude modulated stimuli in the inferior colliculus. *Hearing Research*, *168*(1–2), 163–173. https://doi.org/10.1016/S0378-5955(02)00363-5

Čeponiene, R., Westerfield, M., Torki, M., & Townsend, J. (2008). Modality-specificity of sensory aging in vision and audition: evidence from event-related potentials. *Brain Research, 1215*, 53–68. https://doi.org/10.1016/j.brainres.2008.02.010

Chambers, A. R., Resnik, J., Yuan, Y., Whitton, J. P., Edge, A. S., Liberman, M. C., & Polley, D. B. (2016). Central gain restores auditory processing following near-complete cochlear denervation. *Neuron*, *89*(4), 867–879. https://doi.org/10.1016/j.neuron.2015.12.041

Dias, J. W., McClaskey, C. M., & Harris, K. C. (2019). Time-compressed speech identification is predicted by auditory neural processing, perceptuomotor speed, and executive functioning in younger and older listeners. *Journal of the Association for Research in Otolaryngology*, *20*(1), 73–88. https://doi.org/10.1007/s10162-018-00703-1

Dimitrijevic, A., Alsamri, J., John, M. S., Purcell, D., George, S., & Zeng, F.-G. (2016). Human envelope following responses to amplitude modulation: effects of aging and modulation depth. *Ear and Hearing*, *37*(5), e322–e335. https://doi.org/10.1097/AUD.0000000000000324

Dimitrijevic, A., John, M. S., & Picton, T. W. (2004). Auditory steady-state responses and word recognition scores in normal-hearing and hearing-impaired adults. *Ear and Hearing*, *25*(1), 68–84. https://doi.org/10.1097/01.AUD.0000111545.71693.48

Eggermont, J. J. (2000). Neural responses in primary auditory cortex mimic psychophysical, across-frequency-channel, gap-detection thresholds. *Journal of Neurophysiology*, *84*(3), 1453–1463. https://doi.org/10.1152/jn.2000.84.3.1453

Friedman, D. (2008). Oxford Handbook of Event-Related Potential Components.

Gleich, O., Hamann, I., Klump, G. M., Kittel, M., & Strutz, J. (2003). Boosting GABA improves impaired auditory temporal resolution in the gerbil. *NeuroReport*, *14*(14), 1877–1880. https://doi.org/10.1097/00001756-200310060-00024

Gleich, O., & Strutz, J. (2011). The effect of gabapentin on gap detection and forward masking in young and old gerbils. *Ear and Hearing*, *32*(6), 741–749. https://doi.org/10.1097/AUD.0b013e318222289f

Harris, K. C., Wilson, S., Eckert, M. A., & Dubno, J. R. (2012). Human evoked cortical activity to silent gaps in noise: effects of age, attention, and cortical processing speed. *Ear and Hearing*, *33*(3), 330–339. https://doi.org/10.1097/AUD.0b013e31823fb585

He, N., Horwitz, A. R., Dubno, J. R., & Mills, J. H. (1999). Psychometric functions for gap detection in noise measured from young and aged subjects. *The Journal of the Acoustical Society of America*, *106*(2), 966. https://doi.org/10.1121/1.427109

Hunter, K. P., & Willott, J. F. (1987). Aging and the auditory brainstem response in mice with severe or minimal presbycusis. *Hearing Research*, *30*(2–3), 207–218. https://doi.org/10.1016/0378-5955(87)90137-7

Hwang, E., Han, H. B., Kim, J. Y., & Choi, J. H. (2020). High-density EEG of auditory steady-state responses during stimulation of basal forebrain parvalbumin neurons. *Scientific Data*, *7*(1), 1–9. https://doi.org/10.1038/s41597-020-00621-z

Ison, J. R., Agrawal, P., Pak, J., & Vaughn, W. J. (1998). Changes in temporal acuity with age and with hearing impairment in the mouse: a study of the acoustic startle reflex and its inhibition by brief decrements in noise level. *The Journal of the Acoustical Society of America*, *104*(3 Pt 1), 1696–1704. https://doi.org/10.1121/1.424382

Johnson, K. R., Erway, L. C., Cook, S. A., & Willott, J. F. (1997). A major gene affecting age-related hearing loss in C57BL / 6J mice. *Hearing Research*, *114*, 83–92. https://doi.org/10.1016/S0378-5955(97)00155-X

Key, A. P. F., Dove, G. O., & Maguire, M. J. (2005). Linking brainwaves to the brain: an ERP primer. *Developmental Neuropsychology*, *27*(2), 183–215. https://doi.org/10.1207/s15326942dn2702_1

Leigh-Paffenroth D.E., & Fowler, C. G. (2006). Amplitude-modulated auditory steady-state responses in younger and older listeners. *Journal of the American Academy of Audiology, 17*(8), 582–597.

Lovelace, J. W., Ethell, I. M., Binder, D. K., & Razak, K. A. (2018). Translation-relevant EEG phenotypes in a mouse model of Fragile X Syndrome. *Neurobiology of Disease, 115*, 39–48. https://doi.org/10.1016/j.nbd.2018.03.012

Lovelace, J. W., Ethell, I. M., Binder, D. K., & Razak, K. A. (2020). Minocycline treatment reverses sound evoked EEG abnormalities in a mouse model of Fragile X Syndrome. *Frontiers in Neuroscience, 14*, 771. https://doi.org/10.3389/fnins.2020.00771

Lovelace, J. W., Wen, T. H., Reinhard, S., Hsu, M. S., Sidhu, H., Ethell, I. M., Binder, D. K., & Razak, K. A. (2016). Matrix metalloproteinase-9 deletion rescues auditory evoked potential habituation deficit in a mouse model of Fragile X Syndrome. *Neurobiology of Disease, 89*, 126–135. https://doi.org/10.1016/j.nbd.2016.02.002

McClaskey, C. M., Dias, J. W., & Harris, K. C. (2019). Sustained envelope periodicity representations are associated with speech-in-noise performance in difficult listening conditions for younger and older adults. *Journal of Neurophysiology, 122*(4), 1685–1696. https://doi.org/10.1152/jn.00845.2018

Parthasarathy, A., Cunningham, P. A., & Bartlett, E. L. (2010). Age-related differences in auditory processing as assessed by amplitude-modulation following responses in quiet and in noise. *Frontiers in Aging Neuroscience, 2*, 152. https://doi.org/10.3389/fnagi.2010.00152

Razak, K. A., & Fuzessery, Z. M. (2007). Development of inhibitory mechanisms underlying selectivity for the rate and direction of frequency-modulated sweeps in the auditory cortex. *Journal of Neuroscience, 27*(7), 1769–1781. https://doi.org/10.1523/JNEUROSCI.3851-06.2007

Razak, K. A., & Fuzessery, Z. M. (2013). GABA shapes selectivity for the rate and direction of frequency-modulated sweeps in the auditory cortex. *Journal of Neurophysiology*, *102*, 1366–1378. https://doi.org/10.1152/jn.00334.2009

Rotschafer, S., & Razak, K. (2013). Altered auditory processing in a mouse model of fragile X syndrome. *Brain Research, 1506*, 12–24. https://doi.org/10.1016/j.brainres.2013.02.038

Rumschlag, J. A., Lovelace, J. W., & Razak, K. A. (2020). Age- and movement-related modulation of cortical oscillations in a mouse model of presbycusis. *Hearing*

Research, Advance Online Publication. https://doi.org/10.1016/j.heares.2020.108095

Schneider, B. A., & Hamstra, S. J. (1999). Gap detection thresholds as a function of tonal duration for younger and older listeners. *The Journal of the Acoustical Society of America, 106*(1), 371–380. https://doi.org/10.1121/1.427062

Snell, K. B. (1997). Age-related changes in temporal gap detection. *Journal of the Acoustical Society of America, 101*(4), 2214–2220. https://doi.org/10.1121/1.418205

Snell, K. B., & Frisina, D. R. (2000). Relationships among age related differences in gap detection and word recognition. *The Journal of the Acoustical Society of America, 107*(3), 1615–1626. https://doi.org/10.1121/1.428446

Stothart, G., & Kazanina, N. (2016). Auditory perception in the aging brain: the role of inhibition and facilitation in early processing. *Neurobiology of Aging, 47*, 23–34. https://doi.org/10.1016/j.neurobiolaging.2016.06.022

Tremblay, K. L., Piskosz, M., & Souza, P. (2002). Aging alters the neural representation of speech cues. *NeuroReport, 13*(15), 1865–1870. https://doi.org/10.1097/00001756-200210280-00007

Tremblay, K. L., Piskosz, M., & Souza, P. (2003). Effects of age and age-related hearing loss on the neural representation of speech cues. *Clinical Neurophysiology, 114*(7), 1332–1343. https://doi.org/10.1016/S1388-2457(03)00114-7

Trujillo, M., Measor, K., Carrasco, M. M., & Razak, K. A. (2011). Selectivity for the rate of frequency-modulated sweeps in the mouse auditory cortex. *Journal of Neurophysiology, 106*(6), 2825–2837. https://doi.org/10.1152/jn.00480.2011

Uhlhaas, P. J., & Singer, W. (2010). Abnormal neural oscillations and synchrony in schizophrenia. *Nature Reviews Neuroscience, 11*(2), 100–113. https://doi.org/10.1038/nrn2774

Umbricht, D., Vyssotky, D., Latanov, A., Nitsch, R., Brambilla, R., D'Adamo, P., & Lipp, H.-P. (2004). Midlatency auditory event-related potentials in mice: comparison to midlatency auditory ERPs in humans. *Brain Research, 1019*(1-2), 189–200. https://doi.org/10.1016/j.brainres.2004.05.097

Walton, J. P., Frisina, R. D., & O'Neill, W. E. (1998). Age-related alteration in processing of temporal sound features in the auditory midbrain of the CBA

mouse. *Journal of Neuroscience, 18*(7), 2764–2776. https://doi.org/10.1523/JNEUROSCI.18-07-02764.1998

Wen, T. H., Lovelace, J. W., Ethell, I. M., Binder, D. K., & Razak, K. A. (2019). Developmental changes in EEG phenotypes in a mouse model of Fragile X Syndrome. *Neuroscience, 398*, 126–143. https://doi.org/10.1016/j.neuroscience.2018.11.047

Willott, J. F., Aitkin, L. M., & McFadden, S. L. (1993). Plasticity of auditory cortex associated with sensorineural hearing loss in adult C57BL/6J mice. *The Journal of Comparative Neurology, 329*(3), 402–411. https://doi.org/10.1002/cne.903290310

Wilson, T. W., Rojas, D. C., Reite, M. L., Teale, P. D., & Rogers, S. J. (2007). Children and adolescents with autism exhibit reduced MEG steady-state gamma responses. *Biological Psychiatry, 62*(3), 192–197. https://doi.org/10.1016/j.biopsych.2006.07.002

Woods, D. L., & Clayworth, C. C. (1986). Age-related changes in human middle latency auditory evoked potentials. *Electroencephalography and Clinical Neurophysiology, 65*, 297–303. https://doi.org/10.1016/0168-5597(86)90008-0

Yokota, Y., & Naruse, Y. (2015). Phase coherence of auditory steady-state response reflects the amount of cognitive workload in a modified N-back task. *Neuroscience Research, 100*, 39–45. https://doi.org/10.1016/j.neures.2015.06.010

Zhao, Y., Xu, X., He, J., Xu, J., & Zhang, J. (2015). Age-related changes in neural gap detection thresholds in the rat auditory cortex. *European Journal of Neuroscience, 41*(3), 285–292. https://doi.org/10.1111/ejn.12791

Chapter 5

Conclusions

The chapters in this dissertation profile auditory changes in aging mice with and without age-related hearing loss. Some findings, such as a decrease in resting gamma power, are shared between the two mouse models. Measures of auditory temporal processing, however, differentiate between presbycusis and typical age-related hearing changes. Although the C57bl/6 mice show strong event-related potentials in response to broadband noise bursts, they show severe deficits in synchronized responses to any sort of amplitude modulated stimuli. On the other hand, the older FVB mice, which age without showing signs of presbycusis, have similar ERPs to younger mice, and show only small reductions in synchronized responses to salient AM noise when the stimuli are not adjusted for the observed minor hearing loss.

The gap-ASSR stimulus shows a temporal processing deficit in old mice without severe hearing loss. The gap-ASSR stimulus tests the ability of the auditory system to consistently detect brief gaps presented rapidly within noise (measured as ITPC; inter-trial phase clustering). When the modulation depth is 100%, such that the gaps are silent, the older FVB mice show similar consistency values to the younger FVB mice. However, when the gaps are partial reductions in level, rather than silence, the older mice show deficits. In that case, the older mice show nearly identical consistency values when the sound is presented at either 70 dB SPL or 80 dB SPL, both of which are lower than the consistency values of the younger mice. This finding demonstrates that the older mice with normal hearing have temporal processing deficits, even when the signal gain is

increased. When the stimulus has a higher signal to noise ratio, as in the pulse-ASSR stimulus, there is no difference between the consistency measure of temporal processing.

These findings demonstrate the utility of using mice as preclinical models of auditory processing deficits in aging. I have developed a series of measures that differentiate between young and old mice, and between mice with and without hearing loss. These measures have strong translational potential. Similar measures can be and have been recorded from older adults. For example, the decreases in P2 and N2 amplitudes in the ERPs of older FVB mice mirror age-related changes observed in humans (Čeponiene et al., 2008). Neither humans nor FVB mice show a significant decrease in measures of click/pulse ASSR with age (McClaskey et al., 2019). However, more subtle measures of temporal processing show differences in FVB mice, as shown in this study. In C57 mice and in humans with severe presbycusis, temporal processing is impaired. Altogether, the age-related changes in cortical auditory processing measured in mice show similarities to those seen in humans. Further studies are warranted to confirm that the findings from the passive listening paradigm used in the preceding chapters persist in experiments controlling for attention and arousal. However, the initial results are promising. The changes to responses following nicotine administration show that this model can be used to test potential therapeutic avenues for age-related hearing changes. Recording cortical EEG signals from mice provides increased translational power, compared to measures of auditory processing at lower auditory stations. Many of the results detailed in this dissertation are directly comparable to findings in older humans.

Methodological considerations

Though the described method of measuring EEG is versatile and shows significant age-related differences, the resulting data contains ambiguities that complicate interpretation. For example, the measures of cortical activity do not take into account subcortical changes. In the presbycusis model mice, for example, morphological and physiological changes occur in the cochlea, which have downstream effects on auditory processing. With this recording technique, we are forced to treat the subcortical auditory system as a black box. However, chemogenetic or optogenetic techniques can be used to show how specific changes in the cortex alter population-level activity. For example, PV cells density is reduced in aging C57 mice (Brewton et al., 2016; Martin del Campo et al., 2012). To determine which of the age-related differences we see are likely caused by decreased PV cell density, we could use a chemogenetic approach, expressing inhibitory DREADDs specifically in PV neurons in the auditory cortex. If the responses recorded from younger mice while PV cells are silenced are similar to responses recorded from aged mice, then we may assert that the age-related changes we see are likely due to changes in PV neuron activity. This has specific implications for treatment options. If faulty inhibitory signaling plays a role in age-related changes to auditory processing, as is suggested by numerous studies (Caspary et al., 2008), then treatments should focus on restoring inhibition in the auditory system.

Because the mice were moving freely during stimulus presentations, there is a concern that they may have perceived different sound levels depending on which direction they were facing. However, the speaker was suspended high enough that the

sound level measured at all points in the arena was uniform. If the mice reared, they may perceive a slightly different sound level, but rearing was not observed in the recorded video.

Future studies

One of the next steps to take in this project is to test the effect of acute nicotine administration on the gap-ASSR in older mice. Chapter 3 demonstrated that acute nicotine can alter the impulse response of the cortex (ERP) and improve synchronization to an AM stimulus in older mice without severe hearing loss. The natural hypothesis stemming from the previously presented findings is that nicotine should improve auditory temporal processing, as measured by the gap-ASSR.

To evaluate the utility of the gap-ASSR stimulus, a behavioral study must be conducted. Younger and older mice without hearing loss would be trained in a go/no go task, in which they would respond to stimuli containing gaps with a nose poke and ignore continuous stimuli. Extending the EEG recording protocol to allow for simultaneous behavioral testing should not pose a significant challenge and would allow for a stronger interpretation of the electrophysiological changes with age.

The gap-ASSR stimulus should also be tested in humans, to determine whether the stimulus has translational potential. To do this experiment, a cohort of human participants without severe hearing loss would be tested for speech in noise comprehension (SPIN), which is perhaps the most important measure of age-related changes to auditory temporal processing. Next, scalp EEG would be recorded while the participants passively listen to the sound while engaging in an unrelated viewing activity.

Finally, to measure the behavioral relevance of the gap-ASSR in humans, scalp EEG would be recorded from the participants as they engaged in a forced choice task, in which they would listen to noise bursts, either uninterrupted or interrupted by short gaps spaced at 40 Hz. The gap width and modulation depth would be varied, as described previously. The SPIN, passive EEG, and active EEG task results would then be analyzed using regression, to determine whether the passive or active EEG predict the ability to hear speech in noise.

To more closely compare the resting EEG of aged mice with and without severe hearing loss, B6.CAST-Cdh23Ahl+ (CAST) mice should be compared to C57bl/6. The CAST mice have the same genetic background as the C57bl/6 mice, but do not have the Cadherin 23 splice variant that causes the early onset of hearing loss.

References

Brewton, D. H., Kokash, J., Jimenez, O., Pena, E. R., & Razak, K. A. (2016). Age-related deterioration of perineuronal nets in the primary auditory cortex of mice. *Frontiers in Aging Neuroscience*, *8*, 270. https://doi.org/10.3389/fnagi.2016.00270

Caspary, D. M., Ling, L., Turner, J. G., & Hughes, L. F. (2008). Inhibitory neurotransmission, plasticity and aging in the mammalian central auditory system. *Journal of Experimental Biology*, *211*(11), 1781–1791. https://doi.org/10.1242/jeb.013581

Čeponiene, R., Westerfield, M., Torki, M., & Townsend, J. (2008). Modality-specificity of sensory aging in vision and audition: evidence from event-related potentials. *Brain Research, 1215*, 53–68. https://doi.org/10.1016/j.brainres.2008.02.010

Martin del Campo, H. N., Measor, K. R., & Razak, K. A. (2012). Parvalbumin immunoreactivity in the auditory cortex of a mouse model of presbycusis. *Hearing Research, 294*(1–2), 31–39. https://doi.org/10.1016/j.heares.2012.08.017

McClaskey, C. M., Dias, J. W., & Harris, K. C. (2019). Sustained envelope periodicity representations are associated with speech-in-noise performance in difficult listening conditions for younger and older adults. *Journal of Neurophysiology, 122*(4), 1685–1696. https://doi.org/10.1152/jn.00845.2018

Compiled References

Anderson, S., Parbery-Clark, A., White-Schwoch, T., & Kraus, N. (2012). Aging affects neural precision of speech encoding. *The Journal of Neuroscience*, *32*(41), 14156–14164. https://doi.org/10.1523/JNEUROSCI.2176-12.2012

Askew, C. E., Lopez, A. J., Wood, M. A., & Metherate, R. (2019). Nicotine excites VIP interneurons to disinhibit pyramidal neurons in auditory cortex. *Synapse*, *73*(9), 1–12. https://doi.org/10.1002/syn.22116

Askew, C., Intskirveli, I., & Metherate, R. (2017). Systemic nicotine increases gain and narrows receptive fields in a1 via integrated cortical and subcortical actions. *ENeuro*, *4*(3). https://doi.org/10.1523/ENEURO.0192-17.2017

Ball, T., Demandt, E., Mutschler, I., Neitzel, E., Mehring, C., Vogt, K., Aertsen, A., & Schulze-Bonhage, A. (2008). Movement related activity in the high gamma range of the human EEG. *NeuroImage*, *41*(2), 302–310. https://doi.org/10.1016/j.neuroimage.2008.02.032

Balmer, T. S. (2016). Perineuronal nets enhance the excitability of fast-spiking neurons. *ENeuro*, *3*(4), 745–751. https://doi.org/10.1523/ENEURO.0112-16.2016

Barr, R. S., Culhane, M. A., Jubelt, L. E., Mufti, R. S., Dyer, M. A., Weiss, A. P., Deckersbach, T., Kelly, J. F., Freudenreich, O., Goff, D. C., & Evins, A. E. (2008). The effects of transdermal nicotine on cognition in nonsmokers with schizophrenia and nonpsychiatric controls. *Neuropsychopharmacology*, *33*(3), 480–490. https://doi.org/10.1038/sj.npp.1301423

Barry, R. J., Clarke, A. R., Johnstone, S. J., Magee, C. A., & Rushby, J. A. (2007). EEG differences between eyes-closed and eyes-open resting conditions. *Clinical Neurophysiology*, *118*(12), 2765–2773. https://doi.org/10.1016/j.clinph.2007.07.028

Barsz, K., Ison, J. R., Snell, K. B., & Walton, J. P. (2002). Behavioral and neural measures of auditory temporal acuity in aging humans and mice. *Neurobiology of Aging*, *23*(4), 565–578. https://doi.org/10.1016/S0197-4580(02)00008-8

Bazanova, O. M., & Vernon, D. (2014). Interpreting EEG alpha activity. *Neuroscience and Biobehavioral Reviews*, *44*, 94–110. https://doi.org/10.1016/j.neubiorev.2013.05.007

Başar, E., Schürmann, M., Demiralp, T., Baar-Eroglu, C., & Ademoglu, A. (2001). Event-related oscillations are “real brain responses” - Wavelet analysis and new

strategies. *International Journal of Psychophysiology*, *39*(2–3), 91–127. https://doi.org/10.1016/S0167-8760(00)00135-5

Brewton, D. H., Kokash, J., Jimenez, O., Pena, E. R., & Razak, K. A. (2016). Age-related deterioration of perineuronal nets in the primary auditory cortex of mice. *Frontiers in Aging Neuroscience*, *8*, 270. https://doi.org/10.3389/fnagi.2016.00270

Brosch, M., Budinger, E., & Scheich, H. (2002). Stimulus-related gamma oscillations in primate auditory cortex. *Journal of Neurophysiology*, *87*(6), 2715–2725. https://doi.org/10.1152/jn.00583.2001

Bueno-Junior, L. S., Simon, N. W., Wegener, M. A., & Moghaddam, B. (2017). Repeated nicotine strengthens gamma oscillations in the prefrontal cortex and improves visual attention. *Neuropsychopharmacology*, *42*(8), 1590–1598. https://doi.org/10.1038/npp.2017.15

Burianova, J., Ouda, L., Profant, O., & Syka, J. (2009). Age-related changes in GAD levels in the central auditory system of the rat. *Experimental Gerontology*, *44*(3), 161–169. https://doi.org/10.1016/j.exger.2008.09.012

Cabungcal, J. H., Steullet, P., Morishita, H., Kraftsik, R., Cuenod, M., Hensch, T. K., & Do, K. Q. (2013). Perineuronal nets protect fast-spiking interneurons against oxidative stress. *Proceedings of the National Academy of Sciences of the United States of America*, *110*(22), 9130–9135. https://doi.org/10.1073/pnas.1300454110

Cacioppo, J. T., & Hawkley, L. C. (2009). Perceived social isolation and cognition. *Trends in Cognitive Sciences 13*(10), 447–454. https://doi.org/10.1016/j.tics.2009.06.005

Cardin, J. A., Carlén, M., Meletis, K., Knoblich, U., Zhang, F., Deisseroth, K., Tsai, L. H., & Moore, C. I. (2009). Driving fast-spiking cells induces gamma rhythm and controls sensory responses. *Nature*, *459*(7247), 663–667. https://doi.org/10.1038/nature08002

Carlson, G. C., Talbot, K., Halene, T. B., Gandal, M. J., Kazi, H. A., Schlosser, L., Phung, Q. H., Gur, R. E., Arnold, S. E., & Siegel, S. J. (2011). Dysbindin-1 mutant mice implicate reduced fast-phasic inhibition as a final common disease mechanism in schizophrenia. *Proceedings of the National Academy of Sciences of the United States of America*, *108*(43). https://doi.org/10.1073/pnas.1109625108

Caspary, D. M., Holder, T. M., Hughes, L. F., Milbrandt, J. C., McKernan, R. M., & Naritoku, D. K. (1999). Age-related changes in GABA(A) receptor subunit

composition and function in rat auditory system. *Neuroscience*, *93*(1), 307–312. https://doi.org/10.1016/S0306-4522(99)00121-9

Caspary, D. M., Hughes, L. F., & Ling, L. L. (2013). Age-related GABAA receptor changes in rat auditory cortex. *Neurobiology of Aging*, *34*(5), 1486–1496. https://doi.org/10.1016/j.neurobiolaging.2012.11.009

Caspary, D. M., Ling, L., Turner, J. G., & Hughes, L. F. (2008). Inhibitory neurotransmission, plasticity and aging in the mammalian central auditory system. *Journal of Experimental Biology*, *211*(11), 1781–1791. https://doi.org/10.1242/jeb.013581

Caspary, Donald M., Palombi, P. S., & Hughes, L. F. (2002). GABAergic inputs shape responses to amplitude modulated stimuli in the inferior colliculus. *Hearing Research*, *168*(1–2), 163–173. https://doi.org/10.1016/S0378-5955(02)00363-5

Čeponiene, R., Westerfield, M., Torki, M., & Townsend, J. (2008). Modality-specificity of sensory aging in vision and audition: evidence from event-related potentials. *Brain Research, 1215*, 53–68. https://doi.org/10.1016/j.brainres.2008.02.010

Cervenka, M. C., Nagleb, S., & Boatman-Reich, D. (2011). Cortical high-gamma responses in auditory processing. *American Journal of Audiology*, *20*(2). https://doi.org/10.1038/jid.2014.371

Chambers, A. R., Resnik, J., Yuan, Y., Whitton, J. P., Edge, A. S., Liberman, M. C., & Polley, D. B. (2016). Central gain restores auditory processing following near-complete cochlear denervation. *Neuron*, *89*(4), 867–879. https://doi.org/10.1016/j.neuron.2015.12.041

Chen, G., Zhang, Y., Li, X., Zhao, X., Ye, Q., Lin, Y., Tao, H. W., Rasch, M. J., & Zhang, X. (2017). Distinct inhibitory circuits orchestrate cortical beta and gamma band oscillations. *Neuron*, *96*(6), 1403-1418. https://doi.org/10.1016/j.neuron.2017.11.033

Chen, J. E., & Glover, G. H. (2015). Functional magnetic resonance imaging methods. *Neuropsychology Review*, *25*(3), 289–313. https://doi.org/10.1007/s11065-015-9294-9

Cheyne, D., Bells, S., Ferrari, P., Gaetz, W., & Bostan, A. C. (2008). Self-paced movements induce high-frequency gamma oscillations in primary motor cortex. *NeuroImage*, *42*(1), 332–342. https://doi.org/10.1016/j.neuroimage.2008.04.178

Chiang, A. K. I., Rennie, C. J., Robinson, P. A., van Albada, S. J., & Kerr, C. C. (2011). Age trends and sex differences of alpha rhythms including split alpha peaks. *Clinical Neurophysiology*, *122*(8), 1505–1517. https://doi.org/10.1016/j.clinph.2011.01.040

Christov, M., & Dushanova, J. (2016). Functional correlates of brain aging: beta and gamma components of event-related band responses. *Acta Neurobiologiae Experimentalis*, *76*(2), 98–109. https://doi.org/10.21307/ane-2017-009

Clinard, C. G., & Cotter, C. M. (2015). Neural representation of dynamic frequency is degraded in older adults. *Hearing Research*, *323*, 91–98. https://doi.org/10.1016/j.heares.2015.02.002

Cohen, M. X. (2014). Analyzing neural time series data: theory and practice. *MIT press*.

Cook, I. A., O'Hara, R., Uijtdehaage, S. H. J., Mandelkern, M., & Leuchter, A. F. (1998). Assessing the accuracy of topographic EEG mapping for determining local brain function. *Electroencephalography and Clinical Neurophysiology*, *107*(6), 408–414. https://doi.org/10.1016/S0013-4694(98)00092-3

Crone, N., Boatman, D., Gordon, B., & Hao, L. (2001). Induced electrocorticographic gamma activity during auditory perception. *Clinical Neurophysiology*, *112*, 565–582. https://doi.org/10.1016/S1388-2457(00)00545-9

Curio, G., Neuloh, G., Numminen, J., Jousmäki, V., & Hari, R. (2000). Speaking modifies utterance-related activity of the human auditory cortex. *Human Brain Mapping*, *9*, 183–191. https://doi.org/10.1016/s1053-8119(18)30881-4

Davis, A., McMahon, C. M., Pichora-Fuller, K. M., Russ, S., Lin, F., Olusanya, B. O., Chadha, S., & Tremblay, K. L. (2016). Aging and hearing health: the life-course approach. *Gerontologist*, *56*, S256–S267. https://doi.org/10.1093/geront/gnw033

De Villers-Sidani, E., Alzghoul, L., Zhou, X., Simpson, K. L., Lin, R. C. S., & Merzenich, M. M. (2010). Recovery of functional and structural age-related changes in the rat primary auditory cortex with operant training. *Proceedings of the National Academy of Sciences of the United States of America*, *107*(31), 13900–13905. https://doi.org/10.1073/pnas.1007885107

Desmedt, J. E., & Tomberg, C. (1994). Transient phase-locking of 40 Hz electrical oscillations in prefrontal and parietal human cortex reflects the process of conscious somatic perception. *Neuroscience Letters*, *168*, 126–129. https://doi.org/10.1016/0304-3940(94)90432-4

Dias, J. W., McClaskey, C. M., & Harris, K. C. (2019). Time-compressed speech identification is predicted by auditory neural processing, perceptuomotor speed, and executive functioning in younger and older listeners. *Journal of the Association for Research in Otolaryngology*, *20*(1), 73–88. https://doi.org/10.1007/s10162-018-00703-1

Dimitrijevic, A., Alsamri, J., John, M. S., Purcell, D., George, S., & Zeng, F.-G. (2016). Human envelope following responses to amplitude modulation: effects of aging and modulation depth. *Ear and Hearing*, *37*(5), e322–e335. https://doi.org/10.1097/AUD.0000000000000324

Dimitrijevic, A., John, M. S., & Picton, T. W. (2004). Auditory steady-state responses and word recognition scores in normal-hearing and hearing-impaired adults. *Ear and Hearing*, *25*(1), 68–84. https://doi.org/10.1097/01.AUD.0000111545.71693.48

Edwards, E., Soltani, M., Deouell, L. Y., Berger, M. S., & Knight, R. T. (2005). High gamma activity in response to deviant auditory stimuli recorded directly from human cortex. *Journal of Neurophysiology*, *94*(6), 4269–4280. https://doi.org/10.1152/jn.00324.2005

Eggermont, J. J. (2000). Neural responses in primary auditory cortex mimic psychophysical, across-frequency-channel, gap-detection thresholds. *Journal of Neurophysiology*, *84*(3), 1453–1463. https://doi.org/10.1152/jn.2000.84.3.1453

Ehlers, C. L., & Criado, J. R. (2009). Event-related oscillations in mice: effects of stimulus characteristics. *Journal of Neuroscience Methods*, *181*(1), 52–57. https://doi.org/10.1016/j.jneumeth.2009.04.015

Ethridge, L. E., White, S. P., Mosconi, M. W., Wang, J., Pedapati, E. V., Erickson, C. A., Byerly, M. J., & Sweeney, J. A. (2017). Neural synchronization deficits linked to cortical hyper-excitability and auditory hypersensitivity in fragile X syndrome. *Molecular Autism*, *8*(1), 1–11. https://doi.org/10.1186/s13229-017-0140-1

Featherstone, R. E., Phillips, J. M., Thieu, T., Ehrlichman, R. S., Halene, T. B., Leiser, S. C., Christian, E., Johnson, E., Lerman, C., & Siegel, S. J. (2012). Nicotine receptor subtype-specific effects on auditory evoked oscillations and potentials. *PLoS ONE*, *7*(7). https://doi.org/10.1371/journal.pone.0039775

Feurra, M., Bianco, G., Santarnecchi, E., del Testa, M., Rossi, A., & Rossi, S. (2011). Frequency-dependent tuning of the human motor system induced by transcranial oscillatory potentials. *Journal of Neuroscience*, *31*(34), 12165–12170. https://doi.org/10.1523/JNEUROSCI.0978-11.2011

Finnigan, S., O'Connell, R. G., Cummins, T. D. R., Broughton, M., & Robertson, I. H. (2011). ERP measures indicate both attention and working memory encoding decrements in aging. *Psychophysiology*, *48*(5), 601–611. https://doi.org/10.1111/j.1469-8986.2010.01128.x

Fitzgibbons, P. J., Gordon-Salant, S., & Friedman, S. A. (2006). Effects of age and sequence presentation rate on temporal order recognition. *The Journal of the Acoustical Society of America*, *120*(2), 991–999. https://doi.org/10.1121/1.2214463

Flinker, A., Chang, E. F., Kirsch, H. E., Barbaro, N. M., Crone, N. E., & Knight, R. T. (2010). Single-trial speech suppression of auditory cortex activity in humans. *Journal of Neuroscience*, *30*(49), 16643–16650. https://doi.org/10.1523/JNEUROSCI.1809-10.2010

Franowicz, M. N., & Barth, D. S. (1995). Comparison of evoked potentials and high-frequency (gamma-band) oscillating potentials in rat auditory cortex. Journal of *Neurophysiology*, *74*(1), 96–112. https://doi.org/10.1152/jn.1995.74.1.96

Friedman, D. (2008). Oxford Handbook of Event-Related Potential Components.

Frisina, R. D. (2009). Age-related hearing loss: ear and brain mechanisms. *Annals of the New York Academy of Sciences*, *1170*, 708–717. https://doi.org/10.1111/j.1749-6632.2009.03931.x

Galambos, R. (1992). A comparison of certain gamma band (40-Hz) brain rhythms in cat and man. In E. Baar & T. H. Bullock (Eds.), Induced Rhythms in the Brain, 201–216. *Birkhäuser Boston*. https://doi.org/10.1007/978-1-4757-1281-0_11

Gates, G. A., Beiser, A., Rees, T. S., D'Agostino, R. B., & Wolf, P. A. (2002). Central auditory dysfunction may precede the onset of clinical dementia in people with probable Alzheimer's disease. *Journal of the American Geriatrics Society, 50*(3), 482–488. https://doi.org/10.1046/j.1532-5415.2002.50114.x

Gates, G., & Mills, J. (2005). Presbycusis. *Lancet*, *366*, 1111–1120. https://doi.org/10.1016/S0140-6736(05)67423-5

Ghimire, M., Cai, R., Ling, L., Hackett, T. A., & Caspary, D. M. (2020). Nicotinic receptor subunit distribution in auditory cortex: impact of aging on receptor number and function. *The Journal of Neuroscience*, *40*(30). https://doi.org/10.1523/jneurosci.0093-20.2020

Gil, S. M., & Metherate, R. (2018). Enhanced sensory–cognitive processing by activation of nicotinic acetylcholine receptors. *Nicotine & Tobacco Research*, *21*(3), 377-382. https://doi.org/10.1093/ntr/nty134

Gleich, O., Hamann, I., Klump, G. M., Kittel, M., & Strutz, J. (2003). Boosting GABA improves impaired auditory temporal resolution in the gerbil. *NeuroReport*, *14*(14), 1877–1880. https://doi.org/10.1097/00001756-200310060-00024

Gleich, O., & Strutz, J. (2011). The effect of gabapentin on gap detection and forward masking in young and old gerbils. *Ear and Hearing*, *32*(6), 741–749. https://doi.org/10.1097/AUD.0b013e318222289f

Gordon-Salant, S., Fitzgibbons, P. J., & Yeni-Komshian, G. H. (2011). Auditory temporal processing and aging: implications for speech understanding of older people. *Audiology Research*, *1*(1), 9–15. https://doi.org/10.4081/audiores.2011.e4

Gordon-Salant, S., & Fitzgibbons, P. J. (2001). Sources of age-related recognition difficulty for time-compressed speech. *Journal of Speech Language and Hearing Research*, *44*(4), 709-719. https://doi.org/10.1044/1092-4388(2001/056)

Grossman, M., Cooke, A., DeVita, C., Alsop, D., Detre, J., Chen, W., & Gee, J. (2002). Age-related changes in working memory during sentence comprehension: an fMRI study. *NeuroImage*, *15*(2), 302–317. https://doi.org/10.1006/nimg.2001.0971

Gulledge, A. T., Park, S. B., Kawaguchi, Y., & Stuart, G. J. (2007). Heterogeneity of phasic cholinergic signaling in neocortical neurons. *Journal of Neurophysiology*, *97*(3), 2215–2229. https://doi.org/10.1152/jn.00493.2006

Gürses, E., Türkyılmaz, M. D., & Sennaroğlu, G. (2020). Evaluation of auditory temporal processing in patients fitted with bone-anchored hearing aids. *European Archives of Oto-Rhino-Laryngology*, *277*(2), 351–359. https://doi.org/10.1007/s00405-019-05701-4

Harris, K. C., & Dubno, J. R. (2017). Age-related deficits in auditory temporal processing: unique contributions of neural dyssynchrony and slowed neuronal processing. *Neurobiology of Aging*, *53*, 150–158. https://doi.org/10.1016/j.neurobiolaging.2017.01.008

Harris, K. C., Mills, J. H., He, N. J., & Dubno, J. R. (2008). Age-related differences in sensitivity to small changes in frequency assessed with cortical evoked potentials. *Hearing Research*, *243*(1–2), 47–56. https://doi.org/10.1016/j.heares.2008.05.005

Harris, K. C., Wilson, S., Eckert, M. A., & Dubno, J. R. (2012). Human evoked cortical activity to silent gaps in noise: effects of age, attention, and cortical processing speed. *Ear and Hearing*, *33*(3), 330–339. https://doi.org/10.1097/AUD.0b013e31823fb585

Hasenstaub, A., Shu, Y., Haider, B., Kraushaar, U., Duque, A., & McCormick, D. A. (2005). Inhibitory postsynaptic potentials carry synchronized frequency information in active cortical networks. *Neuron*, *47*(3), 423–435. https://doi.org/10.1016/j.neuron.2005.06.016

He, N., Dubno, J. R., & Mills, J. H. (1998). Frequency and intensity discrimination measured in a maximum-likelihood procedure from young and aged normal-hearing subjects. *The Journal of the Acoustical Society of America*, *103*(1), 553–565. https://doi.org/10.1121/1.421127

He, N., Mills, J. H., & Dubno, J. R. (2007). Frequency modulation detection: effects of age, psychophysical method, and modulation waveform. *The Journal of the Acoustical Society of America*, *122*(1), 467–477. https://doi.org/10.1121/1.2741208

He, N., Horwitz, A. R., Dubno, J. R., & Mills, J. H. (1999). Psychometric functions for gap detection in noise measured from young and aged subjects. *The Journal of the Acoustical Society of America*, *106*(2), 966. https://doi.org/10.1121/1.427109

Herrmann, B., Parthasarathy, A., & Bartlett, E. L. (2017). Ageing affects dual encoding of periodicity and envelope shape in rat inferior colliculus neurons. *European Journal of Neuroscience*, *45*(2), 299-311. https://doi.org/10.1111/ejn.13463

Hestrin, S., & Galarreta, M. (2005). Electrical synapses define networks of neocortical GABAergic neurons. *Trends in neurosciences, 28*(6), 304-309. https://doi.org/10.1016/j.tins.2005.04.001

Hidalgo, J. L. T., Gras, C. B., Lapeira, J. T., Verdejo, M. Á. L., del Campo, J. M. D. C., & Rabadán, F. E. (2009). Functional status of elderly people with hearing loss. *Archives of Gerontology and Geriatrics, 49*(1), 88–92. https://doi.org/10.1016/j.archger.2008.05.006

Hogan, C. A., & Turner, C. W. (1998). High-frequency audibility: benefits for hearing-impaired listeners. *The Journal of the Acoustical Society of America*, *104*(1), 432–441. https://doi.org/10.1121/1.423247

Hopkins, K., & Moore, B. C. J. (2011). The effects of age and cochlear hearing loss on temporal fine structure sensitivity, frequency selectivity, and speech reception in

noise. *The Journal of the Acoustical Society of America*, *130*(1), 334–349. https://doi.org/10.1121/1.3585848

Humes, L. E., Busey, T. A., Craig, J., & Kewley-Port, D. (2013). Are age-related changes in cognitive function driven by age-related changes in sensory processing?. *Attention, Perception, & Psychophysics*, *75*(3), 508-524. https://doi.org/10.3758/s13414-012-0406-9

Hunter, K. P., & Willott, J. F. (1987). Aging and the auditory brainstem response in mice with severe or minimal presbycusis. *Hearing Research*, *30*(2–3), 207–218. https://doi.org/10.1016/0378-5955(87)90137-7

Hwang, E., Han, H. B., Kim, J. Y., & Choi, J. H. (2020). High-density EEG of auditory steady-state responses during stimulation of basal forebrain parvalbumin neurons. *Scientific Data*, *7*(1), 1–9. https://doi.org/10.1038/s41597-020-00621-z

Intskirveli, I., & Metherate, R. (2012). Nicotinic neuromodulation in auditory cortex requires MAPK activation in thalamocortical and intracortical circuits. Journal of *Neurophysiology*, *107*(10), 2782–2793. https://doi.org/10.1152/jn.01129.2011

Ison, J. R., Agrawal, P., Pak, J., & Vaughn, W. J. (1998). Changes in temporal acuity with age and with hearing impairment in the mouse: a study of the acoustic startle reflex and its inhibition by brief decrements in noise level. *The Journal of the Acoustical Society of America*, *104*(3 Pt 1), 1696–1704. https://doi.org/10.1121/1.424382

Jeschke, M., Lenz, D., Budinger, E., Herrmann, C. S., & Ohl, F. W. (2008). Gamma oscillations in gerbil auditory cortex during a target-discrimination task reflect matches with short-term memory. *Brain Research*, *1220*, 70-80. https://doi.org/10.1016/j.brainres.2007.10.047

Johnson, K. R., Erway, L. C., Cook, S. A., & Willott, J. F. (1997). A major gene affecting age-related hearing loss in C57BL / 6J mice. *Hearing Research*, *114*, 83–92. https://doi.org/10.1016/S0378-5955(97)00155-X

Johnson, K. R., Yu, H., Ding, D., Jiang, H., Gagnon, L. H., & Salvi, R. J. (2010). Separate and combined effects of Sod1 and Cdh23 mutations on age-related hearing loss and cochlear pathology in C57BL/6J mice. *Hearing Research*, *268*(1–2), 85–92. https://doi.org/10.1016/j.heares.2010.05.002

Jokeit, H., & Makeig, S. (1994). Different event-related patterns of gamma-band power in brain waves of fast- and slow-reacting subjects. *Proceedings of the National*

Academy of Sciences of the United States of America, *91*(14), 6339–6343. https://doi.org/10.1073/pnas.91.14.6339

Karayanidis, F., Andrews, S., Ward, P. B., & Michie, P. T. (1995). ERP indices of auditory selective attention in aging and Parkinson's disease. *Psychophysiology*, *32*(4), 335–350. https://doi.org/10.1111/j.1469-8986.1995.tb01216.x

Keller, C. H., Kaylegian, K., & Wehr, M. (2018). Gap encoding by parvalbumin-expressing interneurons in auditory cortex. *Journal of Neurophysiology*, *120*(1), 105–114. https://doi.org/10.1152/jn.00911.2017

Key, A. P. F., Dove, G. O., & Maguire, M. J. (2005). Linking brainwaves to the brain: an ERP primer. *Developmental Neuropsychology*, *27*(2), 183–215. https://doi.org/10.1207/s15326942dn2702_1

Kirschstein, T., & Köhling, R. (2009). What is the source of the EEG? *Clinical EEG and Neuroscience, 40*(3), 146–149. https://doi.org/10.1177/155005940904000305

Lai, J., Sommer, A. L., & Bartlett, E. L. (2017). Age-related changes in envelope-following responses at equalized peripheral or central activation. *Neurobiology of Aging*, *58*, 191–200. https://doi.org/10.1016/j.neurobiolaging.2017.06.013

Lawrence, N. S., Ross, T. J., & Stein, E. A. (2002). Cognitive mechanisms of nicotine on visual attention. *Neuron, 36*(3), 539–548. https://doi.org/10.1016/S0896-6273(02)01004-8

Lee, G. T., Lee, C., Kim, K. H., & Jung, K. Y. (2014). Regional and inter-regional theta oscillation during episodic novelty processing. *Brain and Cognition, 90*, 70–75. https://doi.org/10.1016/j.bandc.2014.06.009

Lee, S., Kruglikov, I., Huang, Z. J., Fishell, G., & Rudy, B. (2013). A disinhibitory circuit mediates motor integration in the somatosensory cortex. *Nature Neuroscience, 16*(11), 1662–1670. https://doi.org/10.1038/nn.3544

Leigh-Paffenroth D.E., & Fowler, C. G. (2006). Amplitude-modulated auditory steady-state responses in younger and older listeners. *Journal of the American Academy of Audiology, 17*(8), 582–597.

Levin, E. D., McClernon, F. J., & Rezvani, A. H. (2006). Nicotinic effects on cognitive function: behavioral characterization, pharmacological specification, and anatomic localization. *Psychopharmacology, 184*(3–4), 523–539. https://doi.org/10.1007/s00213-005-0164-7

Li, J., Hu, H., Chen, N., Jones, J. A., Wu, D., Liu, P., & Liu, H. (2018). Aging and sex influence cortical auditory-motor integration for speech control. *Frontiers in Neuroscience, 12*, 749. https://doi.org/10.3389/fnins.2018.00749

Liao, W., Gandal, M. J., Ehrlichman, R. S., Siegel, S. J., & Carlson, G. C. (2012). MeCP2+/- mouse model of RTT reproduces auditory phenotypes associated with Rett syndrome and replicate select EEG endophenotypes of autism spectrum disorder. *Neurobiology of Disease, 46*(1), 88–92. https://doi.org/10.1016/j.nbd.2011.12.048

Lin, F. R., Ferrucci, L., An, Y., Goh, J. O., Doshi, J., Metter, E. J., Davatzikos, C., Kraut, M. A., & Resnick, S. M. (2014). Association of hearing impairment with brain volume changes in older adults. *NeuroImage, 90*, 84-92. https://doi.org/10.1016/j.neuroimage.2013.12.059

Ling, L. L., Hughes, L. F., & Caspary, D. M. (2005). Age-related loss of the GABA synthetic enzyme glutamic acid decarboxylase in rat primary auditory cortex. *Neuroscience, 132*(4), 1103–1113. https://doi.org/10.1016/j.neuroscience.2004.12.043

Lisman, J. E., & Idiart, M. A. P. (1995). Storage of 7 +/- 2 short-term memories in oscillatory subcycles. *Science, 267*(5203), 1512–1515.

Liu, P., Chen, Z., Jones, J. A., Huang, D., & Liu, H. (2011). Auditory feedback control of vocal pitch during sustained vocalization: a cross-sectional study of adult aging. *PLoS ONE, 6*(7). https://doi.org/10.1371/journal.pone.0022791

Livingston, G., Sommerlad, A., Orgeta, V., Costafreda, S. G., Huntley, J., Ames, D., Ballard, C., Banerjee, S., Cohen-Mansfield, J., Cooper, C., Gitlin, L. N., & Howard, R. (2017). Dementia prevention, intervention, and care. *Lancet, 390*(2673–734). https://doi.org/10.1016/ S0140-6736(17)31363-6

Lovelace, J. W., Ethell, I. M., Binder, D. K., & Razak, K. A. (2018). Translation-relevant EEG phenotypes in a mouse model of Fragile X Syndrome. *Neurobiology of Disease, 115*, 39–48. https://doi.org/10.1016/j.nbd.2018.03.012

Lovelace, J. W., Ethell, I. M., Binder, D. K., & Razak, K. A. (2020). Minocycline treatment reverses sound evoked EEG abnormalities in a mouse model of Fragile X Syndrome. *Frontiers in Neuroscience, 14*, 771. https://doi.org/10.3389/fnins.2020.00771

Lovelace, J. W., Wen, T. H., Reinhard, S., Hsu, M. S., Sidhu, H., Ethell, I. M., Binder, D. K., & Razak, K. A. (2016). Matrix metalloproteinase-9 deletion rescues auditory

evoked potential habituation deficit in a mouse model of Fragile X Syndrome. *Neurobiology of Disease, 89*, 126–135. https://doi.org/10.1016/j.nbd.2016.02.002

MacDonald, K. D., Brett, B., & Barth, D. S. (1996). Inter- and intra-hemispheric spatiotemporal organization of spontaneous electrocortical oscillations. *Journal of Neurophysiology, 76*(1), 423–437. https://doi.org/10.1152/jn.1996.76.1.423

MacDonald, K. D., Fifkova, E., Jones, M. S., & Barth, D. S. (1998). Focal stimulation of the thalamic reticular nucleus induces focal gamma waves in cortex. *Somatosensory and Motor Research, 15*(1), 76.

Makeig, S. (1993). Auditory event-related dynamics of the EEG spectrum and effects of exposure to tones. *Electroencephalography and Clinical Neurophysiology, 86*(4), 283–293. https://doi.org/10.1016/0013-4694(93)90110-H

Maris, E., & Oostenveld, R. (2007). Nonparametric statistical testing of EEG- and MEG-data. *Journal of Neuroscience Methods, 164*(1), 177–190. https://doi.org/10.1016/j.jneumeth.2007.03.024

Martin del Campo, H. N., Measor, K. R., & Razak, K. A. (2012). Parvalbumin immunoreactivity in the auditory cortex of a mouse model of presbycusis. *Hearing Research, 294*(1–2), 31–39. https://doi.org/10.1016/j.heares.2012.08.017

Martins, R., Joanette, Y., & Monchi, O. (2015). The implications of age-related neurofunctional compensatory mechanisms in executive function and language processing including the new temporal hypothesis for compensation. *Frontiers in Human Neuroscience, 9*, 221. https://doi.org/10.3389/fnhum.2015.00221

Matta, S. G., Balfour, D. J., Benowitz, N. L., Boyd, R. T., Buccafusco, J. J., Caggiula, A. R., Craig, C. R., Collins, A. C., Damaj, M. I., Donny, E. C., Gardiner, P. S., Grady, S. R., Heberlein, U., Leonard, S. S., Levin, E. D., Lukas, R. J., Markou, A., Marks, M. J., McCallum, S. E., … Zirger, J. M. (2007). Guidelines on nicotine dose selection for in vivo research. *Psychopharmacology, 190*(3), 269–319. https://doi.org/10.1007/s00213-006-0441-0

Mazelová, J., Popelar, J., & Syka, J. (2003). Auditory function in presbycusis: peripheral vs. central changes. *Experimental Gerontology, 38*(1), 87–94. https://doi.org/https://doi.org/10.1016/S0531-5565(02)00155-9

McClaskey, C. M., Dias, J. W., & Harris, K. C. (2019). Sustained envelope periodicity representations are associated with speech-in-noise performance in difficult listening conditions for younger and older adults. *Journal of Neurophysiology, 122*(4), 1685–1696. https://doi.org/10.1152/jn.00845.2018

Mendelson, J. R., & Ricketts, C. (2001). Age-related temporal processing speed deterioration in auditory cortex. *Hearing Research, 158*(1–2), 84–94. https://doi.org/10.1016/S0378-5955(01)00294-5

Metherate, R. (2011). Functional connectivity and cholinergic modulation in auditory cortex. *Neuroscience and Biobehavioral Reviews, 35*(10), 2058–2063. https://doi.org/10.1016/j.neubiorev.2010.11.010

Metherate, R., & Cruikshank, S. J. (1999). Thalamocortical inputs trigger a propagating envelope of gamma-band activity in auditory cortex in vitro. *Experimental Brain Research, 126*(2), 160–174. https://doi.org/10.1007/s002210050726

Metzger, K. L., Maxwell, C. R., Liang, Y., & Siegel, S. J. (2007). Effects of nicotine vary across two auditory evoked potentials in the mouse. Biological *Psychiatry, 61*(1), 23–30. https://doi.org/10.1016/j.biopsych.2005.12.011

Moore, B. C. J., Peters, R. W., & Glasberg, B. R. (1992). Detection of temporal gaps in sinusoids by elderly subjects with and without hearing loss. *The Journal of the Acoustical Society of America*, *92*(4), 1923–1932. https://doi.org/10.1121/1.405240

Nelson, A., Schneider, D. M., Takatoh, J., Sakurai, K., Wang, F., & Mooney, R. (2013). A circuit for motor cortical modulation of auditory cortical activity. *Journal of Neuroscience, 33*(36), 14342–14353. https://doi.org/10.1523/JNEUROSCI.2275-13.2013

Newhouse, P. A., Potter, A., & Singh, A. (2004). Effects of nicotinic stimulation on cognitive performance. *Current Opinion in Pharmacology, 4*(1), 36–46. https://doi.org/10.1016/j.coph.2003.11.001

Ng, C. W., & Recanzone, G. H. (2018). Age-related changes in temporal processing of rapidly-presented sound sequences in the macaque auditory cortex. *Cerebral Cortex, 28*(11), 3775–3796. https://doi.org/10.1093/cercor/bhx240

Niell, C. M., & Stryker, M. P. (2010). Modulation of visual responses by behavioral state in mouse visual cortex. *Neuron, 65*(4), 472–479. https://doi.org/10.1016/j.neuron.2010.01.033

Ouda, L., Druga, R., & Syka, J. (2008). Changes in parvalbumin immunoreactivity with aging in the central auditory system of the rat. *Experimental Gerontology, 43*(8), 782–789. https://doi.org/10.1016/j.exger.2008.04.001

Ouellet, L., & de Villers-Sidani, E. (2014). Trajectory of the main GABAergic interneuron populations from early development to old age in the rat primary

auditory cortex. *Frontiers in Neuroanatomy, 8*, 40. https://doi.org/10.3389/fnana.2014.00040

Overton, J. A., & Recanzone, G. H. (2016). Effects of aging on the response of single neurons to amplitude-modulated noise in primary auditory cortex of rhesus macaque. *Journal of Neurophysiology, 115*(6), 2911–2923. https://doi.org/10.1152/jn.01098.2015

Packer, A. M., & Yuste, R. (2011). Dense, unspecific connectivity of neocortical parvalbumin-positive interneurons: a canonical microcircuit for inhibition? *Journal of Neuroscience, 31*(37), 13260–13271. https://doi.org/10.1523/JNEUROSCI.3131-11.2011

Pantev, C. (1995). Evoked and induced gamma-band activity of the human cortex. *Brain Topography, 7*(4), 321–330. https://doi.org/10.1007/BF01195258

Panza, F., Lozupone, M., Sardone, R., Battista, P., Piccininni, M., Dibello, V., La Montagna, M., Stallone, R., Venezia, P., Liguori, A., Giannelli, G., Bellomo, A., Greco, A., Daniele, A., Seripa, D., Quaranta, N., & Logroscino, G. (2018). Sensorial frailty: age-related hearing loss and the risk of cognitive impairment and dementia in later life. *Therapeutic Advances in Chronic Disease*, *10*. https://doi.org/10.1177/2040622318811000

Parthasarathy, A, & Bartlett, E. L. (2011). Age-related auditory deficits in temporal processing in F-344 rats. *Neuroscience, 192*, 619–630. https://doi.org/https://doi.org/10.1016/j.neuroscience.2011.06.042

Parthasarathy, A., & Bartlett, E. L. (2012). Two-channel recording of auditory-evoked potentials to detect age-related deficits in temporal processing. *Hearing Research, 289*(1–2), 52–62. https://doi.org/10.1016/j.heares.2012.04.014

Parthasarathy, A., Cunningham, P. A., & Bartlett, E. L. (2010). Age-related differences in auditory processing as assessed by amplitude-modulation following responses in quiet and in noise. *Frontiers in Aging Neuroscience, 2*, 152. https://doi.org/10.3389/fnagi.2010.00152

Parthasarathy, A., Datta, J., Torres, J. A. L., Hopkins, C., & Bartlett, E. L. (2014). Age-related changes in the relationship between auditory brainstem responses and envelope-following responses. *Journal of the Association for Research in Otolaryngology*, *15*(4), 649–661. https://doi.org/10.1007/s10162-014-0460-1

Parthasarathy, A., Herrmann, B., & Bartlett, E. L. (2019). Aging alters envelope representations of speech-like sounds in the inferior colliculus. *Neurobiology of Aging, 73*, 30–40. https://doi.org/10.1016/j.neurobiolaging.2018.08.023

Peelle, J. E., & Wingfield, A. (2016). The neural consequences of age-related hearing loss. *Trends in neurosciences, 39*(7), 486-497. https://doi.org/10.1016/j.tins.2016.05.001

Pfeffer, C. K., Xue, M., He, M., Huang, Z. J., & Scanziani, M. (2013). Inhibition of inhibition in visual cortex: the logic of connections between molecularly distinct interneurons. *Nature Neuroscience, 16*(8), 1068–1076. https://doi.org/10.1038/nn.3446.Inhibition

Pfurtscheller, G., & Lopes da Silva, F. H. (1999). Event-related EEG/MEG synchronization and desynchronization: basic principles. *Clinical Neurophysiology, 110*, 1842–1857. https://doi.org/10.1016/S1388-2457(99)00141-8

Phillips, J. M., Ehrlichman, R. S., & Siegel, S. J. (2007). Mecamylamine blocks nicotine-induced enhancement of the P20 auditory event-related potential and evoked gamma. *Neuroscience, 144*(4), 1314–1323. https://doi.org/10.1016/j.neuroscience.2006.11.003

Polack, P. O., Friedman, J., & Golshani, P. (2013). Cellular mechanisms of brain state-dependent gain modulation in visual cortex. *Nature Neuroscience, 16*(9), 1331–1339. https://doi.org/10.1038/nn.3464

Polich, J. (1997). EEG and ERP assessment of normal aging. *Electroencephalography and Clinical Neurophysiology/Evoked Potentials Section, 104*(3), 244–256. https://doi.org/https://doi.org/10.1016/S0168-5597(97)96139-6

Purcell, D. W., John, S. M., Schneider, B. A., & Picton, T. W. (2004). Human temporal auditory acuity as assessed by envelope following responses. *The Journal of the Acoustical Society of America, 116*(6), 3581–3593. https://doi.org/10.1121/1.1798354

Ray, S., Niebur, E., Hsiao, S. S., Sinai, A., & Crone, N. E. (2008). High-frequency gamma activity (80-150 Hz) is increased in human cortex during selective attention. *Clinical Neurophysiology, 119*(1), 116–133. https://doi.org/10.1016/j.clinph.2007.09.136

Raza, A., Milbrandt, J. C., Arneric, S. P., & Caspary, D. M. (1994). Age-related changes in brainstem auditory neurotransmitters: measures of GABA and acetylcholine

function. *Hearing Research, 77*(1–2), 221–230. https://doi.org/10.1016/0378-5955(94)90270-4

Razak, K. A., & Fuzessery, Z. M. (2007). Development of inhibitory mechanisms underlying selectivity for the rate and direction of frequency-modulated sweeps in the auditory cortex. *Journal of Neuroscience, 27*(7), 1769–1781. https://doi.org/10.1523/JNEUROSCI.3851-06.2007

Razak, K. A., & Fuzessery, Z. M. (2013). GABA shapes selectivity for the rate and direction of frequency-modulated sweeps in the auditory cortex. *Journal of Neurophysiology*, *102*, 1366–1378. https://doi.org/10.1152/jn.00334.2009

Rezvani, A., & Levin, E. (2001). Cognitive effects of nicotine. *Biological Psychiatry, 49*(3), 258–267. https://doi.org/10.1016/S0006-3223(00)01094-5

Richardson, B. D., Ling, L. L., Uteshev, V. V., & Caspary, D. M. (2013). Reduced GABAA receptor-mediated tonic inhibition in aged rat auditory thalamus. *Journal of Neuroscience, 33*(3), 1218–1227. https://doi.org/10.1523/JNEUROSCI.3277-12.2013

Robinson, L. C., Barat, O., & Mellott, J. G. (2019). GABAergic and glutamatergic cells in the inferior colliculus dynamically express the GABAAR 1 subunit during aging. *Neurobiology of Aging, 80*, 99–110. https://doi.org/10.1016/j.neurobiolaging.2019.04.007

Rogalla, M. M., & Hildebrandt, J. K. (2020). Aging but not age-related hearing loss dominates the decrease of parvalbumin immunoreactivity in the primary auditory cortex of mice. *ENeuro, 7*(3). https://doi.org/ENEURO.0511-19.2020

Rotschafer, S., & Razak, K. (2013). Altered auditory processing in a mouse model of fragile X syndrome. *Brain Research, 1506*, 12–24. https://doi.org/10.1016/j.brainres.2013.02.038

Rumschlag, J. A., Lovelace, J. W., & Razak, K. A. (2020). Age- and movement-related modulation of cortical oscillations in a mouse model of presbycusis. *Hearing Research*, Advance Online Publication. https://doi.org/10.1016/j.heares.2020.108095

Sanz-Fernández, R., Sánchez-Rodriguez, C., Granizo, J. J., Durio-Calero, E., & Martín-Sanz, E. (2015). Utility of auditory steady-state and brainstem responses in age-related hearing loss in rats. *Acta Oto-Laryngologica*, *135*(1), 35–41. https://doi.org/10.3109/00016489.2014.953203

Samuel, I. B. H., Wang, C., Hu, Z., & Ding, M. (2018). The frequency of alpha oscillations: task-dependent modulation and its functional significance. *NeuroImage, 183*, 897–906. https://doi.org/10.1016/j.neuroimage.2018.08.063

Saoud, H., Josse, G., Bertasi, E., Truy, E., Chait, M., & Giraud, A. L. (2012). Brain-speech alignment enhances auditory cortical responses and speech perception. *Journal of Neuroscience, 32*(1), 275–281. https://doi.org/10.1523/JNEUROSCI.3970-11.2012

Schneider, B. A., & Hamstra, S. J. (1999). Gap detection thresholds as a function of tonal duration for younger and older listeners. *The Journal of the Acoustical Society of America, 106*(1), 371–380. https://doi.org/10.1121/1.427062

Schneider, B. A., Pichora-Fuller, M. K., Kowalchuk, D., & Lamb, M. (1994). Gap detection and the precedence effect in young and old adults. *The Journal of the Acoustical Society of America*, *95*(2), 980–991. https://doi.org/10.1121/1.408403

Schneider, D. M., & Mooney, R. (2018). How movement modulates hearing. *Annual Review of Neuroscience, 41*, 553–572. https://doi.org/10.1146/annurev-neuro-072116-031215

Schneider, D. M., Nelson, A., & Mooney, R. (2014). A synaptic and circuit basis for corollary discharge in the auditory cortex. *Nature, 513*(7517), 189–194. https://doi.org/10.1038/nature13724

Schofield, B. R., Motts, S. D., & Mellott, J. G. (2011). Cholinergic cells of the pontomesencephalic tegmentum: connections with auditory structures from cochlear nucleus to cortex. *Hearing Research, 279*(1–2), 85–95. https://doi.org/10.1016/j.heares.2010.12.019

Simon, H., Frisina, R. D., & Walton, J. P. (2004). Age reduces response latency of mouse inferior colliculus neurons to AM sounds. *The Journal of the Acoustical Society of America, 116*(1), 469–477. https://doi.org/10.1121/1.1760796

Sinai, A., Crone, N. E., Wied, H. M., Franaszczuk, P. J., Miglioretti, D., & Boatman-Reich, D. (2009). Intracranial mapping of auditory perception: event-related responses and electrocortical stimulation. *Clinical Neurophysiology, 120*(1), 140–149. https://doi.org/10.1016/j.clinph.2008.10.152

Sinai, Alon, Bowers, C. W., Crainiceanu, C. M., Boatman, D., Gordon, B., Lesser, R. P., Lenz, F. A., & Crone, N. E. (2005). Electrocorticographic high gamma activity versus electrical cortical stimulation mapping of naming. *Brain, 128*(7), 1556–1570. https://doi.org/10.1093/brain/awh491

Snell, K. B. (1997). Age-related changes in temporal gap detection. *Journal of the Acoustical Society of America, 101*(4), 2214–2220. https://doi.org/10.1121/1.418205

Snell, K. B., & Frisina, D. R. (2000). Relationships among age related differences in gap detection and word recognition. *The Journal of the Acoustical Society of America, 107*(3), 1615–1626. https://doi.org/10.1121/1.428446

Sohal, V. S., Zhang, F., Yizhar, O., & Deisseroth, K. (2009). Parvalbumin neurons and gamma rhythms enhance cortical circuit performance. *Nature, 459*(7247), 698–702. https://doi.org/10.1038/nature07991

Sottile, S. Y., Ling, L., Cox, B. C., & Caspary, D. M. (2017). Impact of ageing on postsynaptic neuronal nicotinic neurotransmission in auditory thalamus. *Journal of Physiology, 595*(15), 5375–5385. https://doi.org/10.1113/JP274467

Stothart, G., & Kazanina, N. (2016). Auditory perception in the aging brain: the role of inhibition and facilitation in early processing. *Neurobiology of Aging, 47*, 23–34. https://doi.org/10.1016/j.neurobiolaging.2016.06.022

Sukov, W., & Barth, D. S. (2001). Cellular mechanisms of thalamically evoked gamma oscillations in auditory cortex. *Journal of Neurophysiology, 85*(3), 1235–1245. https://doi.org/10.1152/jn.2001.85.3.1235

Šuta, D., Rybalko, N., Pelánová, J., Popelář, J., & Syka, J. (2011). Age-related changes in auditory temporal processing in the rat. *Experimental Gerontology*, *46*(9), 739–746. https://doi.org/10.1016/j.exger.2011.05.004

Tallon-Baudry, C., Bertrand, O., Delpuech, C., & Pernier, J. (1996). Stimulus specificity of phase-locked and non-phase-locked 40 Hz visual responses in human. *Journal of Neuroscience, 16*(13), 4240–4249. https://doi.org/10.1523/jneurosci.16-13-04240.1996

Tremblay, K. L., Piskosz, M., & Souza, P. (2002). Aging alters the neural representation of speech cues. *NeuroReport, 13*(15), 1865–1870. https://doi.org/10.1097/00001756-200210280-00007

Tremblay, K. L., Piskosz, M., & Souza, P. (2003). Effects of age and age-related hearing loss on the neural representation of speech cues. *Clinical Neurophysiology, 114*(7), 1332–1343. https://doi.org/10.1016/S1388-2457(03)00114-7

Trujillo, M., & Razak, K. A. (2013). Altered cortical spectrotemporal processing with age-related hearing loss. *Journal of Neurophysiology, 110*(12), 2873–2886. https://doi.org/10.1152/jn.00423.2013

Trujillo, M., Measor, K., Carrasco, M. M., & Razak, K. A. (2011). Selectivity for the rate of frequency-modulated sweeps in the mouse auditory cortex. *Journal of Neurophysiology, 106*(6), 2825–2837. https://doi.org/10.1152/jn.00480.2011

Turner, J. G., Hughes, L. F., & Caspary, D. M. (2005). Affects of aging on receptive fields in rat primary auditory cortex layer V neurons. *Journal of Neurophysiology, 94*(4), 2738–2747. https://doi.org/10.1152/jn.00362.2005

Tyler, L. K., Shafto, M. A., Randall, B., Wright, P., Marslen-Wilson, W. D., & Stamatakis, E. A. (2010). Preserving syntactic processing across the adult life span: the modulation of the frontotemporal language system in the context of age-related atrophy. *Cerebral Cortex, 20*(2), 352–364. https://doi.org/10.1093/cercor/bhp105

Uhlhaas, P. J., & Singer, W. (2010). Abnormal neural oscillations and synchrony in schizophrenia. *Nature Reviews Neuroscience, 11*(2), 100–113. https://doi.org/10.1038/nrn2774

Umbricht, D., Vyssotky, D., Latanov, A., Nitsch, R., Brambilla, R., D'Adamo, P., & Lipp, H.-P. (2004). Midlatency auditory event-related potentials in mice: comparison to midlatency auditory ERPs in humans. *Brain Research, 1019*(1-2), 189–200. https://doi.org/10.1016/j.brainres.2004.05.097

VanRullen, R., Busch, N. A., Drewes, J., & Dubois, J. (2011). Ongoing EEG phase as a trial-by-trial predictor of perceptual and attentional variability. *Frontiers in Psychology, 2*, 60. https://doi.org/10.3389/fpsyg.2011.00060

Volman, V., Behrens, M. M., & Sejnowski, T. J. (2011). Downregulation of parvalbumin at cortical GABA synapses reduces network gamma oscillatory activity. *Journal of Neuroscience, 31*(49), 18137–18148. https://doi.org/10.1523/JNEUROSCI.3041-11.2011

Walton, J. P., Barsz, K., & Wilson, W. W. (2008). Sensorineural hearing loss and neural correlates of temporal acuity in the inferior colliculus of the C57bl/6 mouse. *Journal of the Association for Research in Otolaryngology*, *9*(1), 90–101. https://doi.org/10.1007/s10162-007-0101-z

Walton, J. P., Frisina, R. D., & O'Neill, W. E. (1998). Age-related alteration in processing of temporal sound features in the auditory midbrain of the CBA

mouse. *Journal of Neuroscience, 18*(7), 2764–2776. https://doi.org/10.1523/JNEUROSCI.18-07-02764.1998

Walton, J. P., Simon, H., Frisina, R. D., & Giraudet, P. (2002). Age-related alterations in the neural coding of envelope periodicities. *Journal of Neurophysiology, 88*(2), 565–578. https://doi.org/10.1152/jn.2002.88.2.565

Warburton, D. M. (1992). Nicotine as a cognitive enhancer. *Progress in Neuropsychopharmacology and Biological Psychiatry, 16*(2), 181–192. https://doi.org/10.1016/0278-5846(92)90069-Q

Weible, A. P., Moore, A. K., Liu, C., Deblander, L., Wu, H., Kentros, C., & Wehr, M. (2014). Perceptual gap detection is mediated by gap termination responses in auditory cortex. *Current Biology*, *24*(13), 1447–1455. https://doi.org/10.1016/j.cub.2014.05.031

Weinstein, B. E., & Ventry, I. M. (1982). Hearing impairment and social isolation in the elderly. *Journal of Speech, Language, and Hearing Research, 25*(4), 593–599. https://doi.org/10.1044/jshr.2504.593

Wen, T. H., Afroz, S., Reinhard, S. M., Palacios, A. R., Tapia, K., Binder, D. K., Razak, K. A., & Ethell, I. M. (2018). Genetic reduction of matrix metalloproteinase-9 promotes formation of perineuronal nets around parvalbumin-expressing interneurons and normalizes auditory cortex responses in developing Fmr1 knock-out mice. *Cerebral Cortex, 28*(11), 3951–3964. https://doi.org/10.1093/cercor/bhx258

Wen, T. H., Binder, D. K., Ethell, I. M., & Razak, K. A. (2018). The perineuronal 'safety' net? perineuronal net abnormalities in neurological disorders. *Frontiers in Molecular Neuroscience, 11*, 270. https://doi.org/10.3389/fnmol.2018.00270

Wen, T. H., Lovelace, J. W., Ethell, I. M., Binder, D. K., & Razak, K. A. (2019). Developmental changes in EEG phenotypes in a mouse model of Fragile X Syndrome. *Neuroscience, 398*, 126–143. https://doi.org/10.1016/j.neuroscience.2018.11.047

Willott, J. F., Aitkin, L. M., & McFadden, S. L. (1993). Plasticity of auditory cortex associated with sensorineural hearing loss in adult C57BL/6J mice. *The Journal of Comparative Neurology, 329*(3), 402–411. https://doi.org/10.1002/cne.903290310

Wilson, T. W., Rojas, D. C., Reite, M. L., Teale, P. D., & Rogers, S. J. (2007). Children and adolescents with autism exhibit reduced MEG steady-state gamma responses.

Biological Psychiatry, 62(3), 192–197. https://doi.org/10.1016/j.biopsych.2006.07.002

Woods, D. L., & Clayworth, C. C. (1986). Age-related changes in human middle latency auditory evoked potentials. *Electroencephalography and Clinical Neurophysiology, 65*, 297–303. https://doi.org/10.1016/0168-5597(86)90008-0

Wu, P. Z., O'Malley, J. T., de Gruttola, V., & Charles Liberman, M. (2020). Age-related hearing loss is dominated by damage to inner ear sensory cells, not the cellular battery that powers them. *Journal of Neuroscience*, *40*(33), 6357–6366. https://doi.org/10.1523/JNEUROSCI.093720.2020

Yang, Y., Lee, J., & Kim, G. (2020). Integration of locomotion and auditory signals in the mouse inferior colliculus. *ELife, 9*, e52228. https://doi.org/10.7554/eLife.52228

Yokota, Y., & Naruse, Y. (2015). Phase coherence of auditory steady-state response reflects the amount of cognitive workload in a modified N-back task. *Neuroscience Research, 100*, 39–45. https://doi.org/10.1016/j.neures.2015.06.010

Zamir, S., Hennessy, C. H., Taylor, A. H., & Jones, R. B. (2018). Video-calls to reduce loneliness and social isolation within care environments for older people: An implementation study using collaborative action research. *BMC Geriatrics*, *18*(1), 1–13. https://doi.org/10.1186/s12877-018-0746-y

Zhao, Y., Xu, X., He, J., Xu, J., & Zhang, J. (2015). Age-related changes in neural gap detection thresholds in the rat auditory cortex. *European Journal of Neuroscience, 41*(3), 285–292. https://doi.org/10.1111/ejn.12791

Zheng, Q. Y., Johnson, K. R., & Erway, L. C. (1999). Assessment of hearing in 80 inbred strains of mice by ABR threshold analyses. *Hearing Research, 130*(1–2), 94–107. https://doi.org/10.1016/S0378-5955(99)00003-9

Zhou, M., Liang, F., Xiong, X. R., Li, L., Li, H., Xiao, Z., Tao, H. W., & Zhang, L. I. (2014). Scaling down of balanced excitation and inhibition by active behavioral states in auditory cortex. *Nature Neuroscience, 17*(6), 841–850. https://doi.org/10.1038/nn.3701